Geological Characteristics of the Ernie Junior Iron-Oxide-Copper-Gold Ore Body, Mt Isa Inlier, North West Queensland.

Thesis submitted in accordance with the requirements of the University of Adelaide for an Honours Degree in Geology

Ella Sullivan

November 2016

THE UNIVERSITY of ADELAIDE

GEOLOGICAL CHARACTERISTICS OF THE ERNIE JUNIOR IOCG ORE BODY, MT ISA INLIER, NW QUEENSLAND, AUSTRALIA

RUNNING TITLE

Ernie Junior; Characteristics and genesis.

ABSTRACT

The Ernest Henry Iron Oxide Copper Gold (IOCG) deposit is situated ~35km NE of Cloncurry, QLD in the Proterozoic Mount Isa Inlier. It is the second largest IOCG deposit in Australia with a pre-mining resource of 167 Mt @ 1.1% Cu and 0.54 ppm Au). The 'Ernie Junior' orebody exists between Ernest Henry and the bounding Footwall Shear Zone. This study presents the first characterisation and genetic model for the Ernie Junior ore body. Core logging, petrology, SEM, MLA and 3D modelling are undertaken on representative samples. The Ernie Junior ore body is hosted within a meta-volcanic sequence of fractured and clast-supported breccias. Host rocks have been subject to 1) regional albite alteration, 2) localised potassic alteration and 3) K-feldspar alteration associated with host breccias. Ore is also hosted in later stage veins where stage 3 alteration is present. The infill ore assemblage is comprised of chalcopyrite, gold, and gangue minerals magnetite, calcite, quartz, titanite and barite. High intensity K-feldspar alteration is coincident with brittle deformation. Brecciation is not as well developed in Ernie Junior as it is in Ernest Henry, possibly accounting for its lower grade. Outside the breccia zone, foliations and replacement textures indicate ductile deformation linked to the Foot Wall Shear Zone. The paragenetic sequence and lateral zonation of Ernie Junior is comparable to that of Ernest Henry providing evidence that the two ore bodies are highly genetically related. Potential exists for further repetitions of Ernest Henry and Ernie Junior mineralisation north of the footwall shear zone and this may be a viable target for future near-mine exploration.

KEYWORDS

Mount Isa Inlier, Ernie Junior, Ernest Henry, ore genesis, geochemical control, structural control.

TABLE OF CONTENTS

LIST OF FIGURES AND TABLES

1. Introduction

Despite the geological and economic importance of the Eastern Succession of the Mount Isa Inlier as host to Iron Oxide Copper Gold deposits, the variable nature of the mineralising system and burial under cover has meant that the genesis of these deposits is limited to a case-by-case understanding.

Immediately adjacent to the Ernest Henry ore body (Figure 1), the Ernie Junior ore body contains ore grade copper and gold and elevated magnetite. As a consequence of its smaller interpreted extent, there have been no formal studies of this ore body. As such, its host rock assemblage, ore distribution, alteration phases, structural controls and paragenesis have not been formally addressed. Such observations and analyses are of fundamental importance to understanding the genesis of the Ernie Junior ore body and how it may be genetically related to the much larger, structurally hosted and geochemically zoned Ernest Henry ore body (Mark et al, 2006). In addition, understanding the formation of Ernie Junior has direct implications for near mine (brownfields) exploration and adds to the growing understanding of IOCG deposits within the Eastern Succession of the Mount Isa Inlier.

IOCG deposits represent a broad range of mineral deposits, (Williams et al, 2005; Hitzman 2010). Lack of constraints on the nature of this deposit class creates complexity for exploration, yet their large size potential (>1000 Mt) and desirable grades in copper and gold makes them key exploration targets (Williams et al. 2005). Recognised as one of the world's most mineralised provinces, the Eastern Succession of the Mt Isa Inlier in Queensland hosts a diversity of IOCG deposits (Figure 2) that display unique characteristics and mineralising styles (Davidson, 1998).

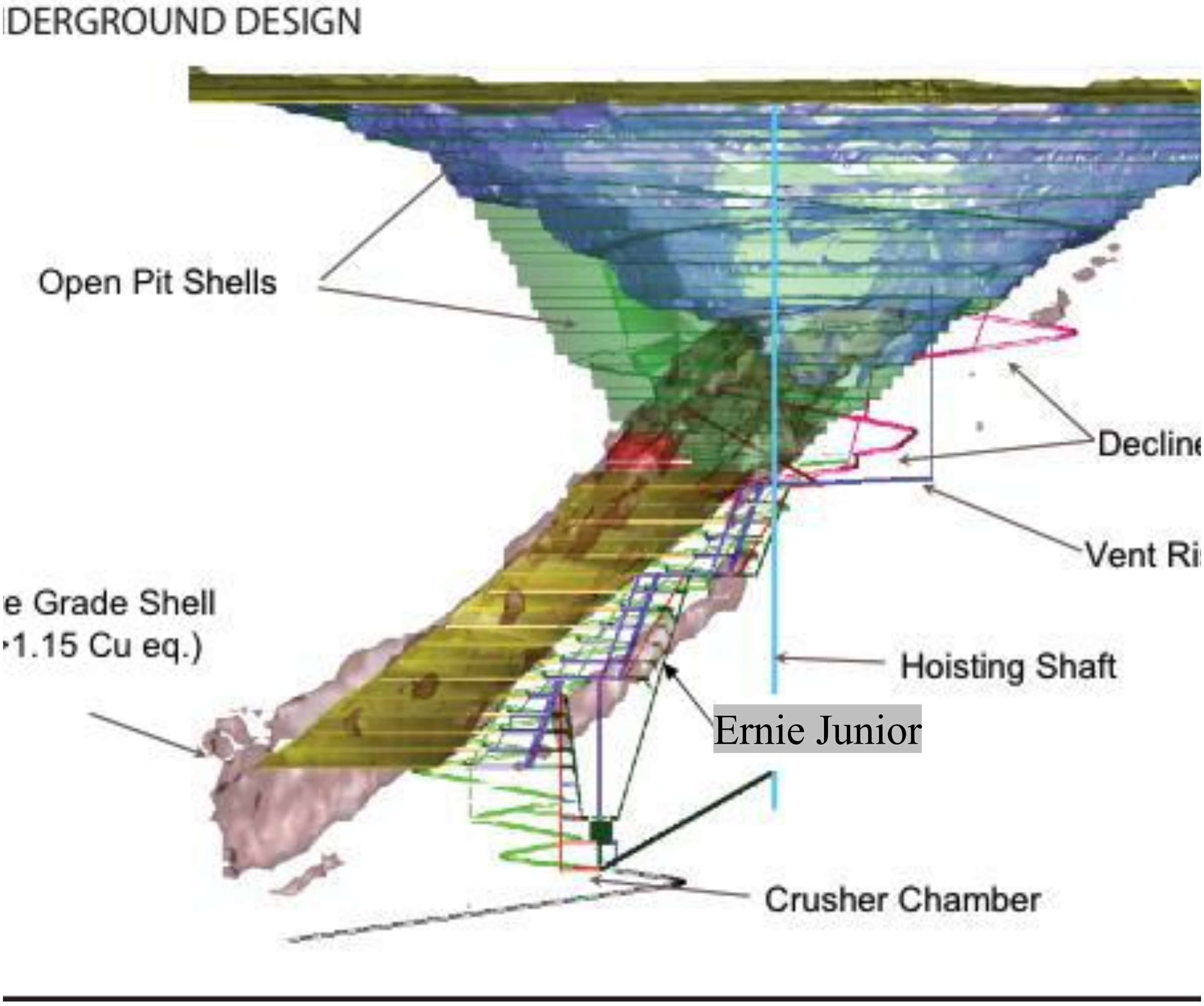

Figure 1 Image of the Ernest Henry Mine illustrating the spatial arrangement of the Ernest Henry and Ernie Junior ore bodies at the grade of >1.15% Cu. Open pit shell and underground workings are also pictured.

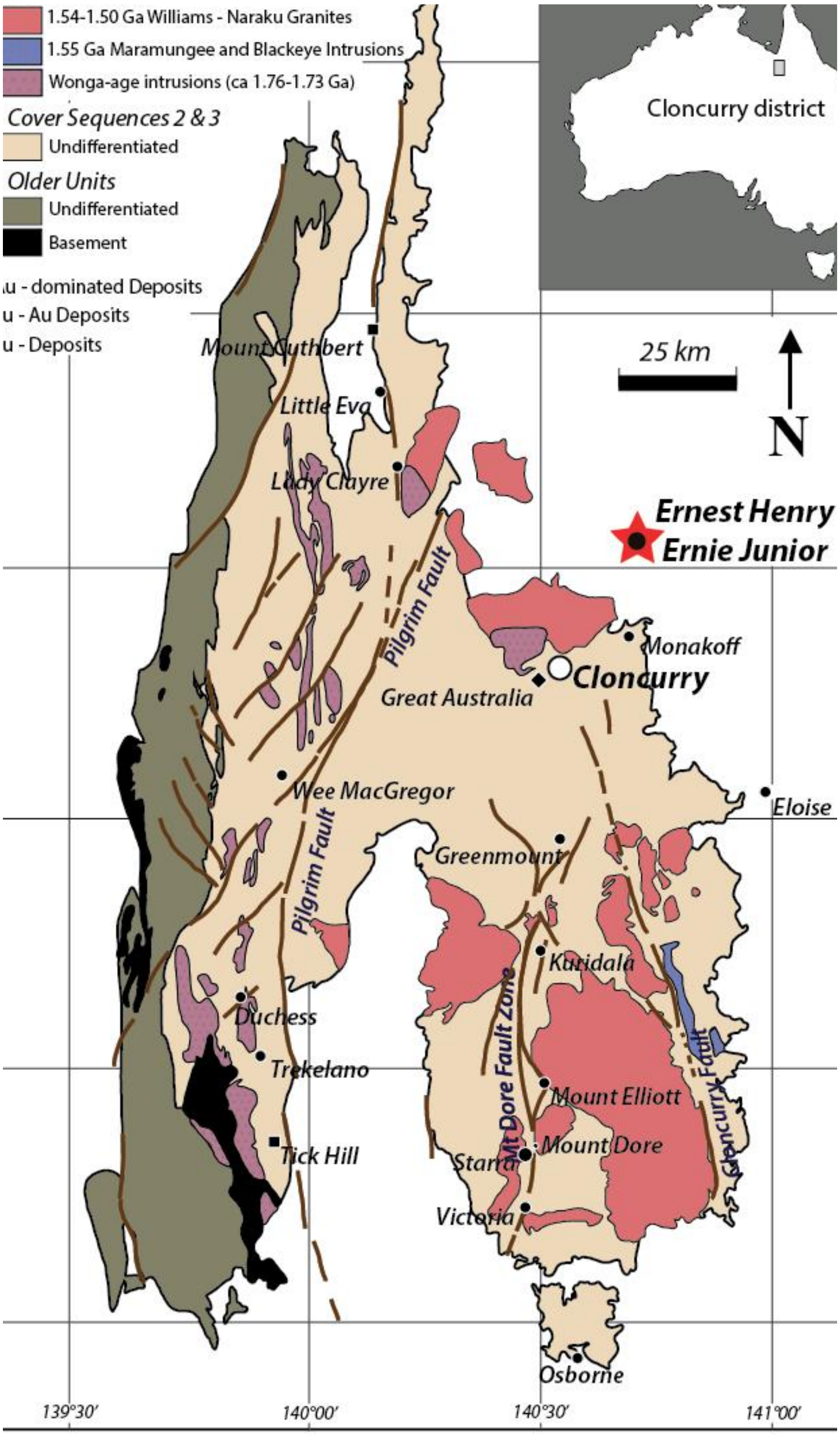

Figure 2. Map of the Mount Isa Inlier, illustrating the locations and styles of significant economic deposits, with inset map of Australia.

Ernest Henry (Figure 2) has been thoroughly characterised in terms of its hydrothermal evolution (Oliver et al, 2004; Mark et al, 2005; Mark et al, 2006, Kendrick et al, 2006), geochemical signature (Rusk et al, 2010), structural control (Coward, 2000) and lateral zonation (Cleverley et al, 2005). Epigenetic mineralisation occurs as co-enriched chalcopyrite and native gold within a breccia matrix (Twyerould, 1997; Ryan, 1998). As Ernie Junior has not yet been completely defined or formally studied, models of genesis for Ernest Henry will provide a reference point for understanding the genesis of Ernie Junior.

1.2 Project aims

This project aims to test the hypotheses that:

- Ernest Henry and Ernie Junior are hosted by the same Mt Fort Constantine Volcanics
- The paragenesis of alteration and mineralisation is consistent across Ernie Junior and Ernest Henry
- The distribution of mineralisation is consistent across Ernie Junior and Ernest Henry
- Deformation fabrics are consistent across the Ernie Junior and Ernest Henry ore bodies

These hypotheses are designed to determine to what extent the Ernie Junior ore body is genetically associated with Ernest Henry, given its spatial proximity, and to highlight any differences in genesis. This research aims to help inform future exploration at the Ernest Henry Mine, as well as within the Eastern Succession.

2. REGIONAL AND LOCAL DEPOSIT GEOLOGY

2.1 Mount Isa Inlier

The Eastern Fold Belt and adjacent Kalkadoon, Leichhardt and Western Fold Belts of the Mount Isa Inlier (Figure 2) comprises >200,000 km2 of Proterozoic meta-sedimentary and metavolcanics sequences. This basement sequence was intruded by 1550 to 1500Ma I-type granites of the Williams and Naraku batholiths prior to the 1620-1550Ma Isan Orogeny metamorphosed basement lithologies to amphibolite facies (Page and Sun, 1998; Foster et al, 2007). Subsequent and regionally extensive metasomatism preserves evidence of at least four hydrothermal events through 1610 to 1500 Ma (Oliver et al., 2004) and widespread Cu mineralisation within the Eastern Succession and wider Mt Isa Inlier (William et al. 2005). Overlying basement lithologies include three major, unconformable Mesozoic volcanoclastic sequences representing three periods of intracratonic rifting 1785 - 1650 Ma post Isan Orogeny (Page and Sun, 1998).

2.2 Deposit Geology

The Ernest Henry deposit is hosted in brecciated and pervasively K-feldspar altered Mount Fort Constantine intermediate volcanics dated at ~1740Ma (Mark et al. 2006). The ore body forms a pipe-like structure, dipping ~40 degrees towards the SSE that extends down plunge for a length >1km and is open at depth (Keys, 2008). The ore body is ~250m long, 300m wide and is structurally controlled by a series of sub-parallel shear zones (Mark et al. 2006). Economic mineralisation lies at the core of alteration zones dominated by K-feldspar in two main plunging lenses and divided by a zone of weak mineralisation and brecciation (Mark et al, 2006, Williams, 2005) known as the inter-lens (O'Brien, 2016). The ore assemblage is dominated by magnetite, chalcopyrite, pyrite, carbonate, quartz and apatite.

Ernest Henry and Ernie Junior interpreted to be hosted within a Paleo-Mesoproterozoic volcano-sedimentary succession deposited in a rift environment (Porter, 2010). Mineralisation is hosted in rocks most analogous to Mt Fort Constantine metavolcanics that outcrop ~10 km from the deposit (Williams and Skirrow, 2000; Marshall and Oliver, 2007). These volcanics consist of andesite and dacite with lesser metabasalts and calc-silicate metasedimentary rocks (Porter, 2010) (Figure 3).

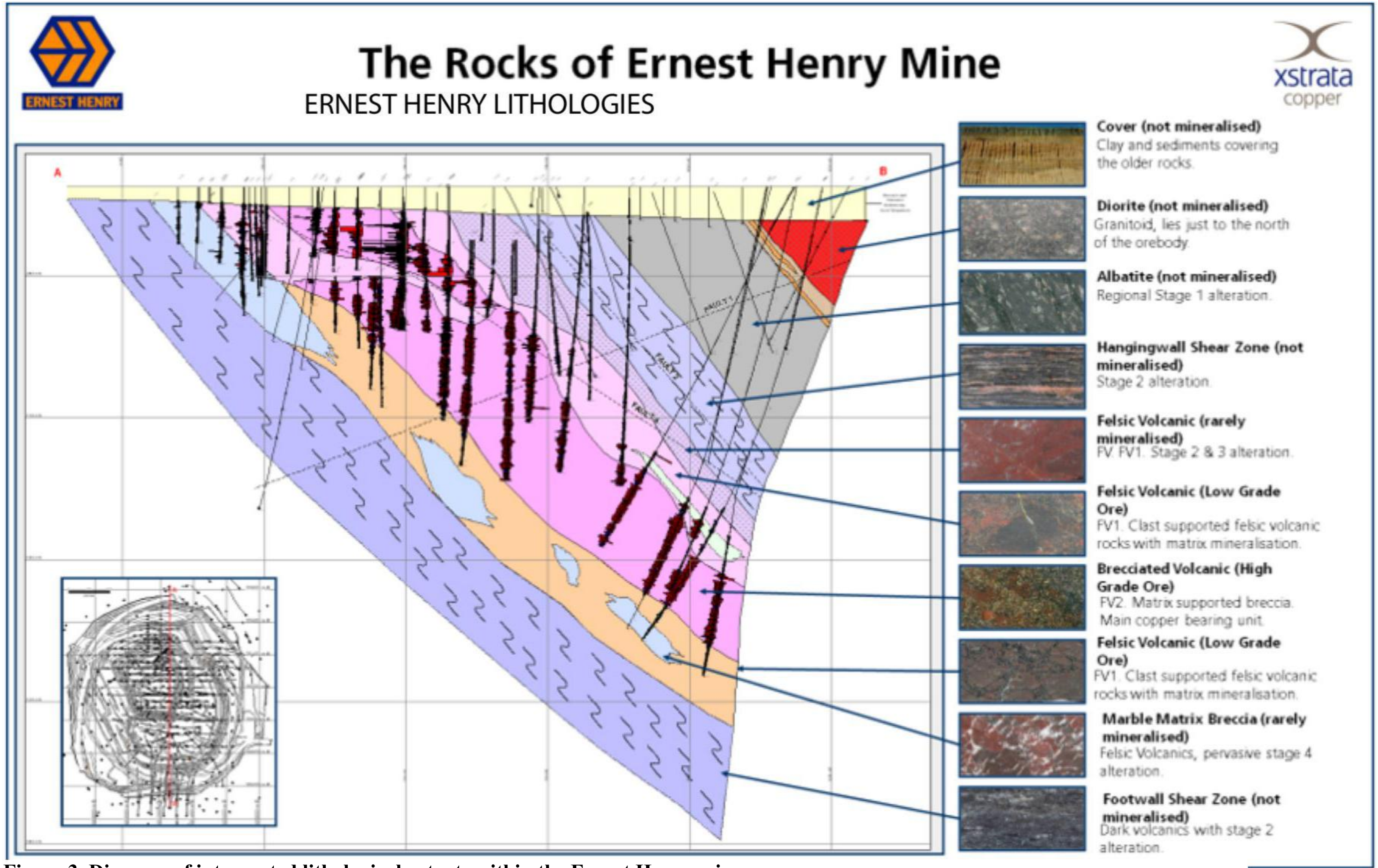

Figure 3. Diagram of interpreted lithological extents within the Ernest Henry mine.

2.3. Structural and geochemical setting

2.3.1. Ernest Henry Structural Setting

Ernest Henry and Ernie Junior are located on the inflection of shear zones (Figure 4). They trend from E-W to NE/SW orientation which has been genetically related to the regional syn- to late regional D3, mineralisation (Valenta, 2000; Coward, 2000; Laing, 2003, Keys, 2008). Control on the flexure in regional structure has been attributed to two resistant diorite bodies to the SE and NE of the deposit (Coward, 2001).

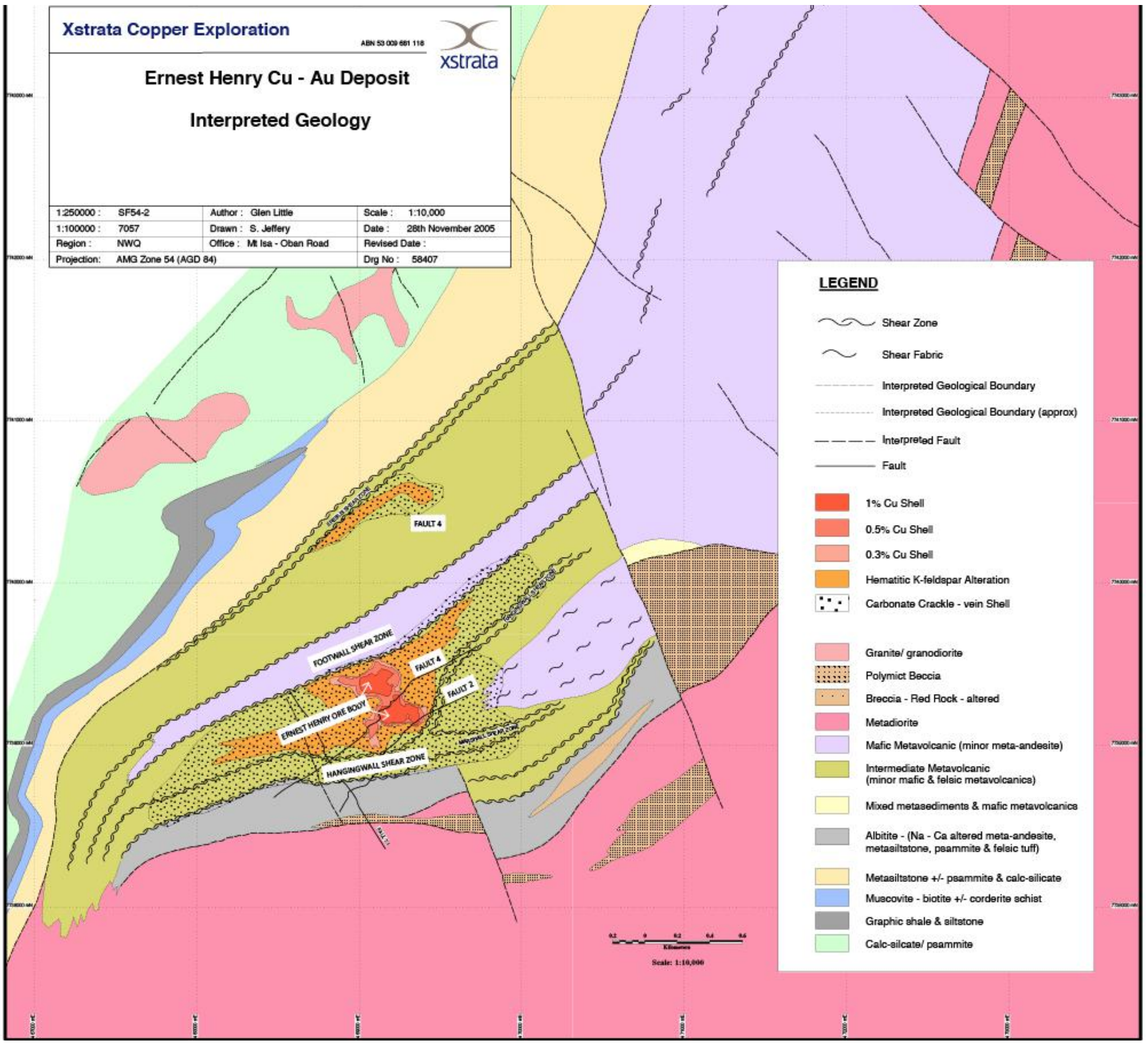

Figure 4. Structural setting of Ernest Henry ore body, with relation to metadiorite intrusions and local shear zones. Image an internal Xstrata Copper report,

Three ductile shear zones are identified around Ernest Henry (**Error! Reference source not found.**), though lack of continuity of fabric intensity along drill core inhibits precise 3D geometry modelling (Mark et al, 2006).

Structural fabric	**Description**	**Preservation within Ernest Henry**
S_1	Bedding-sub parallel feature	Outside of the ore zone as schistosity in graphitic schists
S_2	Crenulation cleavage, broadly synchronous with peak amphibolite metamorphic minerals.	Mica schists
S_3	Hetrogeneous foliation and crenulation development and formation of imbricate breccias. Local overprinting of biotite-magnetite in the footwall rocks.	Biotite and carbonate-rich lithologies within and adjacent to the ore body.

Table 1. Summary of structural fabrics within and around the Ernest Henry deposit, in vicinity to Ernie Junior. Information reference: Mark et al, 2006.

The Ernest Henry deposit is bound by two shear zones - the Hanging Wall Shear Zone (HWSZ) and Footwall Shear Zone (FWSZ) and contains the unmineralised Interlens shear zone within its extent. Ernie Junior is located between Ernest Henry and the FWSZ in proximity to two major faults; Fault 6 and the Angry Man fault (Figure 5). Interpreted as post mineralisation structures, their bounding nature to the ore bodies indicates potential for fault displacement of mineralisation in proximity to the Ernest Henry Deposit (Max Ayliffe, AIG journal, 2009).

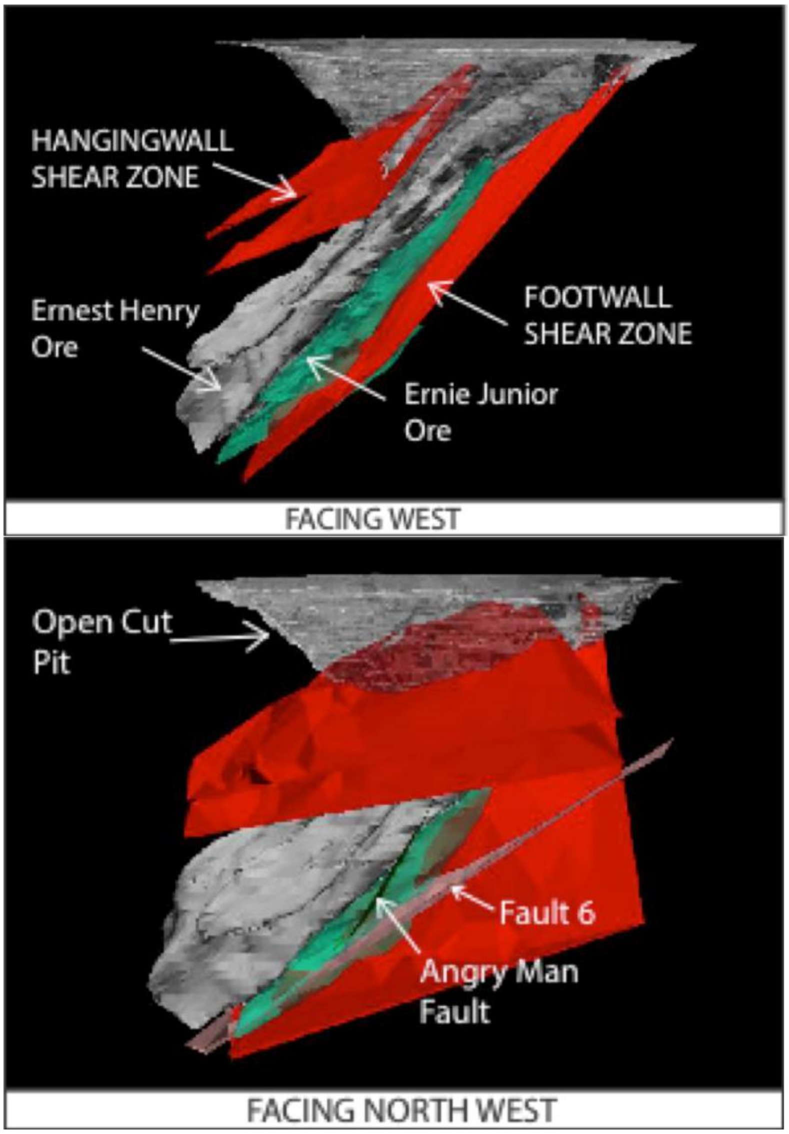

Figure 5 . Illustrating the interpreted extent of the main structures associated with Ernest Henry and Ernie Junior ore bodies. Compiled using ore shells provided by Ernest Henry Mine.

2.3.2 Ernest Henry Geochemistry and Alteration

Cu and Au within the Ernest Henry ore is strongly co-enriched at a ratio of 2:1 with economic mineralisation occurring as chalcopyrite and native gold (95%) and minor electrum (5%) (William, 2000., Rusk et al, 2010). The distribution and intensity of Cu and Au is displayed in Figure 6. Alteration stages and associations are displayed in Table 2.

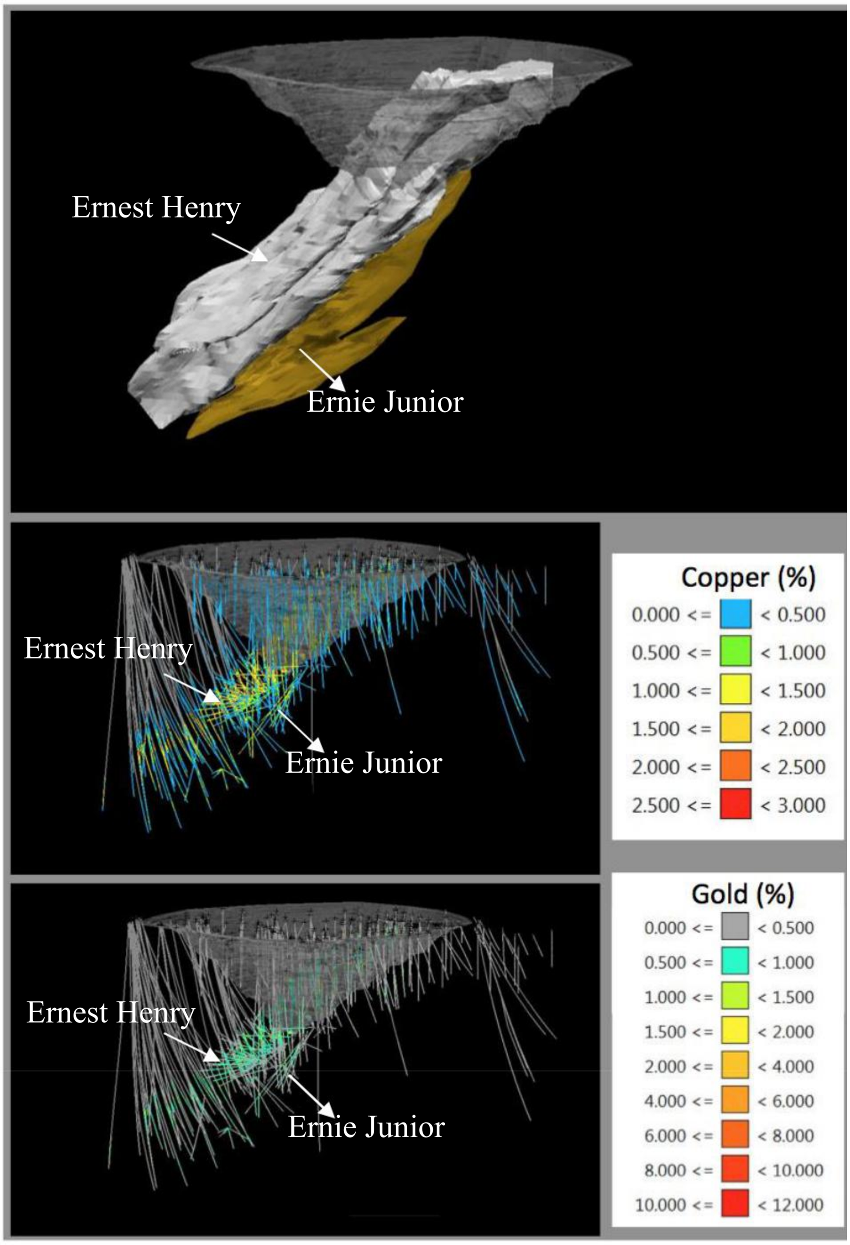

Figure 6. All Ernest Henry Mine (EHM) drilling and interpreted ore body shells a) Interpreted outlines for Ernie Junior (yellow) and Ernest Henry (grey) illustrating their relative position to the open cut pit. Their extent is based on a 1% Cu grade b) Copper assays for EHM illustrating the core of the Ernest Henry ore body and sparse drilling through Ernie Junior. Assay values are taken as an average grade over 2 metre intervals. c) Gold assays for EHM illustrating their spatial association with Cu grade. Assay data courtesy of EHM.

Alteration type	Description	Preservation within Ernest Henry
Albite	Albitisation of plagioclase phenocrysts	Fracture-related hydrothermal breccia, crackle veining, pervasive alteration
Potassic	Fine grained biotite and magnetite rich alteration	Pervasive alteration through all rock types, rare veining
K-feldspar	Equigranular fine-medium grained k-feldspar	Pervasive alteration of volcanic rocks, veining

Table 2. Summary of alteration assemblages within and around the Ernest Henry deposit, in vicinity of Ernie Junior. Alteration stages are ordered by interpreted evolution (Mark et al, 2006).

2.4. Genetic Models for Ernest Henry

The formation of Ernest Henry is recognised within the context of a structurally zoned, post-peak metamorphic hydrothermal system, synchronous with the D3 regional metamorphic event (Mark et al, 2004). Its regional geochemical footprint is dominated by regionally extensive and pervasive albitic and potassic alteration, focussed by local faulting (Blenkinsop and Stark, 2003).

Economic copper and gold mineralisation is restricted to breccia zones with a significant matrix component of more than 10% (Keys, 2008) and is thought to have formed at a depth of 6-10km via circulation of hydrothermal fluids derived from regional ‘A’- type granites associated with, hydrothermal brecciation event (Kendrick and Phillips, 2006;

Ryan, 1998; Williams, 2005). Its genesis however is still contentious (Rusk et al, 2010) and previous studies have suggested a combination of magmatic (Mark et al, 2000; Williams and Skirrow, 2000), non-magmatic (Haynes, 2000) and a hybrid of multiple fluid/metal hydrothermal fluid sources (Mark et al, 2000). More recently, fluid origins have been attributed to a mixture of magmatic, metamorphic and basinal sources (Williams, 2005).

Mark et al, 2006 have interpreted that mineralisation resulted from fluid mixing during dilation and brecciation, concentrated in areas of the initial potassic alteration. An alternate model of genesis attributes breccia host formation to fluid overpressure and explosive brecciation (Oliver, 2004).

3. Methods

3.1 SAMPLING

This thesis is based on fieldwork completed at the Ernest Henry Mine core yard. Drill core logs were produced for seven representative drill holes, within the interpreted extent of the Ernie Junior ore body (Figure 7).

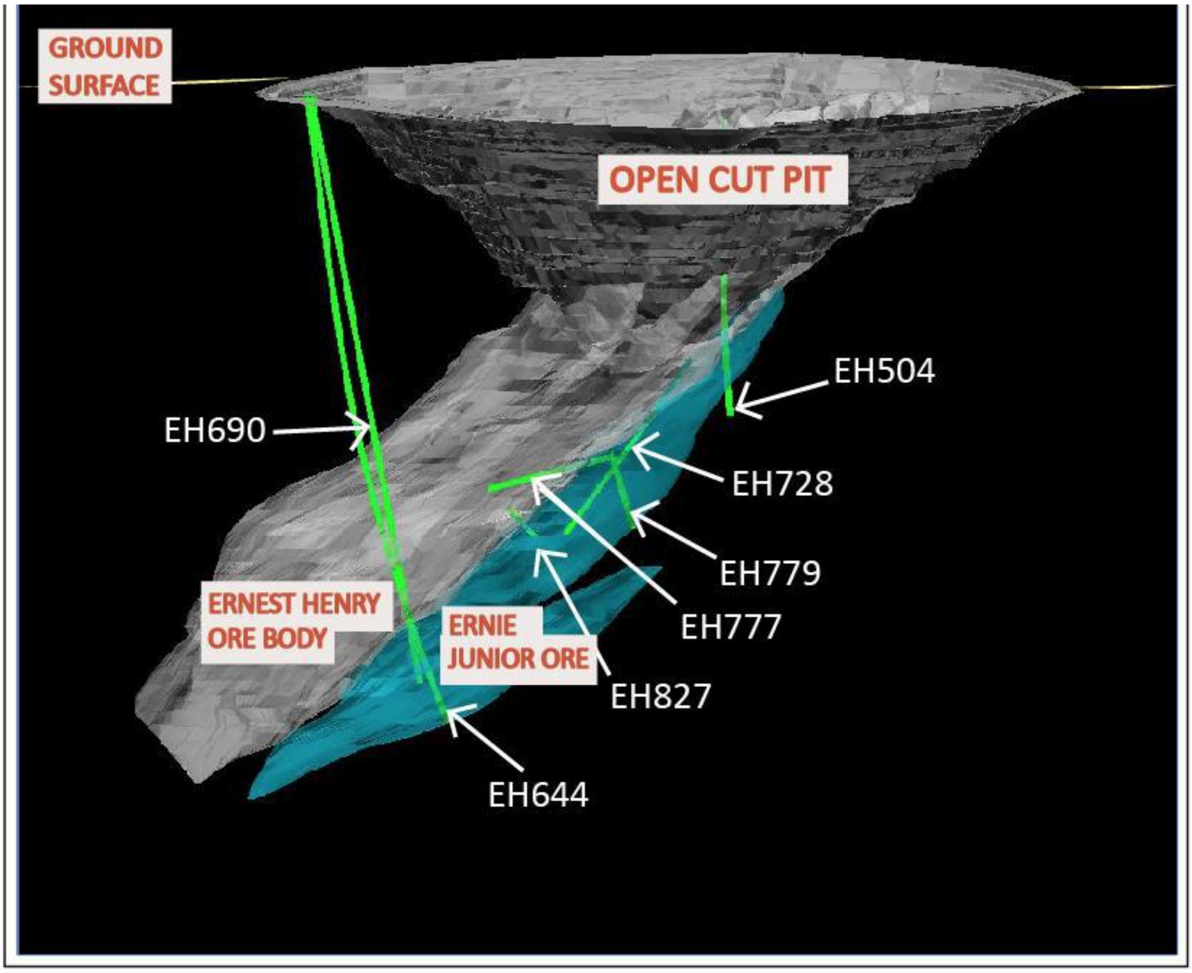

Figure 7. Illustrating the locations and sections of drill holes observed in this study, against the interpreted ore shell. Ore shells represent a 1% Cu grade. Ore shell triangulation courtesy of EHM, 2016.

Drill core was logged for lithology, alteration, sulphides, foliation, brecciation and vein abundance. HQ sized diamond drill core was logged in intervals based on lithology type as listed in **Error! Reference source not found.**The logged data for each drill hole is represented using a scaled interval in Adobe Illustrator and is used to observe the distribution of ore in relation to lithologies and alteration.

Drill Hole ID	Intervals logged (m)
EH504	390-580
EH644	1010-1210
EH690	940 - 1130
EH777	0-150
EH728	80-400
EH779	0-120
EH827	0-35

Table 3. Sections of core logged for drill holes: EH504, EH644, EH690, EH728 EH777, EH779 and EH827.

From these drill holes, a total of 20x 15cm quarter-core samples representative of mineralisation, host rock, veining and alteration were selected for detailed analysis at the hand-sample scale. Samples were selected and cut into thin sections for petrographic analysis through microscopy, scanning electron microscopy (SEM) and mineral liberation acceleration (MLA). Fifteen thin sections were polished for reflected light analyses. The remaining five samples were unpolished. Each section underwent optical microscopy to assess host rock petrology, ore mineralisation and paragenesis.

3.2 Petrology and Ore Microscopy

Twenty Ernie Junior core samples were sent to Ingham Petrographics, Ingham, Queensland, to produce polished thin sections. A DP21 Microscopy digital camera, mounted on an Olympus Bx51 System dual-purpose microscope was used to view and photograph thin sections, facilitating assessment of host rock petrology and ore zone mineralogy for establishment of Ernie Junior paragenesis.

3.3 Scanning Electron Microscopy and Mineral Liberation Acceleration

The Quanta 600 Scanning Electron Microscope (SEM) was used to analyse and describe mineralogy and texture. Analyses were conducted on 15 carbon-coated thin sections of representative Ernie Junior ore. The SEM was equipped with energy-dispersive X-ray spectrometer and was used to identify accessory minerals through semi-qualitative approximation of chemistry. Back-scattered electron (BSE) imaging was used on areas of interest for further textural analyses. In addition, Mineral Liberation Acceleration (MLA) was undertaken on BSE images in order to highlight fine-grained accessory phases and their distribution within samples. The MLA allowed the processing of colour-coded minerals based on chemical composition. Textural complexity provided a limitation to data collection. Limitation of the spectral database was negated by cross-checking with petrological observations to account for any possible identification errors.

3.4 Assay Plots

Relevant drill hole intervals from the Ernest Henry Mine database were selected in order to determine the ratios between copper and gold in the Ernie Junior ore body. Assay data provided by Ernest Henry Mine is based on the average of copper (%) and gold (ppm) over 2 metre intervals down drill holes.

3.5. Structural measurements

Foliation and vein measurements were taken from drill core using survey data from the Ernest Henry Mine and a Majoribanks Core Frame. The core frame was aligned with the orientation of the drill hole as it would be positioned in-situ, using a compass clinometer. Orientation lines indicating the base of the hole on drill core was place facing down on the oriented core frame. Measurements of planes were made with a compass clinometer as per in the field.

3.5 3D Modelling in Vulcan 8.2

Vulcan Envisage and Isis were used to model lithologies and alteration in 3D between studied drill holes. Databases were compiled and lithologies and alteration were colour coded to represent the ore body visually. Structural measurements were likewise plotted presenting measurements in 3D using the Vulcan Isis database complier. Positioning of drill holes by their Northing, Easting and Reduced Level allowed for accurate 3D positioning of textures and structures through the ore body. For an extended method of database design and 3D display refer to Appendix A.

4. RESULTS

4.1. Cu:Au ratio

Cu:Au ratios from drill holes EH690 and EH644 (which intersect both ore bodies) were compiled from each ore body intersection (Figure 8). Results show an R^2 correlation of 0.9 indicating a distinct positive relationship between copper and gold at a ratio of roughly 2:1 within Ernest Henry and Ernie Junior.

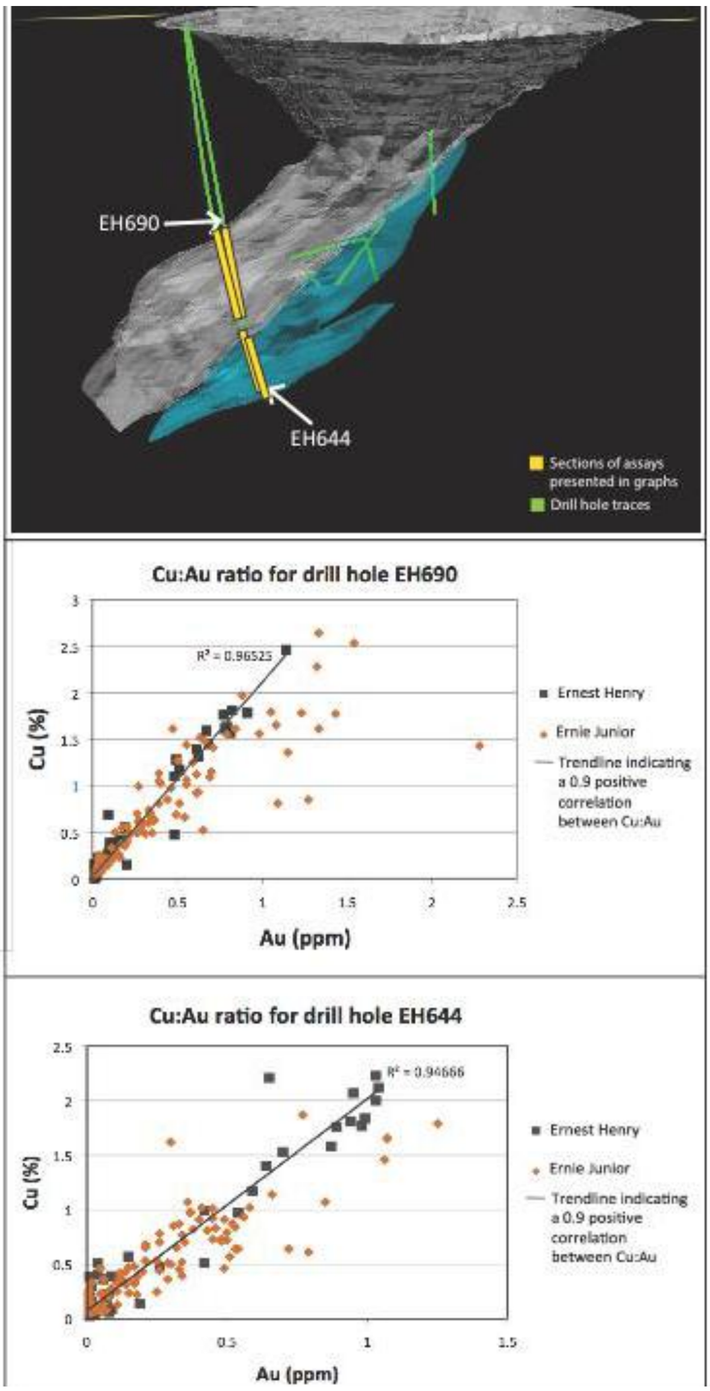

Figure 8. Cu:Au of drill holes EH690 and EH644, intersecting both Ernie Junior and Ernest Henry11 ore bodies.

4.2 Drill Hole Logs

Logs were produced for each drill hole to record the distribution of lithologies, alteration and mineralisation. Correlations were observed between K-feldspar alteration and peaks in Cu and Au. Variable degrees of brecciation within the k-feldspar altered sections and massive sulphide veins outside the k-feldspar altered breccias (0.5-10cm wide) correlate to elevated Cu and Au. Magnetite alteration and infill is pervasive and present through all drill holes. Lower magnetite abundances are observed in intensely K-feldspar altered volcanics (refer to section 7) and in sections where stage 1 regional albite alteration is observed (refer to section 8).

The ore-bearing breccia zone in EH644 and EH960 is highly variable, with contrasting textural repetition of ~3 metre wide units of massive and breccias units that correspond to highly fluctuating Cu/Au grades, within the same lithology and alteration of FV volcanics. Higher matrix component is observed with higher Cu/Au elevations within intense areas of k-feldspar alteration.

Intense magnetite alteration with lesser biotite is a halo to k-feldspar alteration that is present to the extents of drill core logged. Exceptions to this are where trachyandesite textures are preserved in drill hole EH777 (Figure 14), where drill core is less magnetic, preserving an earlier albite alteration stage. Detailed descriptions of lithologies and alteration stages follow below in section 6.3 and 7.

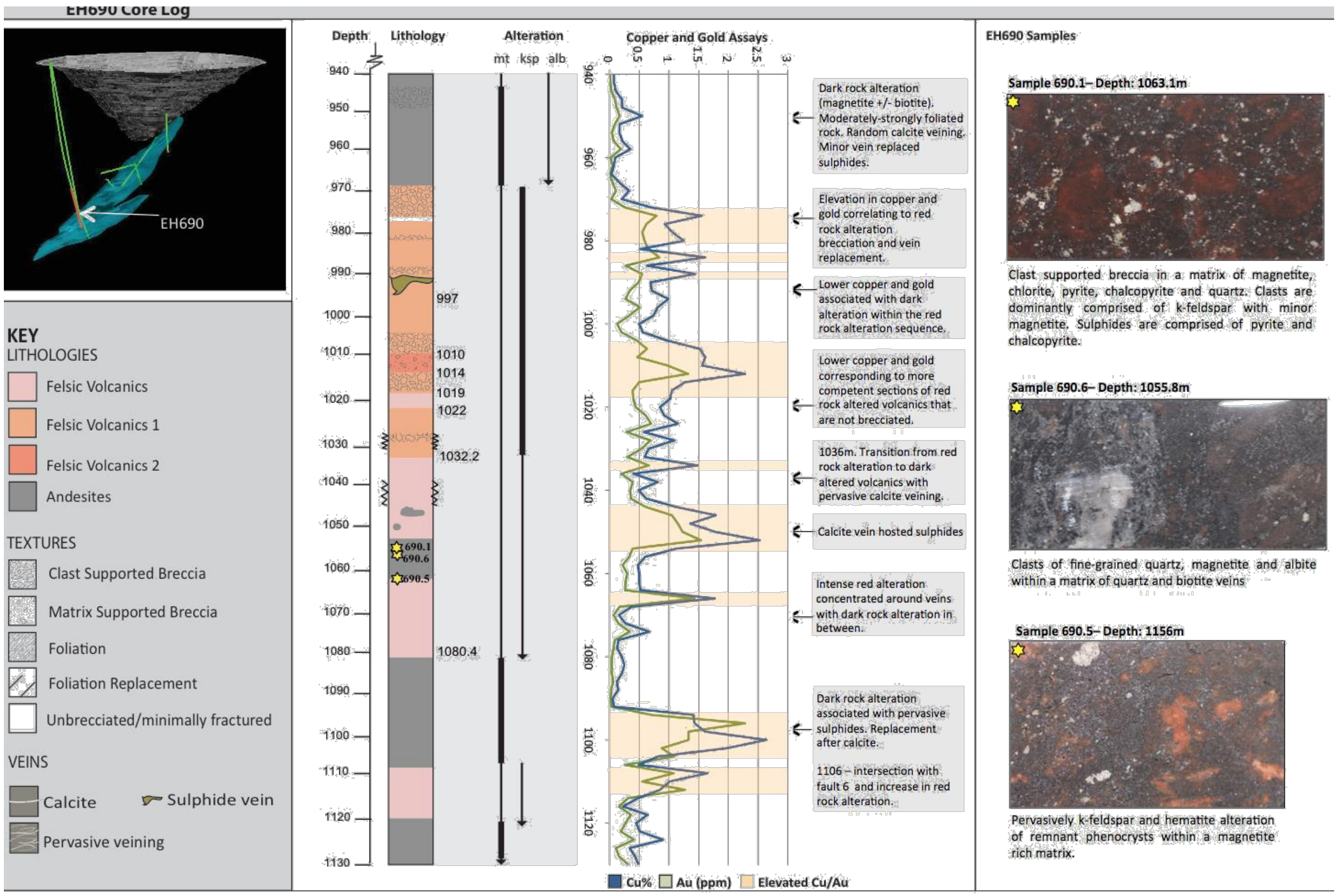

Figure 9. The correlation between lithology, alteration and enrichment of Cu and Au for drill hole EH690. Dark rock alteration, specially increased magnetite correlates with lower copper and gold elevations and comprises a large component of the matrix to red rock altered breccias (refer section 7). Red rock alteration correlates with the majority of sulphide deposition and brecciation. However, the highest elevations of Cu and Au appear to be somewhat irrespective of the alteration stage experienced by the volcanics. Elevations are observed in in the Felsic Volcanics 2 lithology as a breccia, Felsic Volcanics as vein hosted and within andesites, also vein hosted.

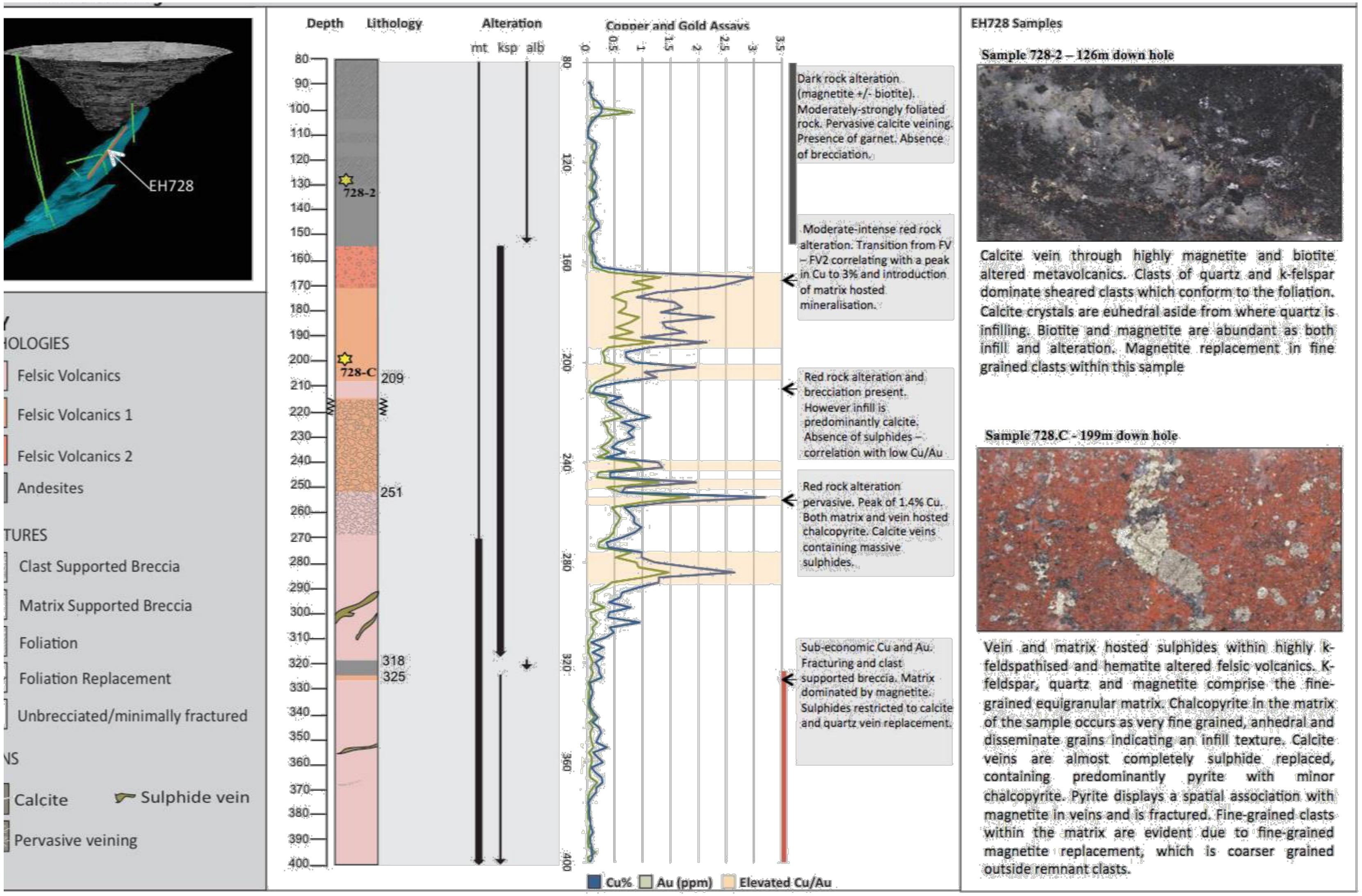

Figure 10. Illustrating the relationship between lithology, alteration and enrichment of Cu and Au and correlating samples. Correlations and core observations indicate that red rock (k-feldspar hematite) alteration and degree of brecciation, are controls on the distribution of Cu and Au. Similar to Ernest Henry ore, a larger matrix component and more pervasive brecciation in ie Junior correlates to high Cu and Au components. Brecciation of red rock altered volcanics and strong foliation of magnetite +/- biotite alteration indicates a competency contrast, related to presence and intensity of k-feldspar and hematite alteration.

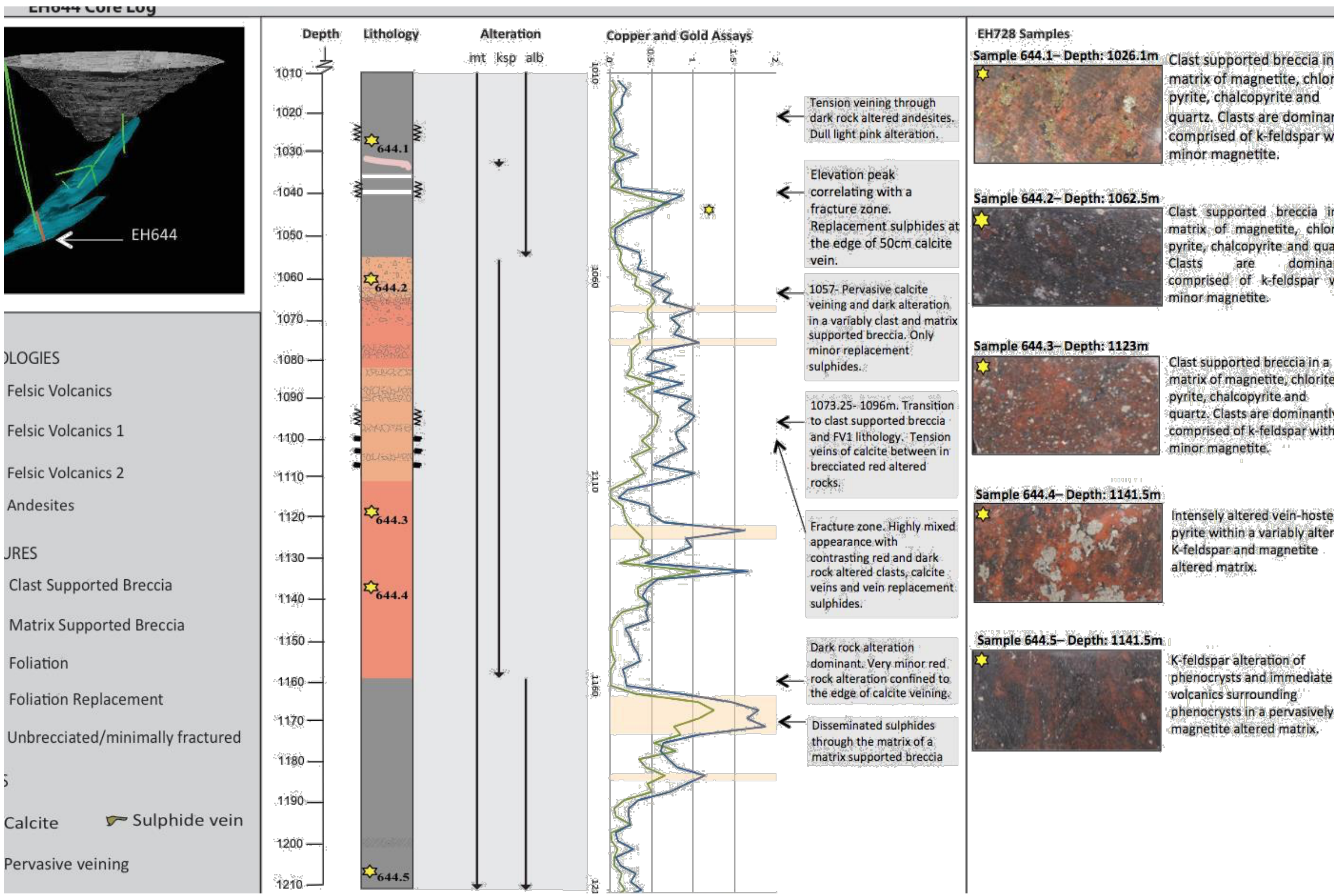

Figure 11. The correlation between lithology, alteration and enrichment of Cu and Au for drill hole EH644. Volcanics lithologies within the red rock altered zone are variably brecciated, with a section from 1055-1110m alternating between breccias and massive host rocks. Massive sections are interpreted to correlate to the low spikes in Cu and Au abundance within this section. Interestingly, the highest ore bearing section of EH644 is within a zone that has been minimally red rock altered. Instead, sulphides are hosted in dark rock altered volcanics.

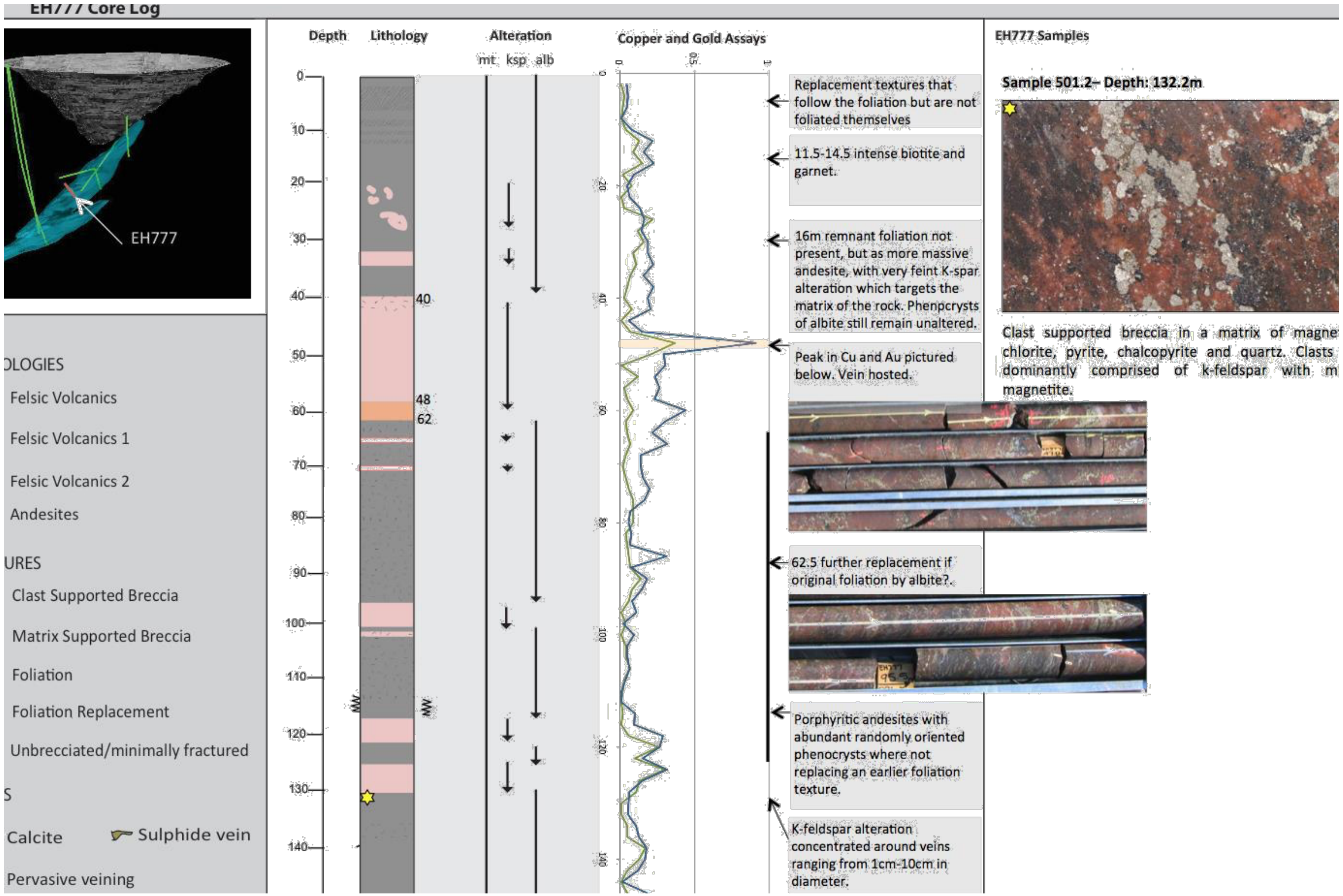

Figure 12. The correlation between lithology, alteration and enrichment of Cu and Au for drill hole EH644.

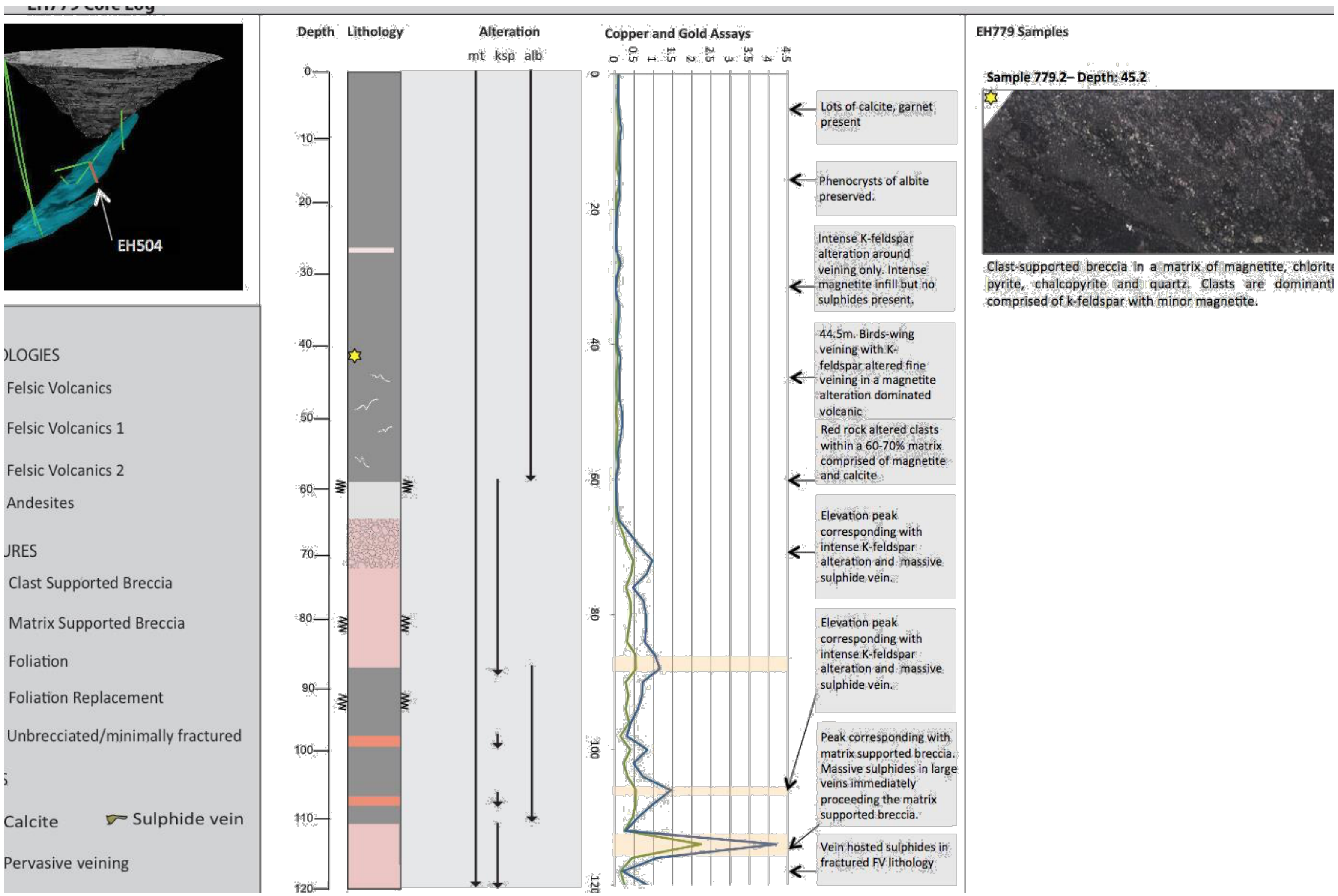

Figure 13. The correlation between lithology, alteration and enrichment of Cu and Au for drill hole EH779. Enrichment in Cu and Au is major peak in elevation observed within the Felsic Volcanics.

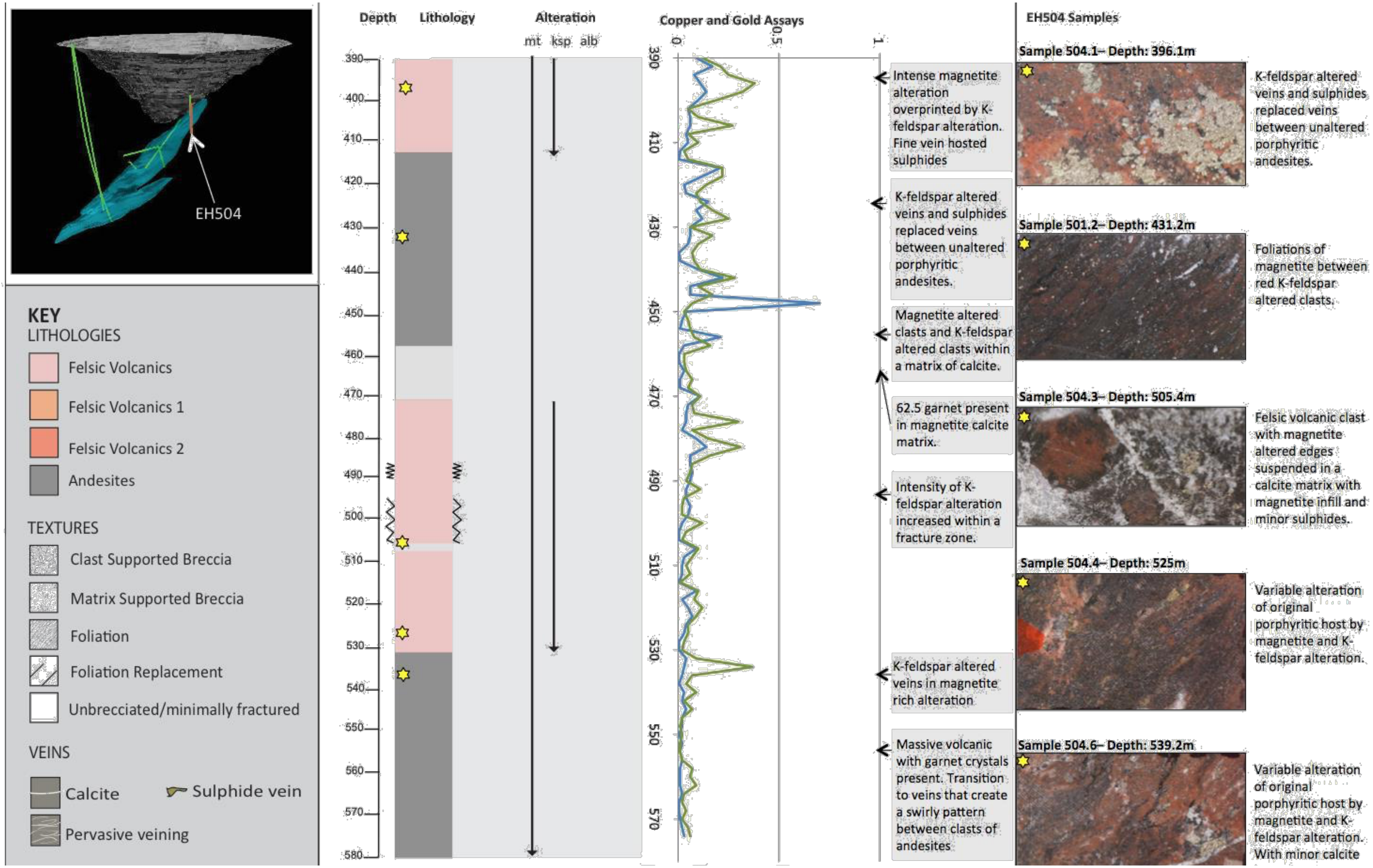

Figure 14. The correlation between lithology, alteration and enrichment of Cu and Au for drill hole EH504.

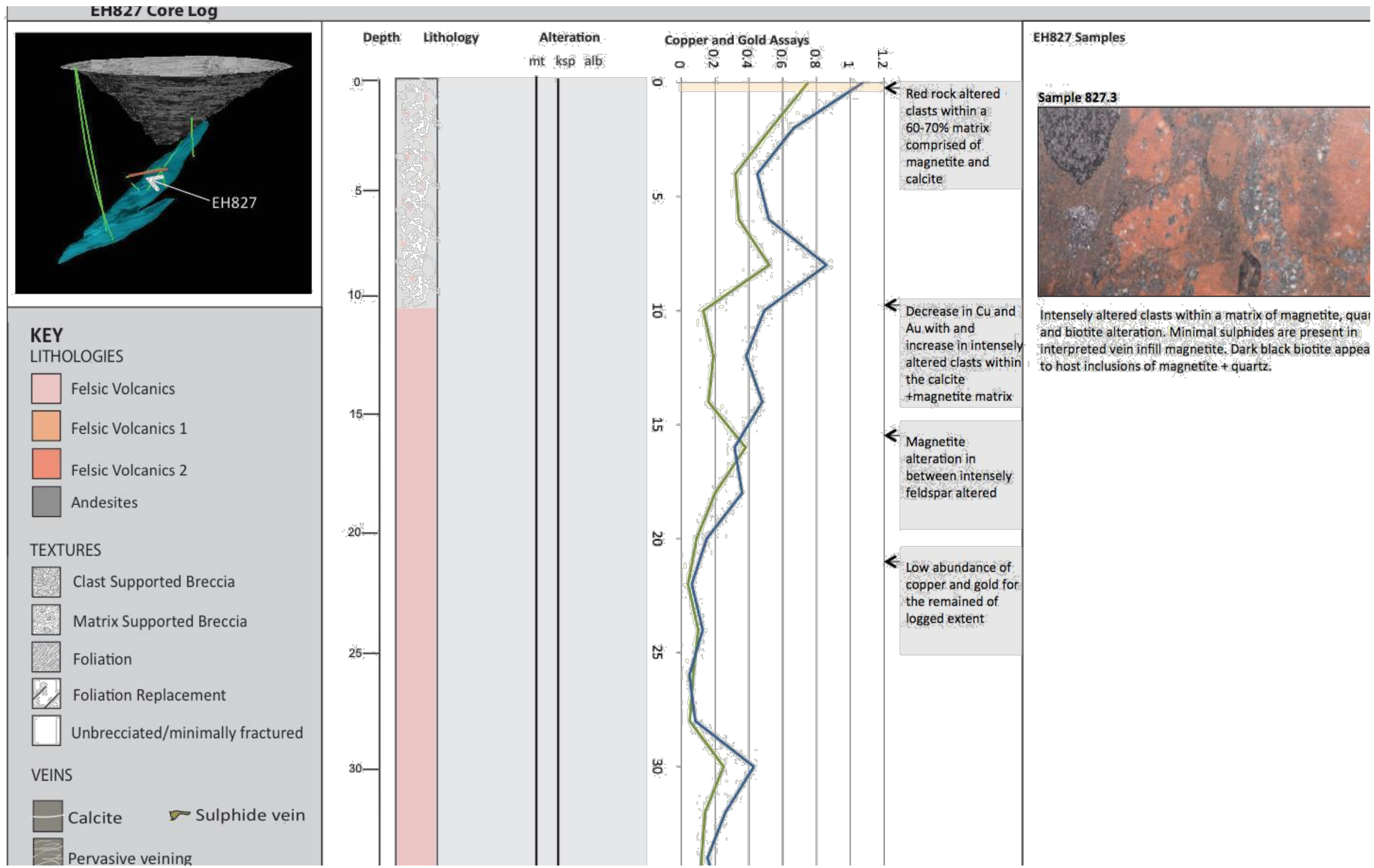

Figure 15. The correlation between lithology, alteration and enrichment of Cu and Au for drill hole EH827.

4.3 Paragenesis of mineralisation

The paragenesis of mineralisation within Ernie Junior, based on optical and SEM microscopy (Figure 19).

	Pre ore alteration			Ore phase	Ore phase outside breccia body	Post ore alteration
	Na(Ca) alteration + replacement	Mt + Biotite alteration	K-feldspar + hematite	Matrix supported	Vein hosted	Veining/retrograde metamorphism
	Dilation and brecciation					Brecciation and shearing ceases. Late stage veining and alteration
Albite	-------					
Magnetite		------------				
Biotite		--------------				-----
Quartz		--------------	--------------		---------	-------------------
K-feldspar			--------------			
Sericite						
Carbonate				----------	----------	--------------------
Pyrite				----------	----------	
Chalcopyrite				----------	----------	
Gold				----------	----------	
Chlorite						-------
Garnet						-------
Titanite				-----		
Barite				-----		

Figure 16. The paragenetic illustrating the sequence of the Ernie Junior mineralisation in relation alteration and structures events. Pre ore alteration includes albite and magnetite ± biotite alteration post shear zone formation. Following this, k-feldspar alteration ± hematite alteration occurs and is subject to brecciation through the ore phase, which in the matrix is comprised predominantly of carbonate, pyrite, chalcopyrite and gold. Distal expression of ore in veins away from the main ore breccia is observed to contain the same assemblage ± quartz. Cross-cutting quartz and calcite veining and alteration of biotite to chlorite also post-dates the ore phase.

4.4 Host Lithologies

Characterisation of host volcanics within the Ernie Junior ore body extent indicate that Ernie Junior host rocks are mineralogically and texturally consistent with the metavolcanic sequence that host Ernest Henry ore (Figure 3). They comprise variably altered intermediate volcanics. Key lithological observations within and around the ore body are documented below.

4.4.1 META-ANDESITES

Meta-andesites are present as a dark-grey porphyritic/non porphyritic volcanic rock comprised of albite, quartz, magnetite ± biotite). Orientated albite phenocrysts define a trachyte texture (Figure 19,c,d). Smaller albite crystals comprise ~80% of the matrix and are variably preserved due to overprinting by K-feldspar (Figure 19a). Variable stages of K-feldspar overprinting is expressed on a continuum from light pink phenocrysts in an unaltered matrix, to intense K-feldspar and hematite alteration in which phenocrysts are just detectable in hand specimen. Spatially, these rocks are preserved both within and outside the ore body and do not contain elevated Cu and Au (refer to drill hole logs figure Figure 11 to Figure 12).

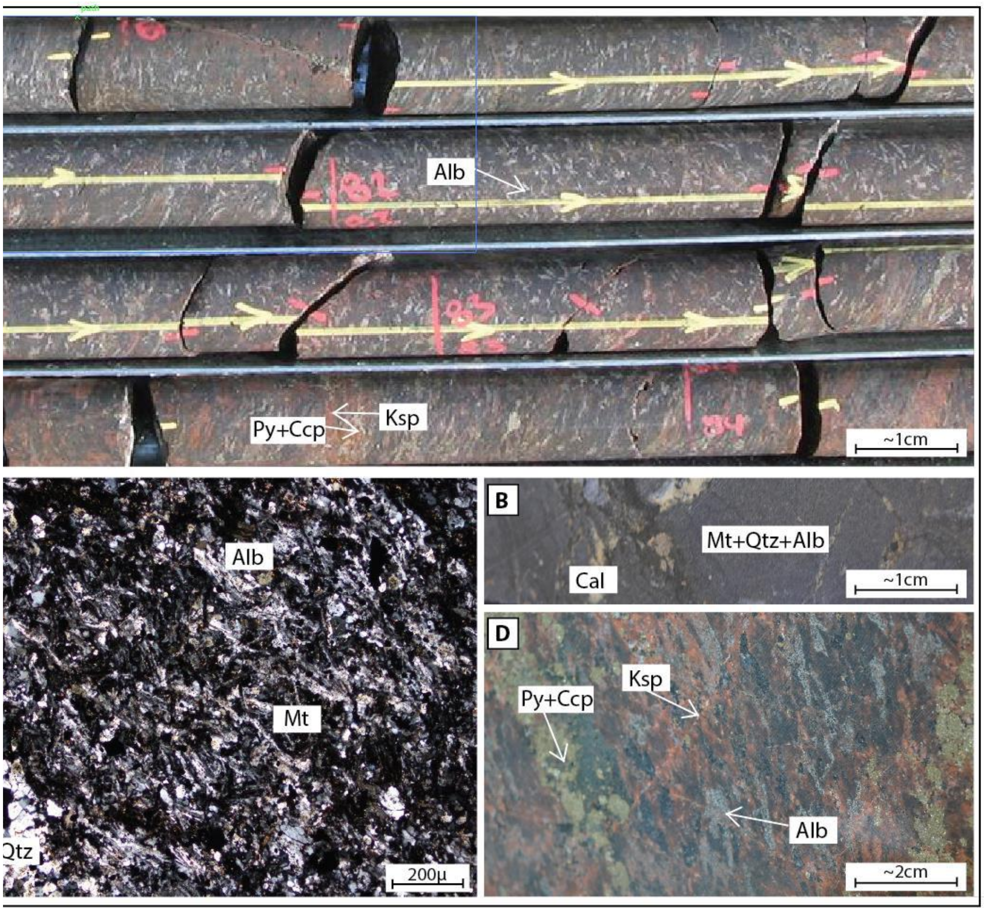

Figure 17. Representative images of meta-andesites in hand specimen and XPL microscopy a) Section of core from drill hole EH504, showing typical porphyritic section and variable overprinting by red k-feldspar and hematite b) Close up trachyte texture comprised of albite phenocrysts c) non-porphyritic andesite d) XPL image of the fine-grained groundmass meta-andesites, comprised albite, magnetite and quartz e) Foliated and unaltered andesite in close proximity to k-feldspar altered veining and subsequent sulphide infill.

4.4.2. FELSIC META-VOLCANICS

Brecciated and variably foliated felsic volcanics comprise the major rock type of the Ernie Junior ore body. These rocks are fine grained, k-feldspar and quartz rich volcanics that have been subject to intense alteration and brecciation (Figures Figure 11-Figure 16). Less pervasive alteration exhibits pink altered phenocrysts of albite, interpreted as remnant andesite texture. Both fracturing and brecciation is common within this lithotype.

Felsic volcanics comprise the majority of the ore bearing rock and are therefore further subdivided based on degree of brecciation and sulphide abundance:

Felsic Volcanics are Porphyritic/non-porhyritic massive to crackle veined volcanics Figure (Figure 20). Pyrite and chalcopyrite are minor components within the intensely K-feldspar + hematite lithotype. This lithotype is recognised by the EHM mine personnel as low-grade ore and waste rock (Internal report, EHM, 2009).

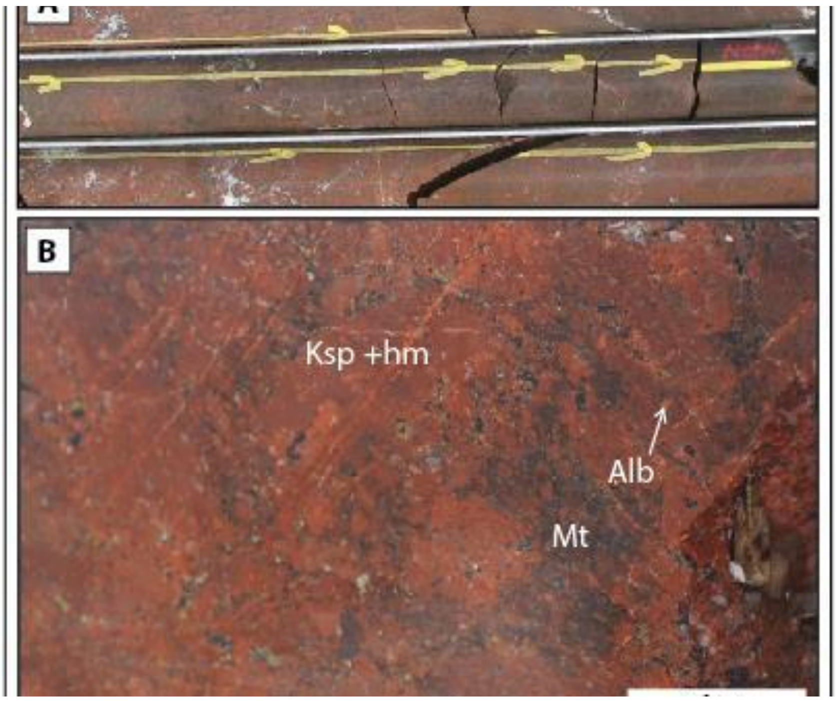

Figure 18. Representative hand specimens of Felsic Volcanics a) Core image from EH644 illustrating the massive texture of this lithology that exhibits magnetite alteration between more intensely altered sections b) Close up hand sample of the felsic volcanics illustrating a pre-breccia texture which is host to minor sulphides.

Felsic Volcanics 1 display tension vein and moderate brecciation (Figure 21). The FV1 (ref. Ernest Henry lithologies in Figure 3) unit within Ernie Junior is comprised of small (up to 10mm) carbonate veins within a red rock altered matrix. This texture, recognised as a sub-parallel feature to shearing within the Ernest Henry ore body (Taylor, 2009) is observed towards the south east of the Ernie Junior ore body within drill holes EH644 and EH777.

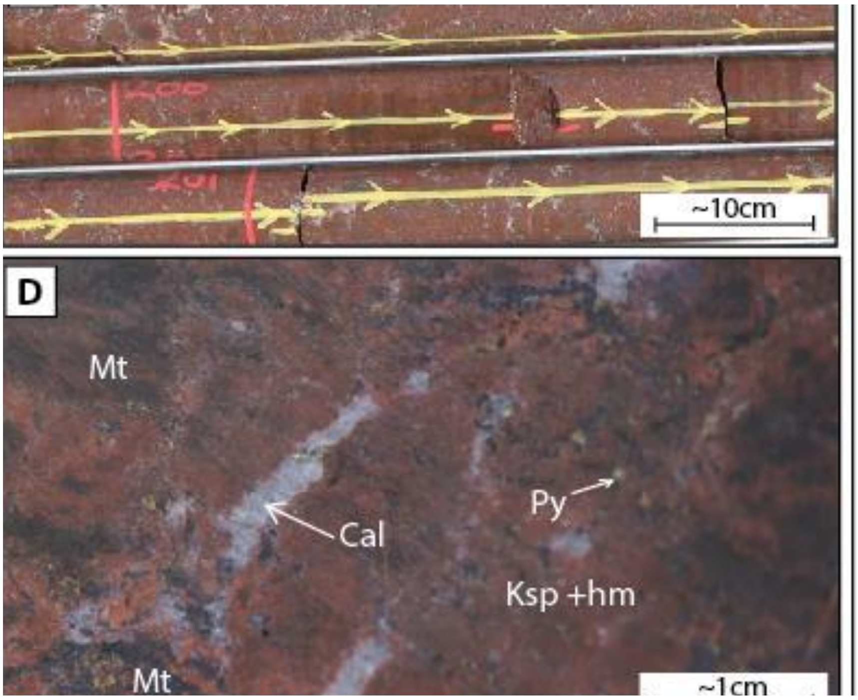

Figure 19. Representative FV1 tension veining a) 'seagull' veining of calcite in a variably but pervasively altered magnetite and k-feldspar matrix b) the same texture, but with a higher magnetite component, illustrating a variable overprint of magnetite alteration.

Felsic volcanics 2 are comprised of FV clasts within a matrix of calcite +/- magnetite +/- pyrite +/- chalcopyrite +/- biotite +/- chlorite and are distinguished from the other two felsic volcanics by a more matrix supported nature (Figure 25). This lithology is observed as a minor component of the drill core studied. Within Ernie Junior, both mineralised and non-mineralised matrix supported breccias are observed. This differs from the matrix supported breccias that comprise the high grade ore zone within Ernest Henry.

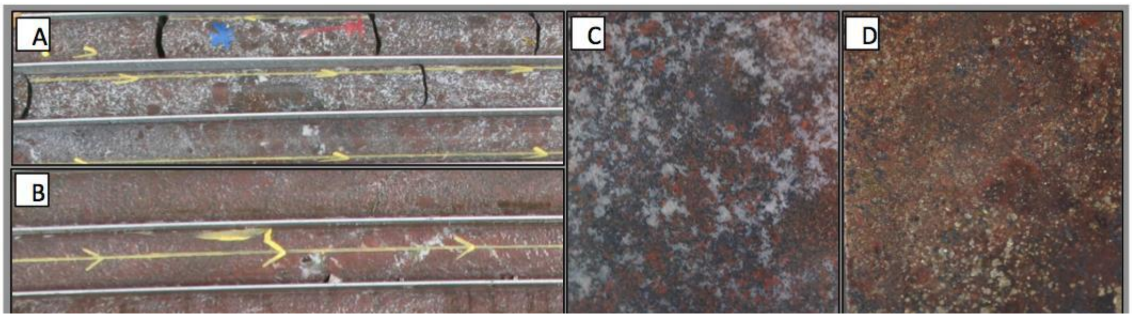

Figure 20. FV2 lithology characterised by development of a higher matrix component a) Illustrates FV2 in drill core, where the matrix is comprised of calcite and magnetite b) Illustrates a less developed FV2 matrix also comprised of calcite and magnetite c) Hand specimen sample of FV2 illustrating an unmineralised matrix supported breccia d) Mineralised sample of FV2 illustrating disseminated sulphides throughout the matrix of the drill core.

4.4.4 Meta-intermediate volcanics

Massive unit, with moderate-strong foliation defined by biotite and magnetite is observed outside the K-feldspar and andesite lithologies, in proximity to the FWSZ. This un-mineralised unit is comprised of magnetite, biotite, and variably garnet rich veining that indicates abrupt transition laterally into non-foliated andesites.

Spatially, this lithology occurs to the South East of the Ernie Junior ore body and is not associated with ore mineralogy as indicated in drill core logs (Figure 24).

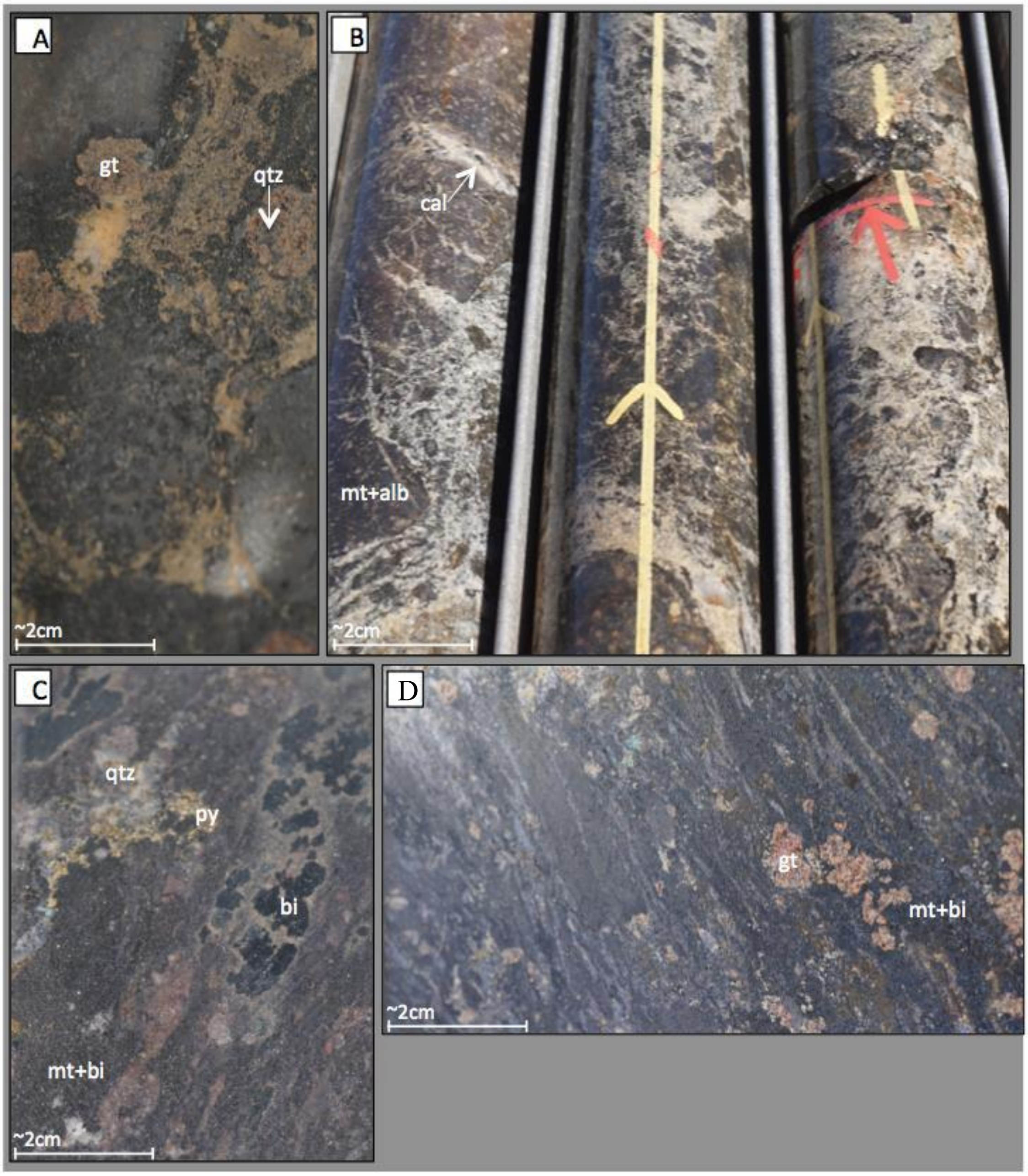

Figure 21. Core specimens of intermediate-mafic volcanics observed outside the extent of Ernie Junior mineralisation a) Garnet with inclusions of quartz associated with magnetite alteration around a calcite vein, b) Pervasive carbonate wash in between highly altered clasts of porphyritic intermediate volcanics, c) biotite aggregates with an unidentified halo d) foliated magnetite and biotite with garnet veining.

4.5. Alteration and veining

The Ernie Junior ore body has undergone three distinct styles of alteration (Figure 24), and displays a complex history of alteration, producing 1) albite, 2a) magnetite ± biotite,

3) K-feldspar volcanic host rocks. Minor chlorite and sericitic alteration is also observed within Ernie Junior. Core logging has indicated that K-feldspar +/- hematite is associated with, but not confined to, the main ore phase of Ernie Junior. Earlier phases of alteration exist outside the dominant ore-bearing zone that is defined by K-feldspar alteration.

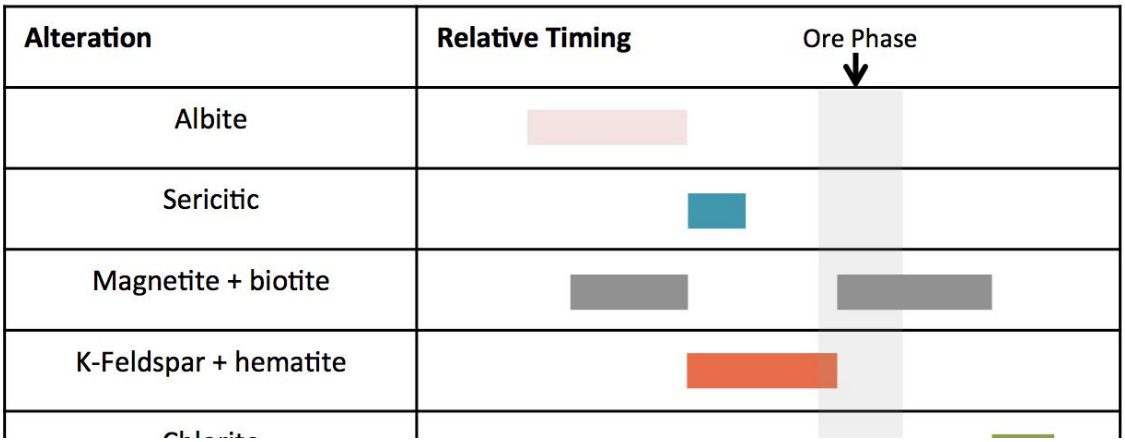

Figure 22. Relative timing of alteration in relation to the ore-bearing phase. Early albite, sericite and magnetite +/- biotite alteration is preserved outside the ore zone. The ore phase is mainly associated with brecciation of red rock altered rocks. Chlorite is observed as an alteration product after the second stage magnetite +/- biotite alteration as a minor phase that is also more present outside the ore bearing red rock altered breccias.

4.4.1 STAGE 1- ALBITE ALTERATION

Albite alteration is observed as the albitisation of plagioclase phenocrysts and groundmass crystals within trachyandesites. Representative samples of the styles of albite alteration are summarised in Figure 25, with the overprinting of this alteration by K-feldspar alteration illustrated inFigure Error! Main Document Only.

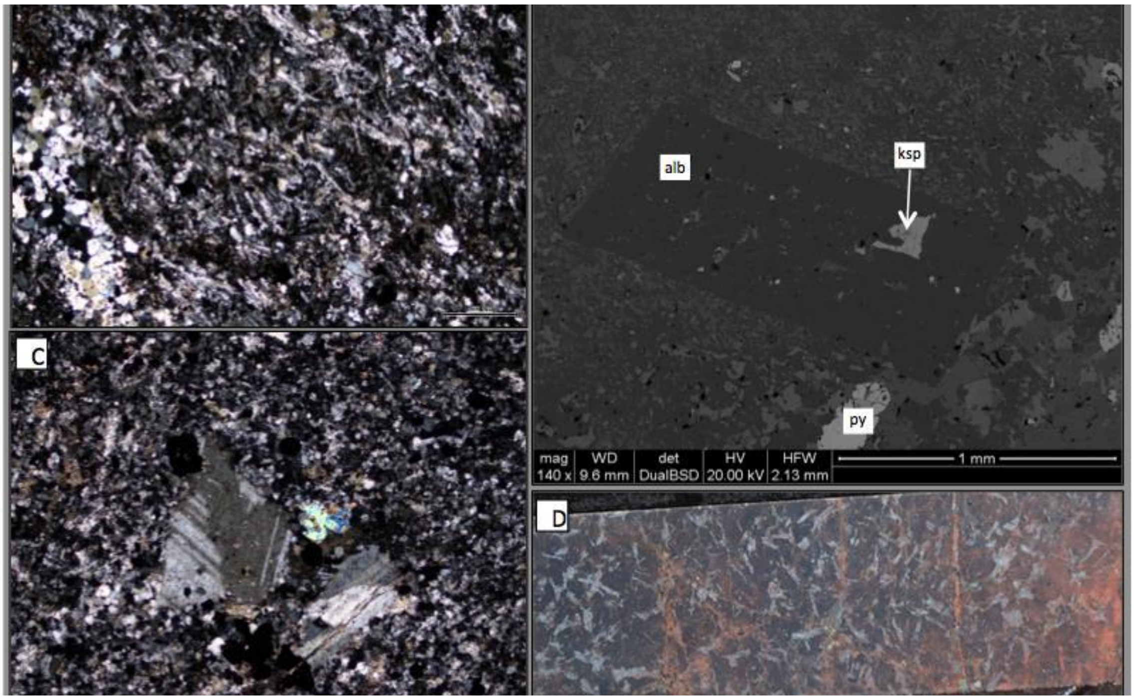

Figure 23. a) Sample EH738.2 illustrating a typical trachytic texture, preserving the earliest alteration preserved in immediate host sequence to Ernie Junior b) SEM image illustrating a sodic-feldspar interpreted to be albite. Inclusions within the phenocryst indicate some textural destruction of albite c) Sample EH 779.2 illustrating destruction of the edges of albite phenocrysts d) gradient k-feldspar overprinting of trachyandesites by fabric destructive k-feldspar alteration.

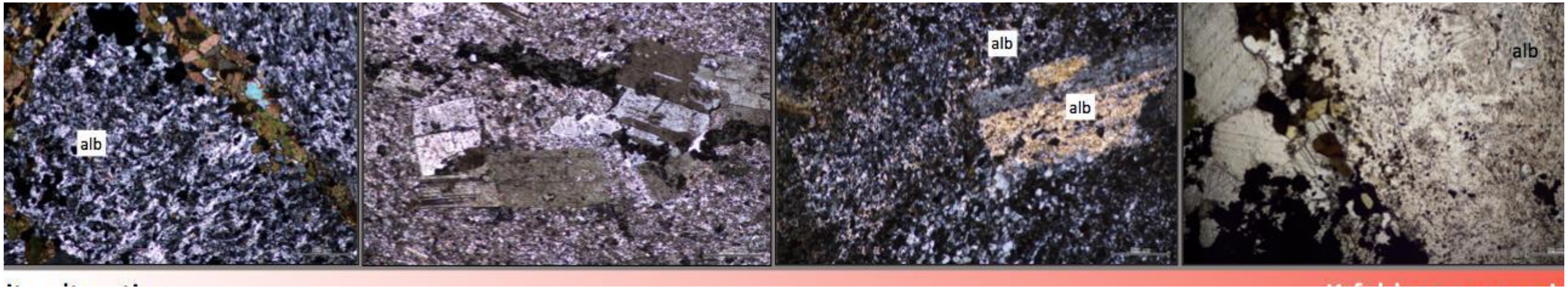

Figure 24. **Illustrating the preservation of host rock trachyandesites and subsequent overprinting. The earliest stage of these volcanics is preserved as a fine-grained groundmass of randomly oriented albite altered as the result of early Na-Ca alteration of plagioclase. Large albite phenocrysts are more resistant to k-feldspar alteration and are preserved or pseudomorphed with further alteration a) Original trachyte texture comprised predominantly of albite as an alteration feature b) Sample 504.4 Albite phenocrysts being overprinted by magnetite +/- biotite alteration. Some albite still evident in the groundmass c) Sample 504.1, Preservation of the host rock occurs as clasts in weakly-moderately k-feldspar + hematite alteration zones. Phenocrysts are preserved yet the groundmass has little remaining albite texture d) Sample 504.3, Remnant phenocryst within a k-feldspar dominated matrix, no evidence of original andesite groundmass.**

4.4.2 STAGE 2-MAGNETITE ± BIOTITE ALTERATION

Magnetite and biotite alteration is abundant outside Ernie Junior in proximity to the FWSZ and throughout the ore body where not overprinted by further K-feldspar related alteration. Magnetite and biotite occur variably as individual crystals or as foliated aggregates within both the felsic volcanic centre of the ore body and within the bounding footwall shear zone. Within the biotite schist, biotite occurs as elongate foliated round lenses from 4-60mm in length. Magnetite is pervasive as an early alteration product and as infill in anhedral aggregates (Figure 26).

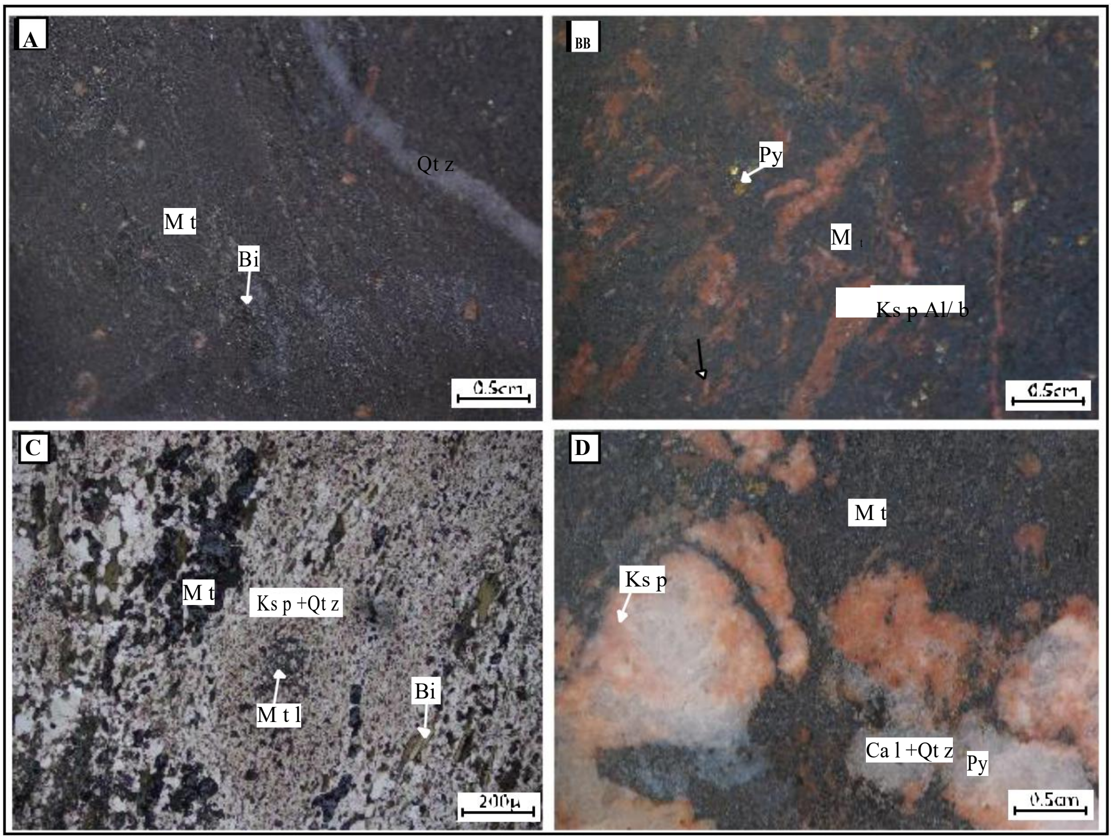

Figure 25. Intense magnetite alteration outside of the ore breccia host to Ernie Junior a) intense magnetite and biotite alteration of what is interpreted to a porphyritic intermediate volcanic b) intense groundmass alteration of magnetite within a porphyritic volcanic. K-feldspar alteration has altered the phenocrysts in this sample to a pinky-red colour c) photomicrograph of sample EH777.3 illustrating intense alteration within the centre of a pre-existing clast of intermediate volcanics which has been nearly entirely overprinted by K-feldspar alteration d) Intense magnetite groundmass alteration showing the same relationships observed in ‘b’ except in this hand specimen, K-feldspar alteration has not completely overprinted the calcite veins present, but has instead just altered the edges.

4.4.3 STAGE 2B- SERICITIC ALTERATION (PRESERVED OUTSIDE ERNIE JUNIOR)

Sericite is observed as a minor alteration phase, observed in association with albite phenocrysts, destructively replacing the crystal faces and interiors (Figure 27). Minor pyrite is also observed within this alteration phase.

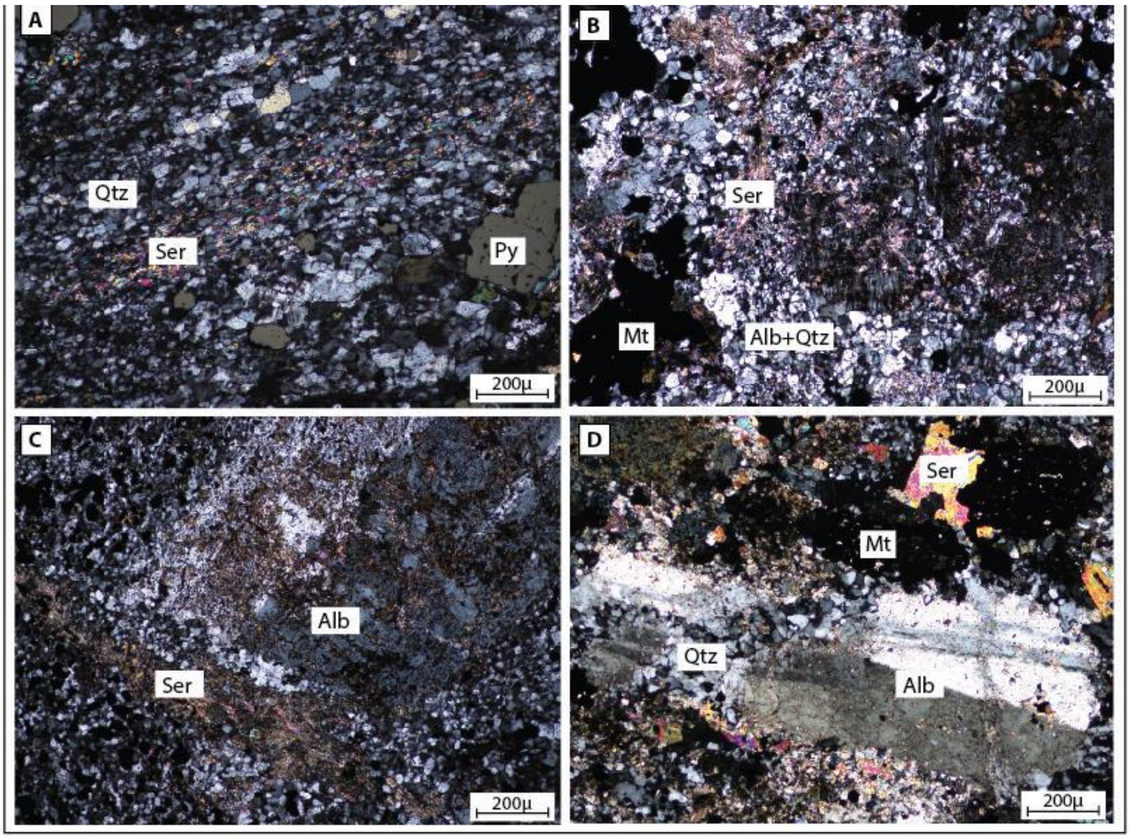

Figure 26. Sericitic destructively alterating albite. a) Sample EH690.2 illustrating sericite alteration within a fine-grained matrix of albite and quartz b) Sample EH644.4 seriticitic alteration of both the matrix and phenocyst of a magnetite altered andesite c) Sample EH504.4 very fine grained sericitis alteration illustrating its destruction of the interior of an albite phenocryst d) Sample EH728.c medium-grained sericite at the edges of an albite phenocryst.

4.4.4. STAGE-3 K-FELDSPAR RICH ALTERATION ± HEMATITE

K-feldspar rich alterationlteration (K-feldspar with hematite dusting) represents the intense overprinting of magnetite +/- biotite alteration and albite bearing andesites. This alteration ranges from pink to intense brick red within Ernie Junior and defines the felsic volcanic lithologies (Figure 28). This alteration correlated strongly to the presence of elevated copper and gold, indicated by drill logs in Figure 11 to Figure 30 displays the intensity and distribution of this alteration.

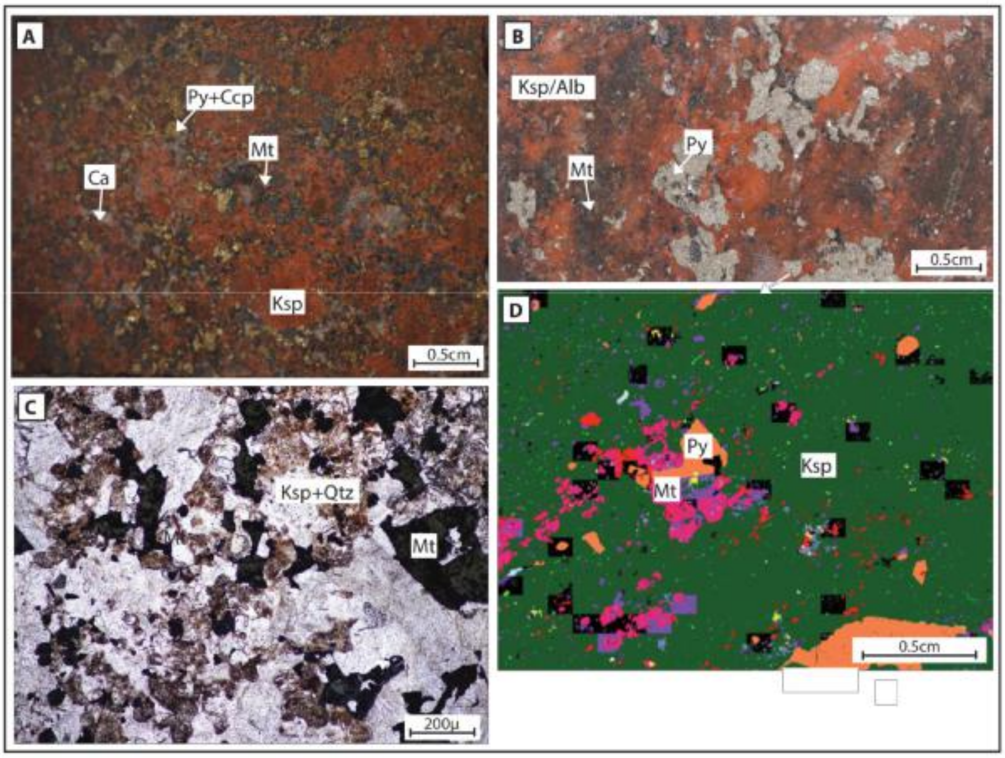

Figure 27. Hand sample, photomicrograph and MLA images illustrating the intense nature of k-feldspar rich alteration a) Hand specimen illustrating a clast supported breccia with stage 3 altered clasts b) sample EH644.2 Illustrating an increased brightness where the red is altering a previous vein texture c) Sample EH504.3 photomicrography of intense K-feldspar alteration of quartz crystals d) MLA image illustrating k-feldspar in green and how pervasive this alteration is through the volcanics.

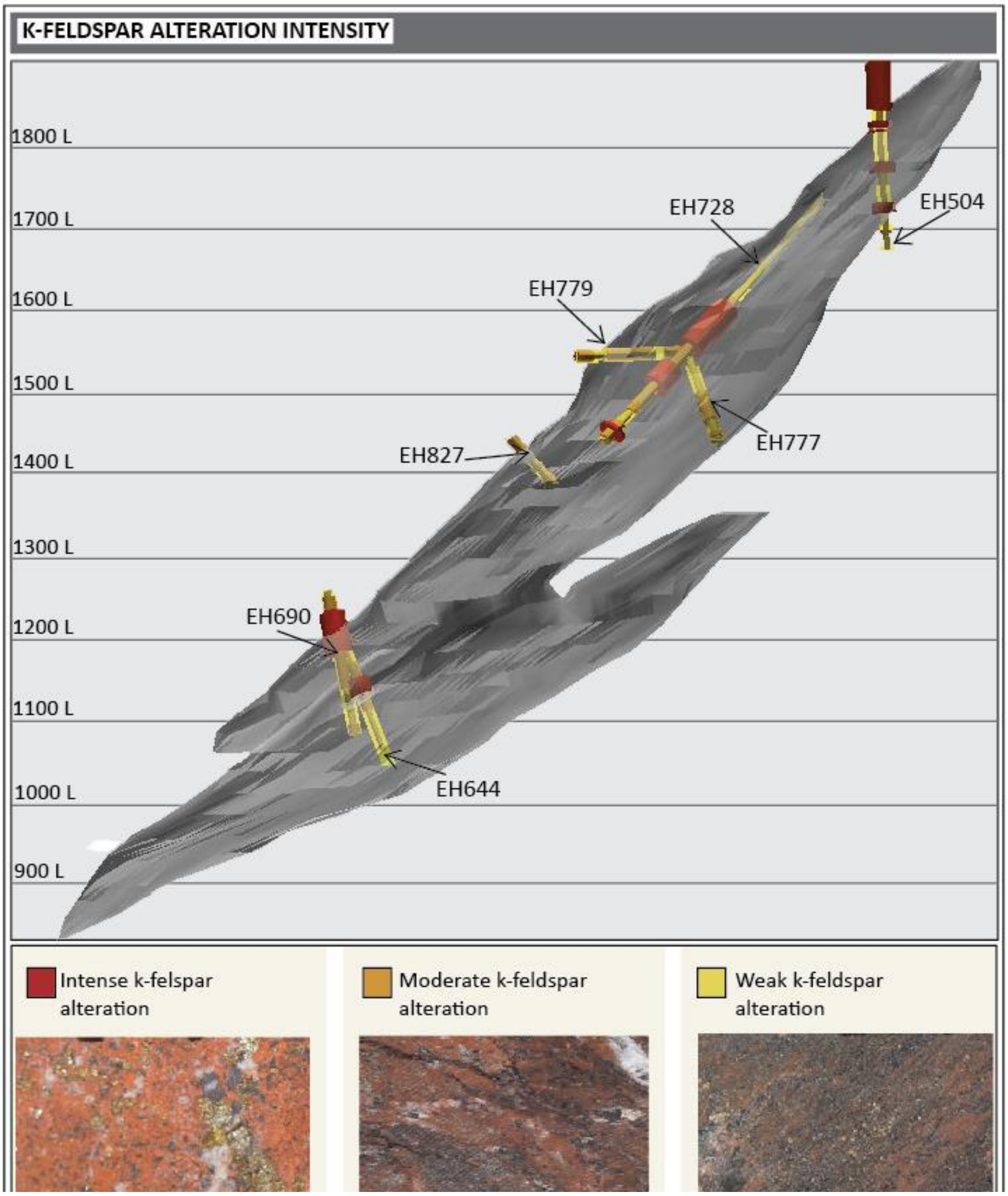

Figure 28. K-feldspar intensity and distribution through Ernie Junior ore body. Indicating that while red rock alteration is associated with a higher copper and gold content and is variable across the ore body.

4.4.5 STAGE 4- CHLORITE ALTERATION

Chlorite alteration is a minor phase, present in felsic sections of the ore body and in veins that bear the ore phase mineralogy of pyrite and chalcopyrite (Figure 30c). Its presence is indicative of a retrograde association. Chlorite is commonly observed as the alteration product after biotite (Figure 30f) and varies in intensity from partial replacement of biotite grains, to vein hosted chlorite masses (<1mm in width) (Figure 30a,c). Alteration is to some extent, controlled by existing grain size, (Figure 30d) and is abundant throughout samples 779.2 and 728.c.

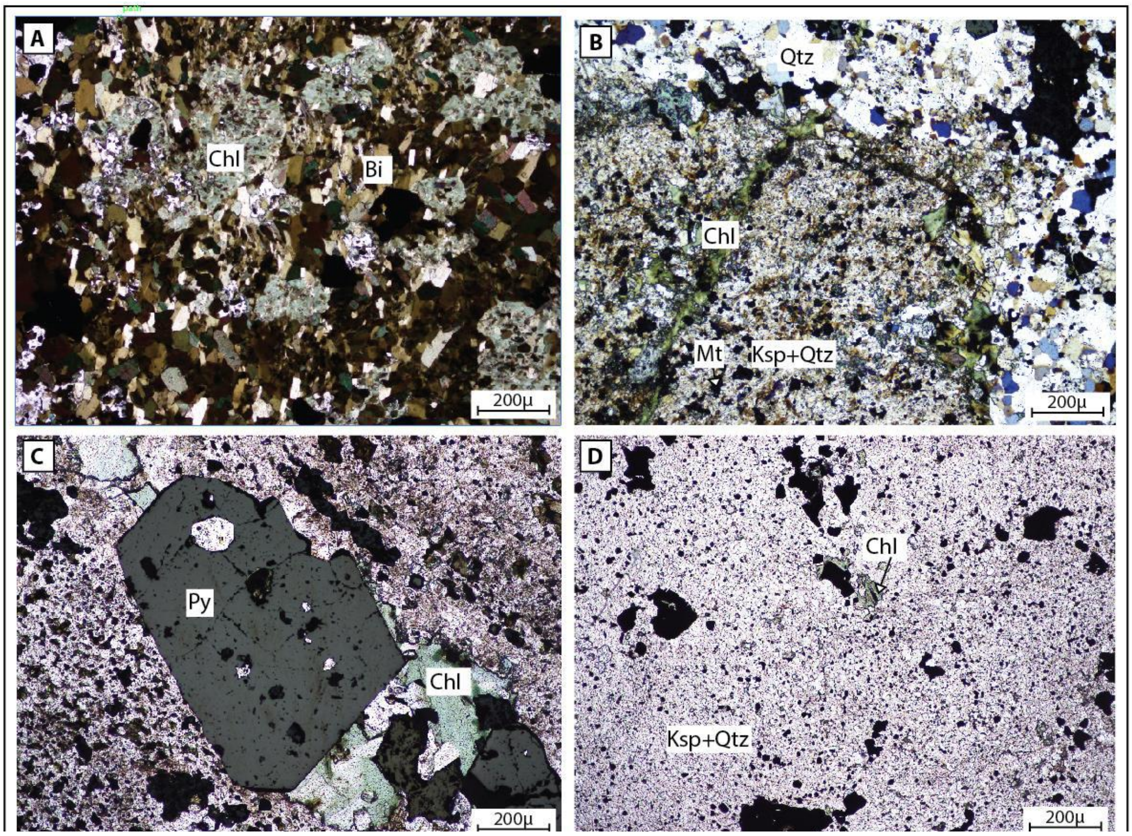

Figure 29. Illustrating late alteration of biotite by chlorite in different styles within the ore body, a) Sample EH Illustrating the alteration of biotite to chlorite b) Veins of chlorite cross-cutting a felsic volcanic clast with remnant plagioclase textures c) Chlorite replacement of infill biotite in a calcite vein, d) Common occurrence of biotite in felsic volcanics, as rare occurrence, spatially associated with magnetite within a K-feldspar and quartz matrix.

4.4.6 VEINING

Calcite veining in Ernie Junior is present as breccia infill, cross-cutting veins (Figure 31a,c,d,e,f,g), 'tension' style veining and a carbonate wash. Calcite dominates breccia infill where it has not been subsequently replaced by magnetite, pyrite, chalcopyrite, biotite ± barite ± titanite. Cross-cutting calcite veins are evident in un-brecciated volcanics with both K-feldspar and magnetite ± biotite alteration (Figure 31f) but are rarely observed to intersect ore breccias.

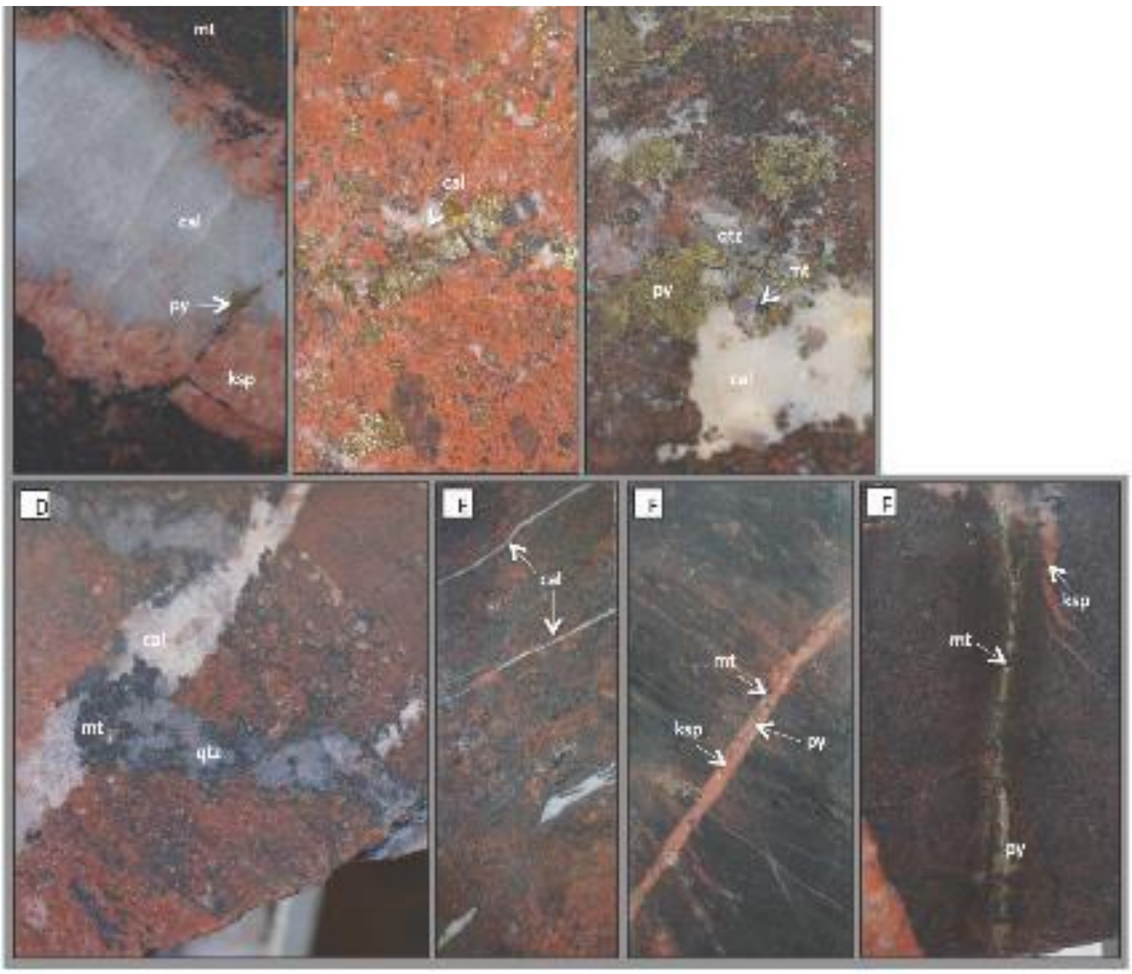

Figure 30. Vein styles across the Ernie Junior ore body. a) cross-cutting calcite vein in highly magnetite altered host rock. K-feldspar alteration at the edges indicating a second flux of fluid through the vein, b) pre-breccia style veining with infill of pyrite, chalcopyrite, calcite and quartz, c) medium veins of quartz + calcite, hosting ore phase mineralisation, d) offsetting calcite and quartz veins with infill of magnetite e) representative sample of fine-grained calcite veining which does not display infill mineralisation f) K-feldspar alteration of a vein and subsequent infill of the ore phase. K-feldspar alteration permeates out of the vein into the surrounding volcanics.

4.4.7 Quartz Veining

Quartz veining occurs as fine-coarse randomly oriented veins that crosscut the mineralisation assemblage (Figure 31d), or as discontinuous aggregates of interlocking, mosaic grains with calcite (Figure 31c). Quartz is also present as inclusions in garnet within the metasediments/mafic FWSZ lithology. This minor veining style not associated with the ore phase.

4.5. Ore minerals and associations

The ore phase of Ernie Junior comprises chalcopyrite, pyrite, magnetite and calcite ± titanite ± barite as infill within breccias and veins in the following paragenetic sequence:

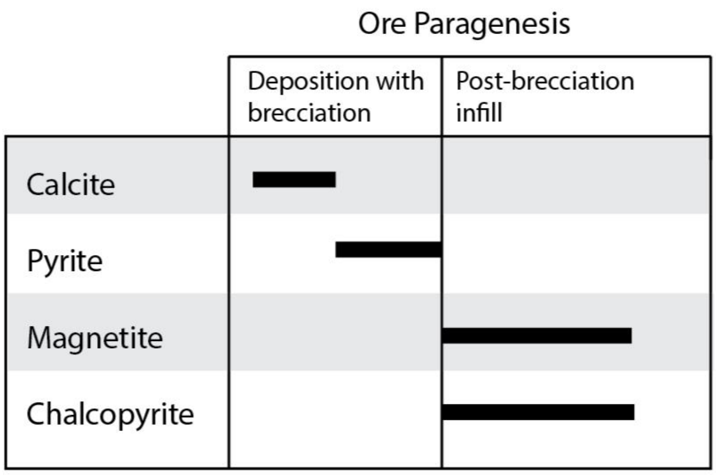

Figure 31. Paragenetic sequence of ore deposition involving veins and matrix components. Calcite forms selvedges most predominantly in felsic volcanic lithologies. Pyrite infills and fractures, providing subsequent space for infill magnetite and chalcopyrite.

Copper within Ernie Junior is present as anhedral grains of chalcopyrite. Chalcopyrite as infill exhibits finer grains than in veins (Figure 33). Chalcopyrite is highly associated with pyrite and magnetite; the three nearly always coexisting except where the ore phase is replacing a fine-grained assemblage in a breccia matrix. Where not associated with pyrite, chalcopyrite occurs as small grains in the matrix of predominantly felsic volcanics in association with magnetite, though minor amounts are hosted within stage 2- magnetite and biotite altered rocks.

Pyrite is strongly associated with chalcopyrite and exists as euhedral-anhedral grains ranging from fine-grained in matrix and medium-large grains within veins Figure 33. Pyrite in Ernie Junior displays variable fracturing with most exhibiting minimal-extreme fracturing (most common and as infill veining) suggesting movement post-deposition. Fractures in pyrite provide infill space for chalcopyrite and other minerals Figure 33. Vein-hosted pyrite grains are up to 4mm across. Non-foliated samples lack the fracturing in pyrite seen in foliated samples.

Gold was not observed under petrographic and SEM analysis .The presence of gold within the drill core studied was determined via assays from the EHM database. Refer to drill logs (Figure 11 to).

4.6. Ernie Junior Ore Styles

Two styles of ore deposition are recognised within Ernie Junior, each comprising an assemblage of chalcopyrite in association with pyrite, magnetite, calcite, +/- biotite +/- chlorite. Chalcopyrite mineralisation occurs 1) matrix hosted- within brecciated felsic volcanics 2) vein hosted- as replacement of late stage calcite +/- quartz veins that crosscut all other textures. Textural variation in ore deposition is shown in Figure 8. Comparable assemblages and lack of cross-cutting ore styles indicate that their deposition is synchronous.

4.6.1 Matrix hosted

Breccia hosted ore occurs almost exclusively within the felsic volcanic lithotypes. Brecciation of felsic volcanic clasts is infilled with an assemblage of calcite, chalcopyrite, pyrite and magnetite with lesser quartz, biotite and titanate.

4.6.2 Vein Hosted

Vein-hosted ore is observed as an ore phase that exists outside the breccia extents. Present in more competent volcanics irrespective of host rock alteration. 1cm-10cm calcite veins host chalcopyrite, and pyrite as larger grains than is observed in matrix breccias (Figure 33 a,c,e).

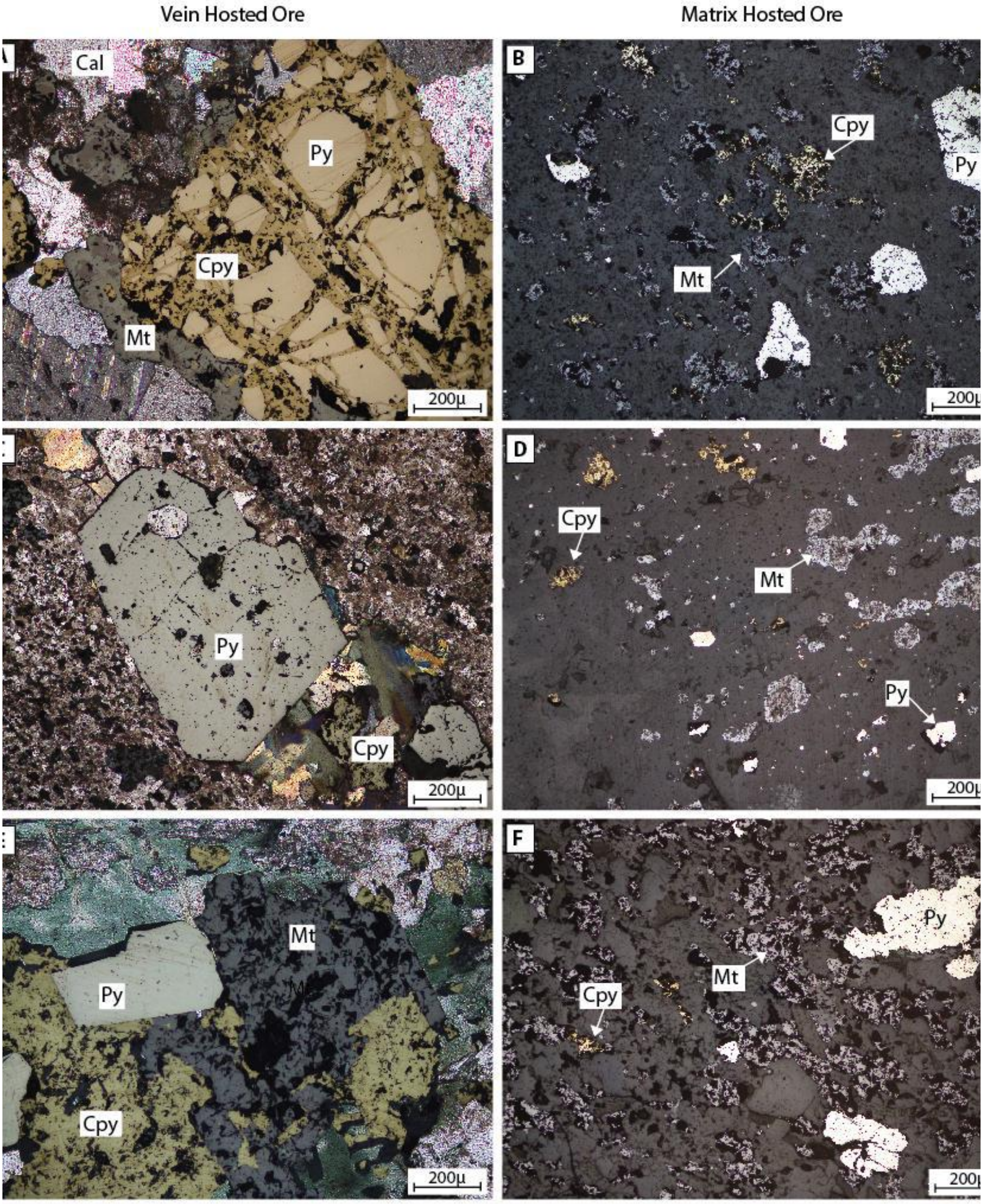

Figure 32. Photomicrographs of vein and matrix hosted ore phases illustrating the difference between the two styles of ore deposition. a) Sample 504.4 under XP and reflected light illustrating vein hosted chalcopyrite in-filling around a fractured grain of pyrite. b) Sample 644.3 under reflected light illustrating matrix hosted anhedral grains of chalcopyrite, exhibiting smaller crystal sizes compared with vein hosted crystals and a close association with magnetite. In comparison to a and c, matrix hosted pyrite displays a lesser degree of fracturing. c) Sample 644.2 under XP and reflected light illustrating micro-fracturing in pyrite and infill chalcopyrite within a carbonate vein. d) Sample 728.C under reflected light illustrating fine-grained chalcopyrite in a k-feldspar matrix. e) Sample 777.3 under XP and reflected light illustrating the close association of magnetite and chalcopyrite in vein-hosted ore. Unlike a and c, Pyrite in this sample is not fractured.

4.7. Accessory Mineralogy

SEM analysis indicates the presence of matrix supported barite and titanite as part of the infill assemblages. While titanite appears to be suspended in the k-feldspar matrix, barite is observed as late stage veining (Figure 34a) and infill (Figure 34c,d). Textural associations indicate that they are present as matrix hosted (Figure 35).

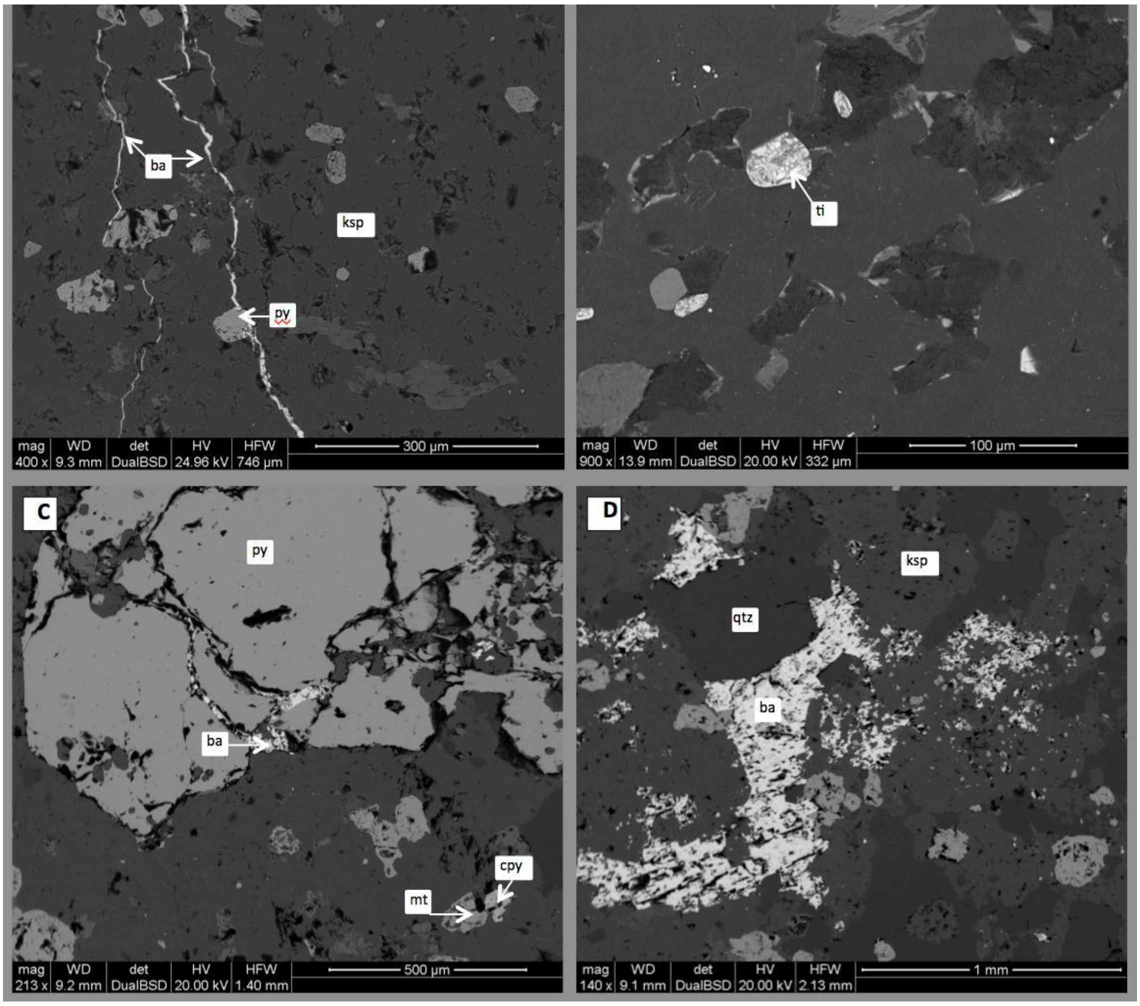

Figure 33. Ernie Junior accessory phase minerals like Ernest Henry, the Ernie Junior ore body is rich in late stage barite (as in Mark et al, 2006) and titanite as lesser phases that comprise the ore body's geochemical signature a) Sample 504-1 late stage fine barite veining within the matrix of k-feldspar at b) Sample 728.c displaying titanite grain and k- feldspar with unidentified alteration edges c) Sample 728.c displaying fractured barite infilling fractures in pyrite d) Sample 728.c displaying large fractured barite grain with disseminations through the quartz and k-feldspar matrix.

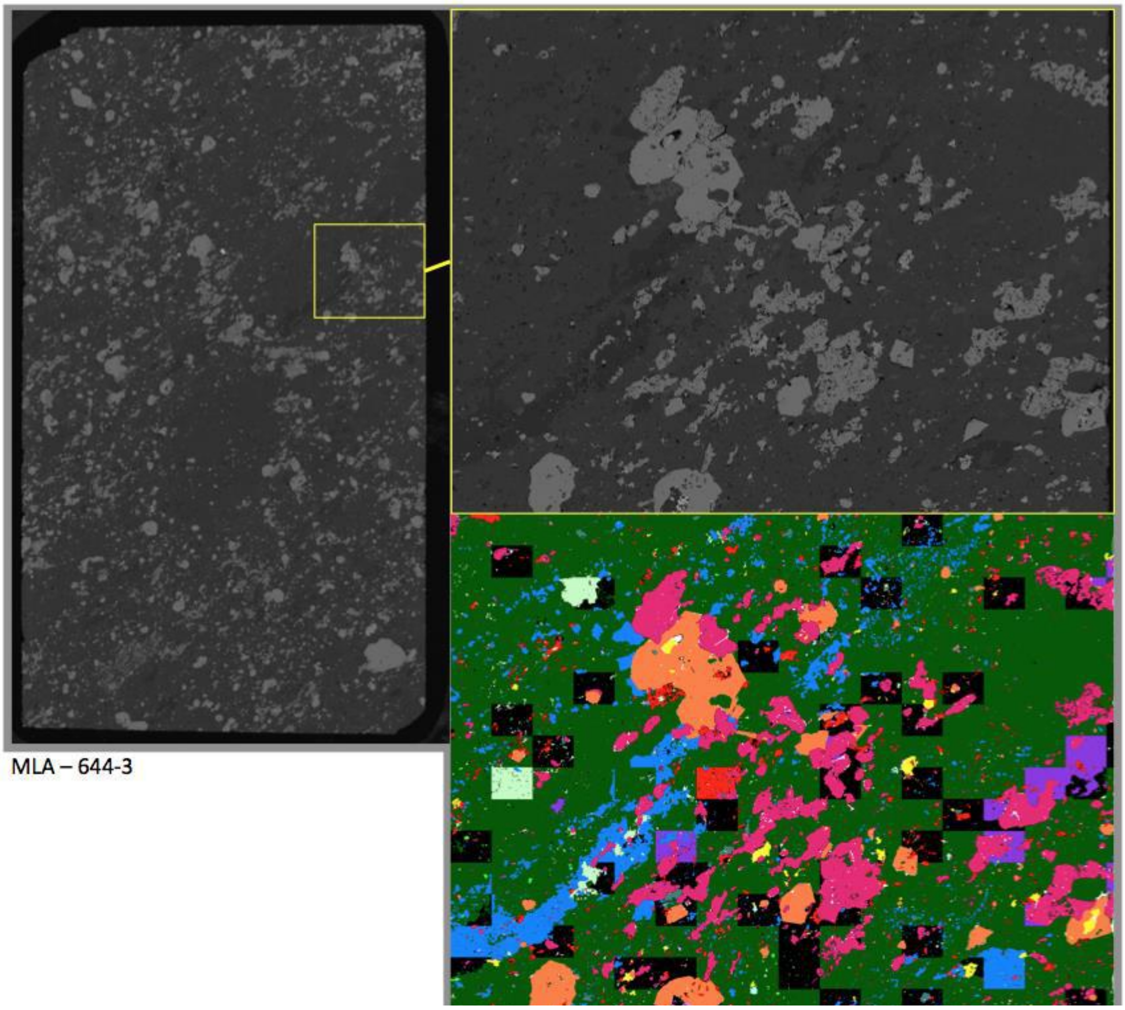

Figure 34. Spatial association of accessory titantie within the matrix of a clast supported breccia. Titanite (bright green) is finely distributed in the matrix of sample 644.3.

4.8. Textural variation and structural control

4.8.1 BRECCIA TEXTURES AND VARIATION

Ernie Junior exhibits variable textures both within the felsic volcanic and dark rock altered lithologies, evident of brecciation (Figure 36a-e) and shearing (Figure 36 f). SEM and MLA analysis provides further distinction between quartz and K-feldspar (Figure 36e and f).

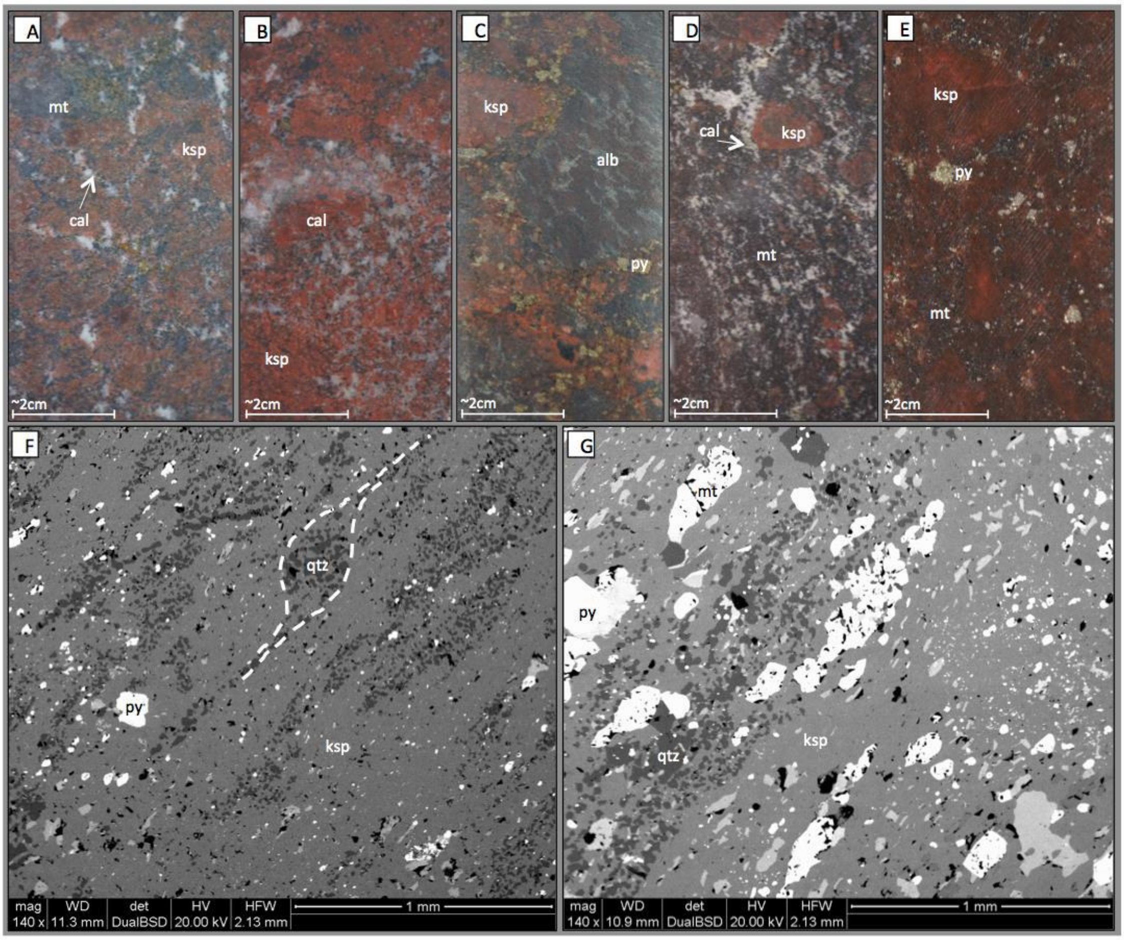

Figure 35. Illustrating breccia styles across the ore body. a) Felsic volcanic 1, dark rock altered matrix with calcite veining also present b) Clast supported breccia without sulphides c) Phenocryst rich clasts within a highly hematite dusted matrix of felsic volcanic clasts sulphides are confined to the matrix. d) Matrix supported breccia, with pervasive red rock alteration of clasts 3-15 mm in size. Matrix comprised of calcite veining and dark rock alteration. e) Clast supported breccia with magnetite and pyrite infill f) shear texture observed within a fractured quartz vein g) alignment of magnetite and quartz within moderate foliation with a background matrix of K-feldspar.

g

The most common texture within the felsic volcanic ore dominated zone, is a clast-supported breccia comprised of subangular-rounded clasts suspended in a matrix of calcite +/- magnetite +/- biotite +/- pyrite +/- chalcopyrite. Clasts exhibit very fine-grained equigranular mosaic textures. Only minor matrix supported brecciation is recognised. Clast sizes range from 2mm to 20cm across and are rounded-angular in nature (Figure 36d,e). Red rock altered breccias contain calcite, magnetite, pyrite and chalcopyrite whereas magnetite alteration dominated breccias display this same infill except with rare pyrite + chalcopyrite.

4.8.2 Structural controls

Ernie Junior is situated between the FWSZ that bounds its lower extent and carbonate vein rich altered andesites within its upper extent. Foliation and vein orientations were measured and presented in stereonets for drill holes that had survey information available and were oriented. These orientations are compared with existing FWSZ structural measurements carried out by Tywerould, 1997 and the Interlens (O'Brien, 2016) (Figure 38). Results indicate a variable but general trend in dip between the SE-E consistent with both the FWSZ and the Interlens Shear Zone. Dips display variation from shallow to sub-vertical (10 -88 degrees). Vein data, though limited, does not appear to follow a consistent trend. For a complete list of measurements refer to Appendix D.

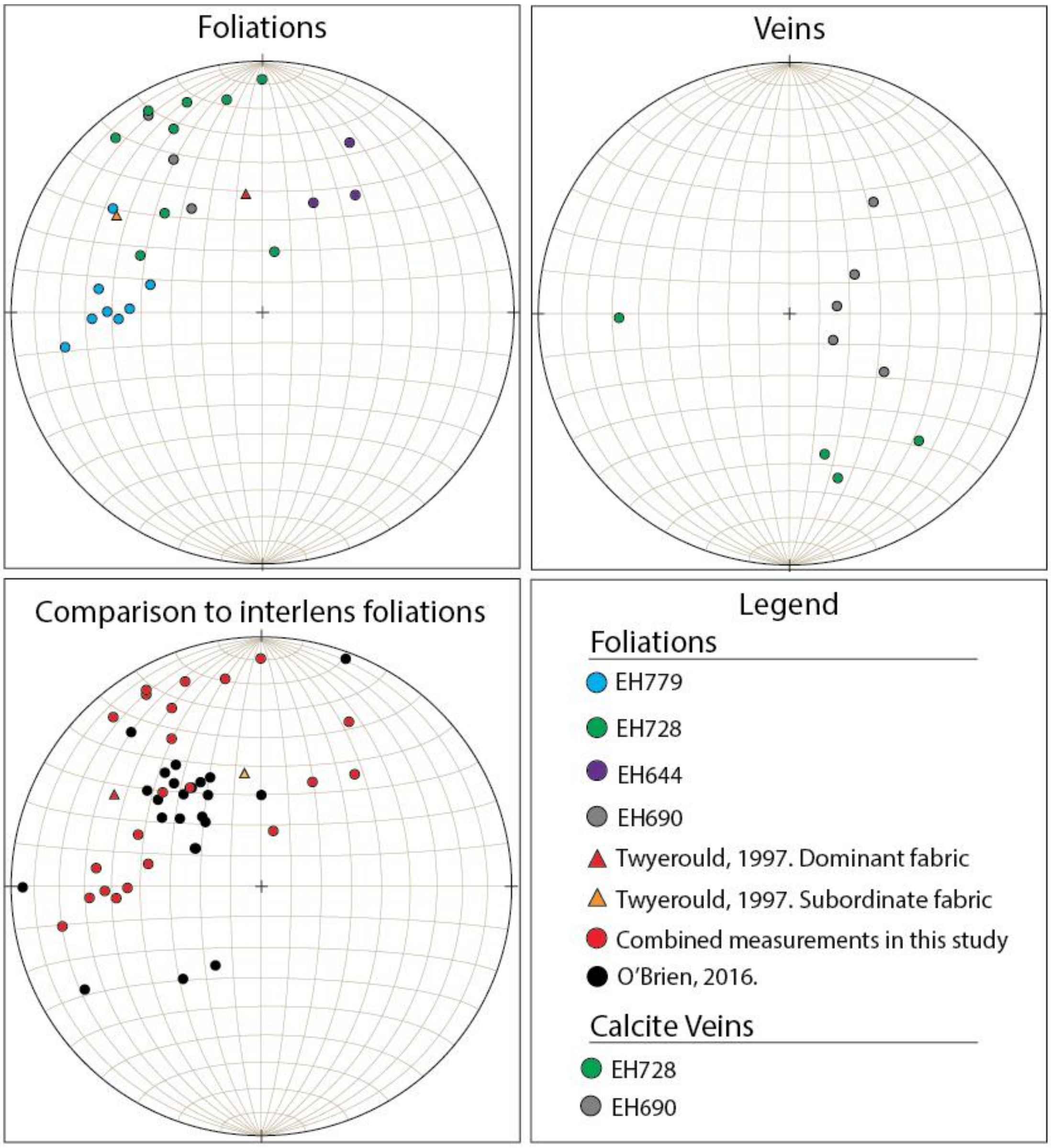

Figure 36. Structural measurements of foliation and veins, plotted as poles to planes, with comparisons to the footwall shear zone and Interlens shear zones. Comparisons illustrate a common SE trending dip. Variation is present between drill holes EH728 and EH690 dip to the SE, EH644 dips more to the East and EH644 trending more the SW.

Spatial distribution of structural textures was logged and displayed in 3D using Vulcan. Distributions in Figure 39 highlights vertical textural change throughout the ore from predominantly foliations/replacement textures of foliations at the bottom bounds of mineralisation, to clast and matrix supported breccias in the central area, leading to tension veining in more massive units towards the top extent of the ore body. This may account for the variation in foliation textures as discussed above.

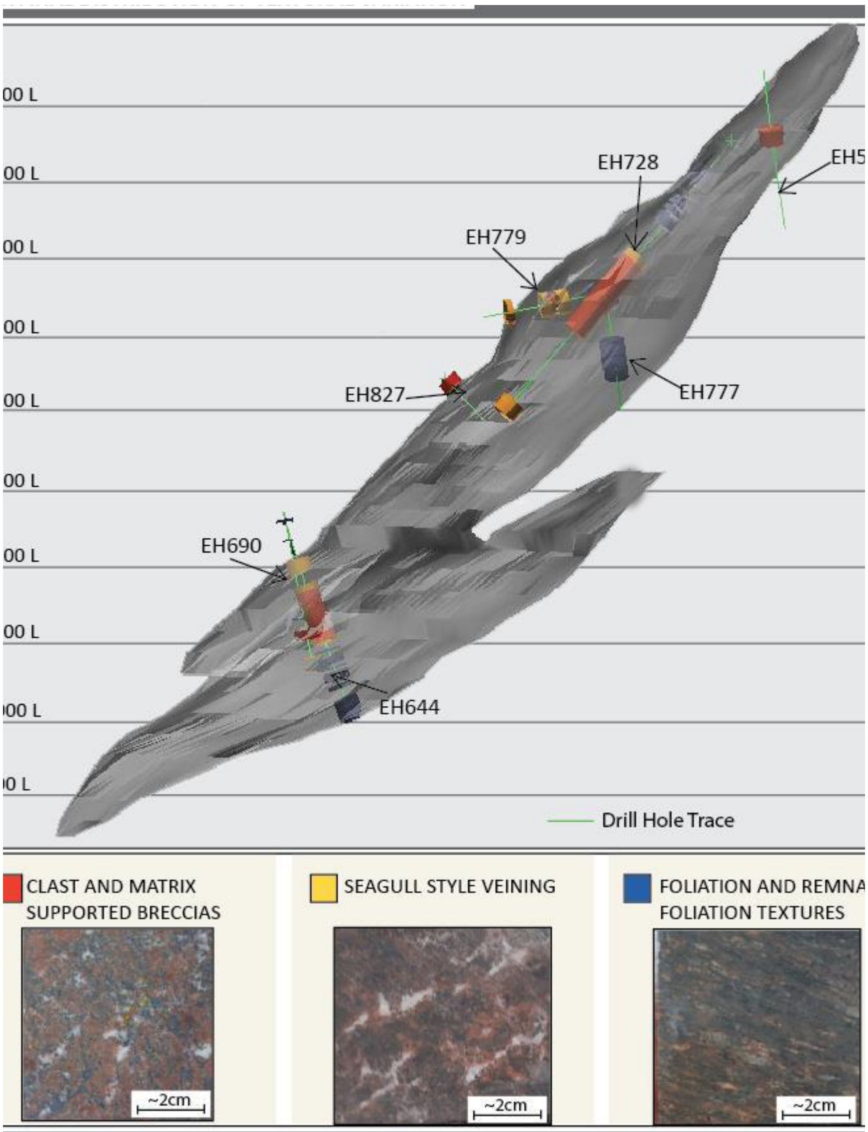

Figure 37. Spatial variation of brecciation, tension style veining and replacement along existing foliation.

Replacement textures identified within andesitic sections of EH504 and EH777 (refer drill logs and Figure 40) indicate that despite the apparent competency contrast between the footwall shear zone and the breccias, some of k-feldspar alteration textures, veining and subsequent sulphides exists due to the replacement of foliation textures which pre-date k-feldspar alteration. Spatially, these textures are preserved in porphyritic sections of EH504 and EH777 and are comprised of albite (Figure 39a,b). These phenocrysts display strong alignment but are not deformed indicating that they post-dated a previous foliation. Replacement phenocrysts are overprinted by k-feldspar alteration and later sulphides-bearing veins that preferentially permeate along these pre-existing foliations, indicating structural control of the peripheral extents of k-feldspar alteration.

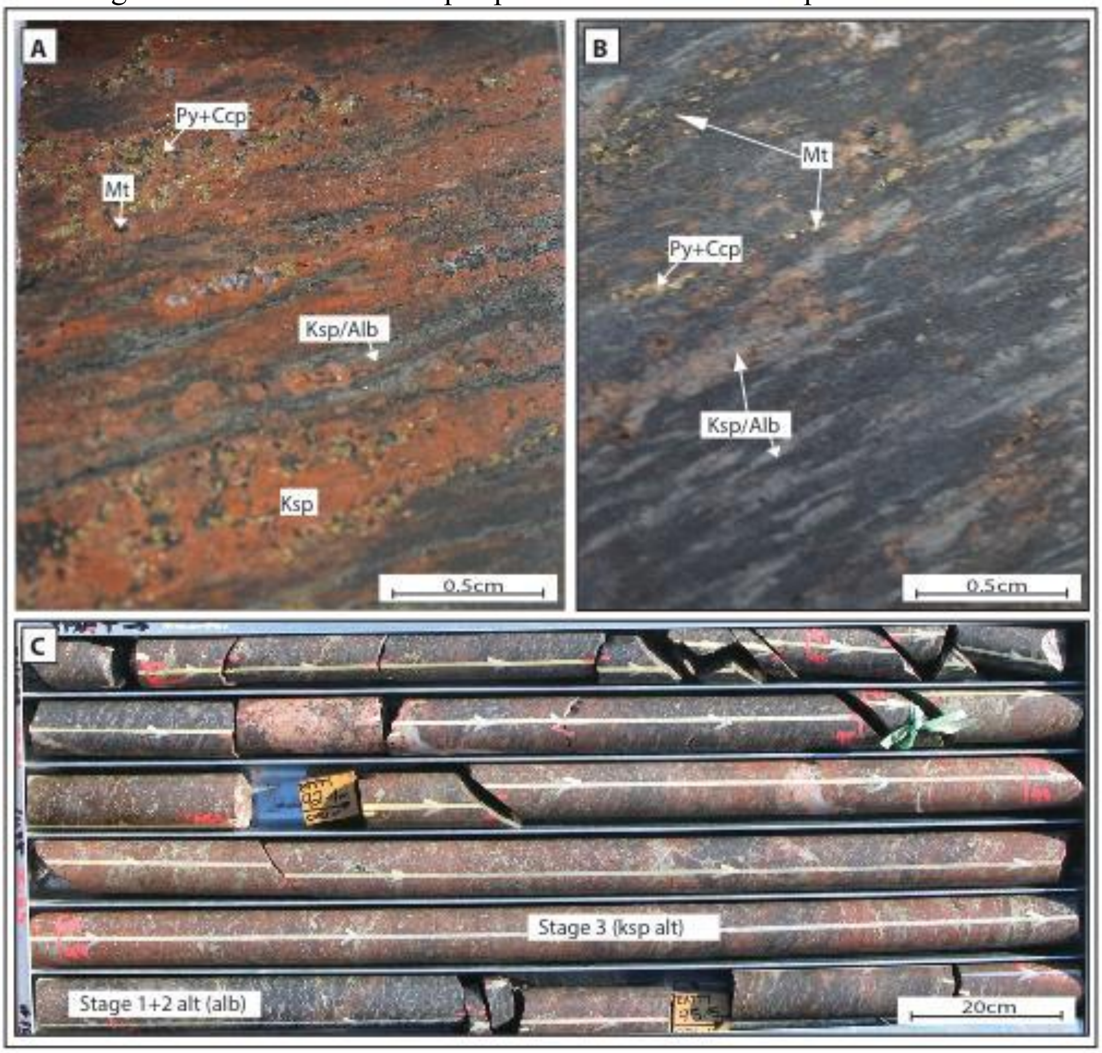

Figure 38. Replacement textures providing pathways for alteration and vein permeation a) Red rock alteration and ore phase magnetite and sulphides altering the spaces between replacement albite which is aligned in a foliation/shear fabric b) Replacement albite textures vein infilled by fine veins, infilled completely by magnetite and pyrite c) Core section of EH777 indicating the variable nature of the K-feldspar overprint in this section and the vein hosted nature of veins where K-feldspar alteration exists.

5. Discussion

Results from drill core logging and petrological observations indicate that Ernie Junior is situated within the same altered host felsic and intermediate volcanics that host Ernest Henry. The main alteration stages observed at Ernest Henry are also observed within Ernie Junior, an exception to this being the presence of chlorite alteration, which is confined only to Ernie Junior. In both ore bodies, correlation between mineralisation occurrence, grade and lithology is consistent, however at Ernie Junior, none of the mineralised veins crosscut the breccias that are observed at EH (eg. Mark et al, 2006). Structurally, there appears to be some control on the location of alteration and subsequent fine sulphide-hosted veins along foliation controlled location of albite/K-feldspar phenocrysts interpreted to be the result of replacement of a pre-existing existing foliation. These replacement textures preserved outside the ore body indicate that while the FWSZ bounds mineralisation, it pre-dates K-feldspar alteration and ore deposition. Structural control is identified in a SE-E dipping foliation fabric on either side of the ore body.

5.1 Interpretation of lithologies

Meta- andesites, felsic volcanics and mafic/sedimentary host rocks observed within and proximal to the Ernie Junior ore body correlate to observations of Ernest Henry carried out by Tywerould (1997) and Mark et al. (2006). Observations are consistent with the hypothesis that Ernie Junior and Ernest Henry are hosted within the same meta-volcanic/sedimentary sequence that has been linked to the Mount Fort Constantine Volcanics (outcropping 15 km to the south) (Mark et al. 2006). The undercover nature of this volcanic sequence means that further extents of these lithologies within the structural setting must be ascertained by additional drilling guided by geophysical magnetics. The felsic volcanics observed in drill holes in this study host the majority of ore; however they are generally clast-supported, which correlates to the outer shell of Ernest Henry that is concentrated around a higher >1.15% copper grade in its centre.

5.2 Alteration events and distributions

Four stages of alteration are observed in the Ernie Junior ore body (Table 4)

Alteration Stage	**Distribution and extent of control of ore**
1) Albite	Regional alteration event with no relevance, or control on subsequent, more localised alteration stages.
2) Potassic; (magnetite + biotite)	Localised to Ernest Henry and Ernie Junior marking the extent of the mineralising system (Mark et al. 2006).
3) K-feldspar rich	Overprints stages 1 and 2 and is confined to both breccia and vein-hosted ore phases of Ernest Henry and Ernie Junior. This alteration of albite phenocrysts is recognised as a vector towards red rock alteration (Tywerould, 1997).
4) Chlorite	Alteration after biotite. Post-ore deposition and therefore no control on ore formation.

Table 4. Distribution of alteration stages and the extent to which they focus ore-bearing mineralisation.

Stage 3 alteration in Ernie Junior widely overprints stage 2 magnetite and biotite that define foliation fabrics. K-feldspar alteration in the presence of a wider stage 2 alteration halo is a desirable target for further exploration. Minor amounts of elevated copper and gold in areas of stage 2 (magnetite + biotite) alteration are observed as a minor phase without the presence of stage 3 (K-feldspar) alteration indicating that it may not be necessary for ore deposition but related more to structural rather than geochemical controls. Biotite/ magnetite rich andesites preserved adjacent to Ernie Junior ore correlate to the outer geochemical extent both within the Ernest Henry Mine area and wider Eastern Succession region (eg Mark et al. 2006; Williams, 2003) that maybe useful pathfinders to k-feldspar alteration (Twyerould, 1997).

The paragenesis of Ernie Junior (Figure 41) is compared to that of Ernest Henry, as proposed by Mark, 2006. Mineralisation stages of Ernie Junior include widespread potassic, magnetite and K-feldspar alteration common throughout the Eastern Succession (Mark et al. 2006; Kendrick et al, 2007). Ernie Junior follows the alteration events observed within Ernest Henry, further illustrating the consistency of their formation and the spatial arrangement in which mineralisation is observed, with minor differences. Though titanite and barite identified were identified under SEM key distinguishing EH minerals apatite and fluorite (eg. Williams et al, 2015) were not observed.

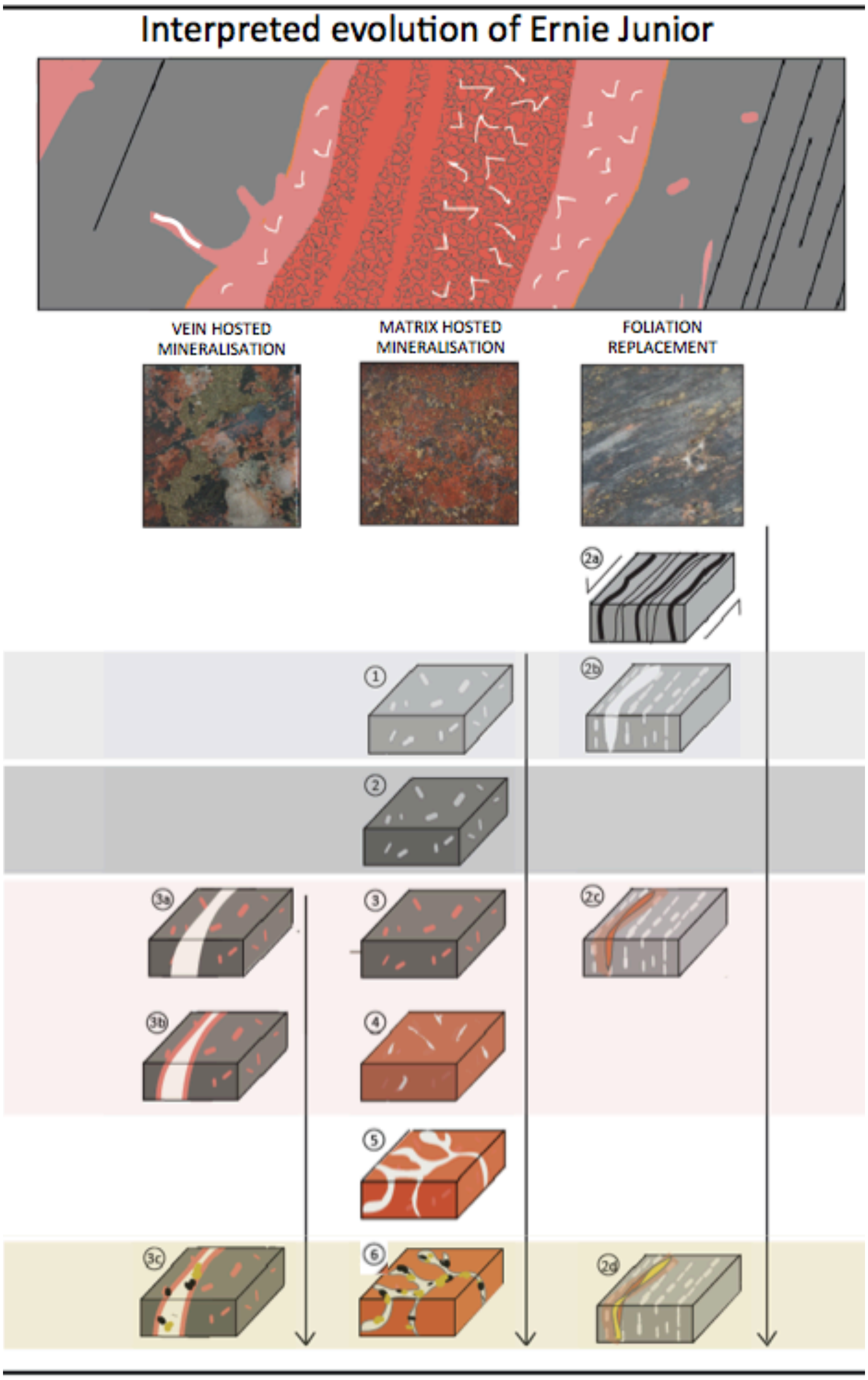

Figure 39. Schematic evolution breccia and vein hosted mineralisation. 1- Stage 1 alteration of albite phenocrysts in a porphyritic andesite. 2- Stage 2 alteration of host rock by magnetite and biotite. 3- Stage 3 alteration as k-feldspar overprints albite and gradually the whole rock texture in 4) where brecciation is initiated and infilled by calcite veins which 5) increase in size with a higher degree of brecciation. 6-magnetite infill is followed by subsequence sulphide deposition in 7.

3a- calcite vein outside of the ore body extent within minor k-feldspar alteration. 3b Alteration of the calcite vein and intrustion of a second calcite vein phase, seperates k-feldspar alteration to the edges of the vein. 3c- sulphides and magnetite infill as with the breccia hosted ore.

2a- foliation of andesites and stage two alteration of magnetite and biotite within the fabric. 2b- replacement along foliation with albite phenocrysts providing a pathway for subsequent calcite veining. 2c-K-feldspar alteration of calcite veining. 2d- subsequent massive sulphide style deposition within the small dialation of space provided by altered veins.

5.3 Comparison of ore styles and paragenesis

A strong positive correlation of 0.9 between copper and gold ratios in both Ernie Junior and Ernest Henry was observed within two drill holes. Accepted variance of Cu:Au ratios between ore deposits within the Eastern Succession (Davidson, 1998) therefore provides evidence for a single fluid source for both deposits. While assays from only two drill holes were used to make this conclusion, the results are strong enough to indicate the commonality.

The ore assemblage of Ernie Junior is comprised of chalcopyrite, gold, pyrite, magnetite, calcite, quartz, biotite chlorite titanite barite. These are also all observed at Ernest Henry (Mark et al, 2006). Two distinct styles of copper-gold mineralisation are present within Ernie Junior.

1) Vein: (Massive sulphides cross cutting un-brecciated andesites and FV volcanics) with coarser grain sizes and
2) Matrix: (FV, FV1 and FV2 lithologies) hosted – disseminated finer grain size

Vein-hosted sulphides are interpreted to be the outer expression of alteration, through andesites that had not been altered to stage 3 alteration and therefore not brecciated.

As both mineralisation styles exist in association with pyrite, magnetite and calcite as infill assemblages is likely they formed synchronously from the same mineralising fluid event. Further evidence of this is the fact vein-hosted ore at EJ is not observed to crosscut mineralised breccias. At Ernest Henry however, vein-hosted ore is observed by Mark et al, 2006, to crosscut ore phases associated with breccias. Further Laser Ablation-Inductively Coupled Plasma -Mass Spectrometry (LA-ICP-MS) geochemical analysis of trace element composition and zonation is required to confirm this suggestion.

5.2 Structural control and deformation fabrics

Measurements of foliations within proximity to the Ernie Junior ore body (refer to Figure 10.2.2 for spatial extent of foliations) indicate a variable dip of 20-30 to the SE-ESE. This correlates with previous observations of the Footwall shear zone (Tywerould, 1997), recently characterised Interlens shear (O'Brien, honours thesis, 2016) and overarching NW-striking, SE dipping Ernest Henry ore body (Mark et al, 2006). Variation the dip of foliations may be attributed to shear structure variation. Incorrect survey information may also account for the variation observed.

The preservation of replacement textures within foliations is observed towards the outermost extent of the stage 3 K-feldspar alteration away from the central brecciation. This replacement: 1) is consistent with observations by Mark et al. 2006, of albite veining and porphyroblastic albite replacement, attributed to local overprinting the S2 fabric also recognised by Coward, 2001, 2) provides evidence of a texture preserved during the earliest stages of the hydrothermal system (observations in this study; Mark et al. 2006) as it displays only the first stage of alteration, and 3) provides further evidence for post-shear zone ore formation of both Ernest Henry (eg those observed by Mark et al. 2006;
O'Brien, honours thesis) and the Ernie Junior.

These textures provide evidence that the FWSZ formed prior to stage 2 and 3 alteration. They also control fine vein-hosted sulphides, due to preferential fluid pathways along in the form of calcite veining and subsequent alteration (Figure 40stages 2a-d) outside the main breccia phase.

Brecciation of the host to Ernie Junior is therefore likely the result of a competency contrast existing between stage 2 magnetite and biotite alteration observed within the FWSZ and texturally destructive stage 3 K-feldspar alteration. The fractured nature of K-feldspar altered volcanics implies that they are more stress resistant/competent. Brecciation provides space for accommodation of mineralising fluids discussed in section. Overall, this indicates that Ernie Junior is strongly structurally controlled

Further structural work on Ernie Junior is recommended to determine a sense of relative movement. This will provide comparison to the reverse, normal and strike-slip movement proposed between the bounding HWSZ and FWSZ to EH (Coward, 2001; Liang, 2003; Valenta, 2000) and EJ. Further investigation of the structural fabric of overlying meta-intermediate volcanics and minor sediments could help structural understanding.

6. CONCLUSIONS

This thesis represents the first formal study of the Ernie Junior IOCG deposit; characterisation, genesis and controls on mineralisation. The genesis of Ernie Junior bears commonalities with the adjacent Ernest Henry deposit, indicating formation within the same hydrothermal system. These two deposits are located between two pre-existing shear zones, which have provided fluid pathways, and resulting alteration and ore deposition. Results indicate:

Ernie Junior is hosted within the same variably altered volcanics as Ernest Henry. Both ore bodies lie at the core of intense k-feldspar alteration in brecciated Felsic Volcanics most likely analogous to the Mount Fort Constantine Volcanics.

The paragenesis of Ernie Junior mineralisation and Ernest Henry are consistent and largely controlled by successive alteration phases and infill of ore phase mineralisation in breccias, central to the most intense K-feldspar alteration.

The ore assemblage of Ernie Junior consists of chalcopyrite, pyrite, magnetite, calcite, titanite, biotite and quartz typical of the Ernest Henry assemblage. Ernie Junior ore is observed in both veins and breccia infill. Vein-hosted ore is peripheral to breccia hosted ore, but given common assemblages, is likely synchronous. Stages 1) (albite), 2) (potassic, magnetite and biotite) and 3) K-feldspar alteration identified in this study are also typical of Ernest Henry.

Deformation fabrics are consistent across Ernie Junior and Ernest Henry ore bodies indicating commonly oriented structural control within bounding FWSZ and HWSZ. SE-ESE dipping, NE striking foliations in Ernie Junior and replacement by albite indicate that they formed before K-feldspar alteration and coincident ore bearing fluids. This supports a post-shear ore deposition model of genesis for both Ernie Junior and Ernest Henry.

ACKNOWLEDGMENTS

Thank you to Richard Lilly, Brad Miller and Glencore for providing the opportunity and funding to conduct this research. Further thanks to Richard Lilly, for your guidance and enthusiasm as well as EHM geologists, Brad, Ness, Dan and Chloe for assistance during fieldwork. Further acknowledgement to Katie Howard her organisational skills and extra advice for NZ, to Ben and Aieofe from Adelaide Microscopy for your assistance and training on the SEM and MLA, to Ioan Sanislav for your structural geology expertise during fieldwork. Thank you to Maptek for providing access to Vulcan software, and Steve Sullivan for his trouble-shooting assistance! Final thanks goes to the rest of the honours students; you've been awesome!

REFERENCES

BAKER, T., AND LAING, W.P., 1998. Eloise Cu-Au deposit, East Mount Isa Block: structural environment and structural controls on ore. *Australian Journal of Earth Sciences 45, 429-444.*

CLEVERLEY, J. AND OLIVER, N. 2005. Comparing closed system, flow-through and fluid infiltration geochemical modelling: examples from K-alteration in the Ernest Henry Fe-oxide-Cu-Au system. *Geofluids* 5, 289-307.

COWARD, M. 2001. Structural Controls on Ore Formation and Distribution at the Ernest Henry Cu-Au Deposit, NW Qld. Honours thesis. James Cook University.

DAVIDSON, G. J. 1998. Variation in copper-gold styles through time in the Proterozoic Cloncurry goldfield, Mt Isa Inlier: a reconnaissance view. *Australian Journal of Earth Sciences*, 45, 445-462.

ERNEST HENRY MINING PTY LTD, 2003. Summary petrography on drill core chips from the Ernest Henry Mine, Northwest Queensland (Armidale: The University of New England).

FOSTER, A., WILLIAMS, P., & RYAN, C. 2007. Distribution of Gold in Hypogene Ore at the Ernest Henry Iron Oxide Copper-Gold Deposit, Cloncurry District, NW Queensland. *Exploration And Mining Geology* 16, 125-143.

FOSTER, D.R. & AUSTIN, J.R., 2008. The 1800–1610Ma stratigraphic and magmatic history of the Eastern Succession, Mount Isa Inlier, and correlations with adjacent Paleoproterozoic terranes. *Precambrian Research,* 163**,** 7-30.

GROVES, D., BIERLEIN, F., MEINERT, L., & HITZMAN, M. 2010. Iron Oxide Copper-Gold (IOCG) Deposits through Earth History: Implications for Origin, Lithospheric Setting, and Distinction from Other Epigenetic Iron Oxide Deposits. *Economic Geology* 105, 641-654.

KENDRICK, M., MARK, G., AND PHILLIPS, D. 2007. Mid-crustal fluid mixing in a Proterozoic Fe oxide–Cu–Au deposit, Ernest Henry, Australia: Evidence from Ar, Kr, Xe, Cl, Br, and I. *Earth And Planetary Science Letters* 256, 328-343.

LAING, W.P., 1993. Structural/metasomatic controls on ore deposits in the East Mount Isa Block: the key to tonnes and grade. *Symposium on recent advances in the Mount Isa Block,* Aust. Inst. Geoscientists Bulletin 13, 17-24.

LAING, W.P., 1998. Structural-metasomatic environment of the East Mount Isa Block base metal-gold province. *Australian Journal of Earth Sciences 45, 413-428.*

MARK, G., OLIVER, N., & CAREW, M. 2006. Insights into the genesis and diversity of epigenetic Cu – Au mineralisation in the Cloncurry district, Mt Isa Inlier, northwest Queensland. *Australian Journal Of Earth Sciences* 53, 109-124.

MARK, G., OLIVER, N., & WILLIAMS, P. 2006. Mineralogical and chemical evolution of the Ernest Henry Fe oxide–Cu–Au ore system, Cloncurry district, northwest Queensland, Australia. *Mineralium Deposita* 40, 769-801.

MARK, G., WILDE, A., OLIVER, N., WILLIAMS, P., & RYAN, C. 2005. Modeling outflow from the Ernest Henry Fe oxide Cu–Au deposit: implications for ore genesis and exploration. *Journal Of Geochemical Exploration* 85, 31-46.

MARSHALL, L. J. & OLIVER, N. H. S. 2005, 'Monitoring fluid chemistry in iron oxide–copper–gold-related metasomatic processes, eastern Mt Isa Block, Australia', Geofluids, vol.5, pp.1–22

PAGE, R. W., AND SUN, S. S., 1998, Aspects of geochronology and crustal evolution in the Eastern Fold Belt, Mt Isa Inlier: Australian Journal of Earth Sciences, v. 45, p. 343-361.

Porter GeoConsultancy Pty Ltd, 2000. Ernest Henry Queensland, Qld, Australia.

RUSK, B., OLIVER, N., CLEVERLEY, J., BLENKINSOP, T., ZANG, D., WILLIAMS, P., & HABERMANN, P. 2016. Physical and chemical characteristics of the Ernest Henry iron oxide copper gold deposit, Australia; implications for IOGC genesis. In Hydrothermal Iron Oxide Copper-Gold & Related Deposits: A Global Perspective - Advances In The Understanding Of IOCG Deposits, T. Porter, ed. (Adelaide: PGC Publishing), pp. 201-218.

TWEROULD, S. 1997. The Geology and Genesis of the Ernest Henry Fe-Cu-Au Deposit, NW Queensland, Australia. PhD thesis. The University of Oregon.

WILLIAMS, M., HOLWELL, D., LILLY, R., CASE, G., & MCDONALD, I. 2015. Mineralogical and fluid characteristics of the fluorite-rich Monakoff and E1 Cu–Au deposits, Cloncurry region, Queensland, Australia: Implications for regional F–Ba-rich IOCG mineralisation. *Ore Geology Reviews* 64, 103-127.

WILLIAMS, P. 2001. Australian Proterozoic Iron Oxide-Cu-Au Deposits: An Overview with New Metallogenic and Exploration Data from the Cloncurry District, Northwest Queensland. *Exploration And Mining Geology* 10, 191-213.

APPENDIX A: EXTENDED METHODS

3D Modelling Creating a Vulcan Isis Database for Figures 27 and 37. *Steps as per the Introduction to Vulcan Training Manual Version 8.2 (2012).*

PART A) CREATING A NEW DATABASE

1) Open Vulcan Envisage and Isis
2) To create a new design click **File > New Design.** Click **Attributes** to define a database **Type**. Select **Drilling** and choose a **Desurvey** style.
3) To create a table with collar, assay, survey and geology data, click **Table > Insert** or **Table > Append**.
4) Each table corresponds with columns of data in .csv files containing drilling information. Name each field and select text or integer depending on the type of data stored in each field of collar, assay, survey and geology.
5) A key field must be defined to tell the database which field ties data across all tables together. To define the Key Field, right click the gray area to the left of the field name and select **Primary Key**.
6) After the primary key is defined, click **File > Save** and close Isis.
7) Open Vulcan Envisage in the primary window and click **File > Import** to import the database into the viewable field. Select **CSV(Databases)** and **OK**.
8) Specify the data file extension, the rows which contain field names in the .csv and the row where records start. Click **Select** to choose a design file.
9) Click File > Import and define fields so that the fields in the dialogue box match the table fields created in Isis.

PART B) CREATING A LEDGEND AND VIEWING DATA

Before you can view the database, a colour legend needs to be defined.

10) Click **Analyse > Legend Edit > Legend editor.**
11) Under *DRILL*, double-click [*] *New legend* to create a new drill legend
12) Select **Numeric** and check **Use database to populate drop menus** and select the name of the database you created.
13) Check **Specify Record** and **Depth** fields. Select a **Record (Table)** name, such as ALTERATION. Select K-feldspar alteration as the **Field Name** and TO as the **To** field.
14) Check **Use From** or **Thickness**. Choose **Use From** and select FROM from the drop down list.
15) Click **Get Range** to automatically populate the Colour Ranges pane with values from the database. You will need to select a respresentative colour for each interval. If a colour is not chosen for an interval, the interval will not display in Envisage.
16) Check **Use Colour for non-logged intervals** and choose a colour which will be used to draw intervals in Envisage when no interval is logged in Isis.
17) Save the legend
18) Display the Drill holes using your new legend by clicking **Geology > Drilling > Load drill holes** and selecting your file name created in Part A.

Extended MLA setup and processing instructions

1) Run the MLA process, following steps on the
2) Verify mineral identification by the MLA using the SEM to spot check and assess the spectral response of the minerals.
3) Repeat until satisfied that the mineral suite is complete.

Limitations:
1) complex textures difficult to identify
2) the chemical similarity between mineral chemistries, and limitation of the spectral database, however this can be mediated by optical and SEM observations to fill gaps.

APPENDIX B: SAMPLE LIST

Appendix A: Sample List **-** Documentation of sample locations and analyses performed on each sample. Hand specimen observations were conducted for all samples. Further analyses were undertaken on samples selected for thin sections. Further detail of observations of listed samples are located in Appendix Two or Three.

Hole ID	**Sample Number**	**Depth (m)**	**Reason for sample/brief description**	**Drillhole Location Nrth/East**	**Location Collected**	**Taken to Adelaide**	**Thin Section**	**Scanning Electron Microscope (SEM)**	**Mineral Liberation Acceleration (MLA)**
EH504	504.1	396.4	Shows vein alteration, cross-cutting matrix of altered volcanics. Representative of red-rock alteration in EH504.	39084.891/ 39084.891	EHM Core Shed	Yes	Yes	Yes	Yes
EH504	504.2	431.2	Shear fabric with pervasive carbonate veining and k-feldspar alteration.	39084.891/ 39084.891	EHM Core Shed	Yes	Yes	Yes	
EH504	504.3	505.4	K-feldspar, calcite and biotite alteration.	39084.891/ 39084.891	EHM Core Shed	Yes	Yes	Yes	
EH504	504.4	525	Foliated sample, k-feldspar alteration of late stage veining.	39084.891/ 39084.891	EHM Core Shed	Yes	Yes	Yes	
EH504	504.5	543.2	Presence of garnet, for use with paragenesis.	39084.891/ 39084.891	EHM Core Shed	Yes			
EH504	504.6	539	Movement of late stage mineralised calcite vein.	39084.891/ 39084.891	EHM Core Shed	Yes	Yes	Yes	
EH504	507.7	554.7	Unknown alteration, albite?	39084.891/ 39084.891	EHM Core Shed	Yes			

Hole	Sample Number	Depth	Brief Description	Drillhole Location	Location Collected	Taken to Adelaide	Thin section	Scanning Electron Microscope (SEM)	Mineral Liberation Acceleration (MLA)
EH777	777.1	3.2	Identification of green mineral. Amphibole?	38879.664/ 38879.664	EHM Core Shed	Yes			
EH777	777.2	7.8	Shows quartz inclusions in garnet and pervasive veining in biotite/magnetite alteration.	38879.664/ 38879.664	EHM Core Shed	Yes			
EH777	777.3	73.7	Infill of green chlorite/amphibole.	38879.664/ 38879.664	EHM Core Shed	Yes	Yes	Yes	
EH777	777.4	91.5	Foliated sample with magnetite veins cross-cutting k-feldspar altered veins.	38879.664/ 38879.664	EHM Core Shed	Yes			
EH777	777.5	107.6	Identification of phenocryss in dark altered rock. Py and chalcopyrite in k-feldspar altered veins.	38879.664/ 38879.664	EHM Core Shed	Yes			
EH777	777.6	112.6	Dark alteration with lighter veining containing magnetite. Process of alteration?	38879.664/ 38879.664	EHM Core Shed	Yes			
EH777	777.7	142	Displays the relationship of alteration of magnetite, k-feldspar, biotite and quartz veining.	38879.664/ 38879.664	EHM Core Shed	Yes			
EH728	728. A	89.6		39025.82/ 69347.029	EHM Core Shed	Yes			
EH728	728.2	126		39025.82/ 69347.029	EHM Core Shed	Yes	Yes	Yes	
EH728	728.B	134		39025.82/ 69347.029	EHM Core Yard	Yes			
EH728	728.4	177		39025.82/ 69347.029	EHM Core Yard	Yes			
EH728	728.C	199		39025.82/ 69347.029	EHM Core Yard	Yes	Yes	Yes	

EH728	728. D	328		39025.82/ 69347.029	EHM Core Yard	Yes			
EH728	728. E	408		39025.82/ 69347.029	EHM Core Yard	Yes			
Hole	**Sample Number**	**Depth**	**Brief Description**	**Drillhole Location**	**Location Collected**	**Taken to Adelaide**	**Thin section**	**Scanning Electron Microscope (SEM)**	**Mineral Liberation Acceleration (MLA)**
EH644	644.1	1026.5	Mineralisation evident at the start of hole. Means for comparison to deeper Cu/Au.	38304.85/ 69378.08	EHM Core Yard	Yes	Yes	Yes	
EH644	644.2	1062.5	Typical matrix supported breccia with calcite infill, with absence on mineralisation.	38304.85/ 69378.08	EHM Core Yard	Yes	Yes	Yes	
EH644	644.3	1123	Mineralised sample, slight foliation and pink clasts..less k-feldspar altered?	38304.85/ 69378.08	EHM Core Yard	Yes	Yes	Yes	
EH644	644.4	1123	Sheared fabric, identification of banded appearance components required.	38304.85/ 69378.08	EHM Core Yard	Yes	Yes	Yes	Yes
EH644	644.5	1204	Shows relationships of shearing to clasts displaying white phenocrysts.	38304.85/ 69378.08	EHM Core Yard	Yes	Yes	Yes	
EH644	644.6	1213.5	Mineralisation in dark altered rock, unusual but present.	38304.85/ 69378.08	EHM Core Yard	Yes	Yes	Yes	
EH690	690.1	1063.1		38312.654/ 69411.904	EHM Core Yard	Yes	Yes	Yes	
EH690	690.2	1112		38312.654/ 69411.904	EHM Core Yard	Yes	Yes	Yes	
EH690	690.3	1115		38312.654/ 69411.904	EHM Core Yard	Yes	Yes	Yes	
EH690	690.4	1150		38312.654/ 69411.904	EHM Core Yard	Yes	Yes	Yes	
EH690	690.5	1156		38312.654/ 69411.904	EHM Core Yard	Yes	Yes	Yes	
EH690	690.6	1055.8		38312.654/ 69411.904	EHM Core Yard	Yes	Yes	Yes	

EH779									

APPENDIX C: PETROLOGY

Appendix B: Petrology- Petrological and hand specimen observations

Minerals	Primary/Alt/Infill	Grain size and Habit	Modal %	Characteristics
K-Feldspar	Primary	Euhedral – well preserved rounded grains ~1 µ	35%	Very fine grained matrix component, creates a mosaic texture with quartz
Quartz	Primary	Euhedral – well preserved rounded grains	25 %	Very fine grained matrix component, creates a mosaic texture with k-feldspar
Pyrite	Infill	Large grains, minimal fracturing.	35%	Late stages pyrite grains are fractured and post date 'red rock' alteration. Small inclusions of quartz at grain boundaries between pyrite grains
Chalcopyrite	Infill	Observed under thin section	2%	Subhedral grains, significantly finer grained than pyrite and occurs predominantly as infill in calcite veins
Magnetite	Infill/replacement	Anhedral grains	3%	Fractured grains and associated with pyrite and chalcopyrite,
Hematite	Alteration	Surface feature		Intense hematite alteration throughout. Intensity of alteration is most intense on remnant clasts.
Calcite	Infill	Large euhedral grains where not overprinted	2%	Large grains, with well preserved cleavage.
Chlorite	Alteration	Diffuse grain boundaries	1%	Alteration of biotite
Biotite	Infill	Randomly oriented	2%	Infill with the ore assemblage in calcite veins

IPLE 504.1 Sulphide Petrology

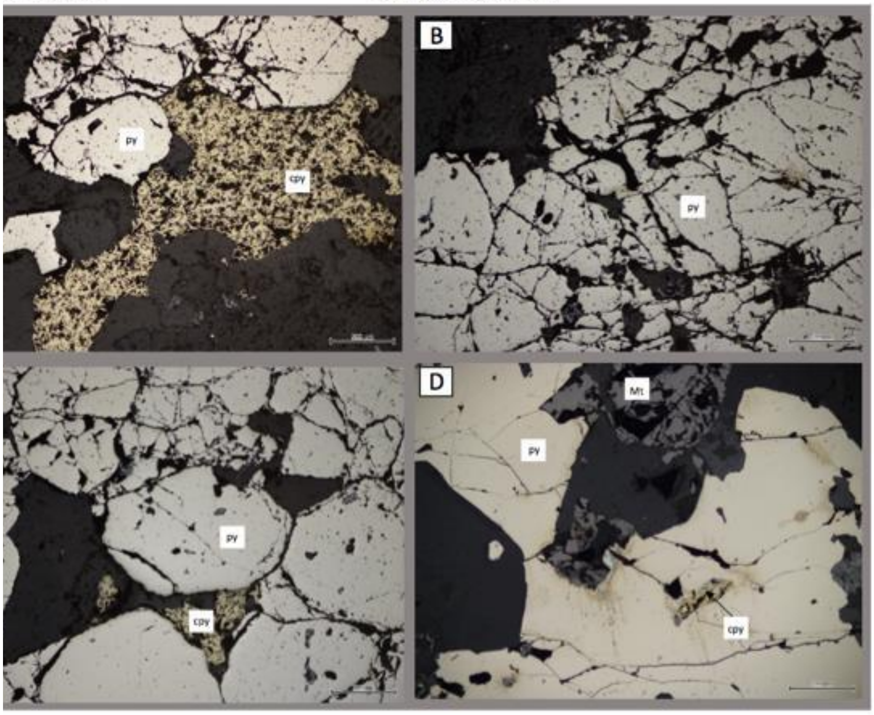

Figure 1. Illustrating the main textural associations of sulphides in sample 504.1.
A – Infill texture exhibited in chalcopyrite with its irregular crystal shape.
B- A highly fractured pyrite grain with smaller magnetite grains infilling in spaces between fractures.
C- Chalcopyrite grains between fractured pyrite grains
D- A less pervasively fractured infill pyrite grain with a small chalcopyrite inclusion.

Observations

Weakly foliated clast supported, rock. Red altered clasts aren't as magnetic as the darker clasts that comprise the majority of the clasts. Soft white, elongate and foliated within the clasts. Magnetite and pyrite +/- chalcopyrite exist in disseminated grain, not elongate and <.5mm. Magnetite grains make up a "developing" matrix. A dark non-magnetic mineral is positioned within hematite alteration at the edge of a quartz vein.

Interpretations

This section has not yet fully developed into a breccia. This rock is not as pervasively magnetite altered. Sulphides are disseminated in both clasts, though occur mostly in the matrix. Hematite alters late stage quartz veins and the dark, non-metallic grains within this could be retrograde biotite. Magnetite infills into calcite veins.

SAMPLE 504.3 DEPTH: 505.2

Minerals	Primary/Alt/Infill	Grain size and Habit	Modal %	Characteristics
K-Feldspar	Primary	Fine grained in the matrix and elongate albite?	30%	Hematite altered clasts comprised of k-spar and quartz
Quartz	Primary	Subhedral rounded crystals	30%	In between calcite grains in veins
Pyrite	Infill	Large grains where present	2%	Highly fractured with magnetite infill in fractures
Chalcopyrite	Infill	Not observed in hand specimen	>1%	Not observed in hand specimen
Biotite	Secondary	Infill between clasts aligned around clasts	15%	Retrograde biotite in calcite veining, much of which is being altered to chlorite.
Magnetite	Alt and infill	Infill aggregates within calcite	4%	Anhedral infill textures in calcite
Calcite	Infill	Hosts clasts of volcanics, medium to large grains	25%	Large grains with a strong cleavage preserved, pervasive in this sample.
Accessory	Infill		4%	

SAMPLE 504.3 Mineral Petrology

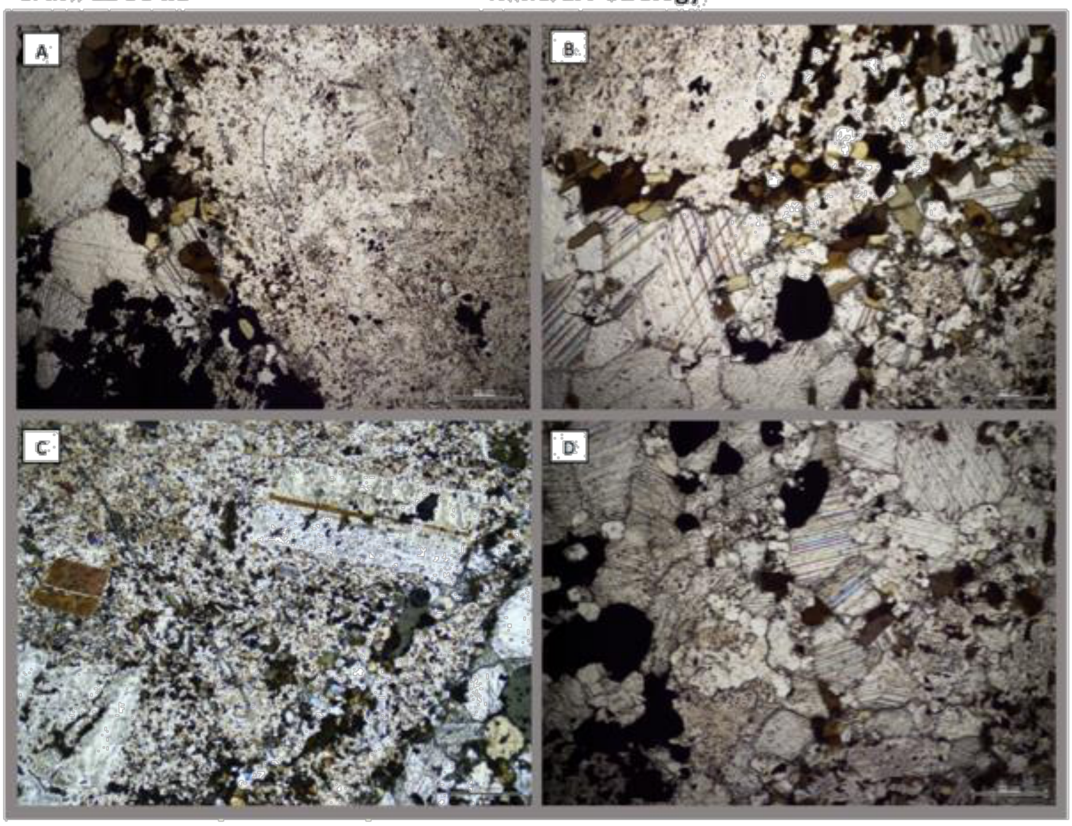

Figure 1. Illustrating the main textural associations of sulphides in sample 504.1.
A - A fine-grained hematite altered clast containing a large phenocryst of k-feldspar that has been replaced/pseudomorphed? To the left, a calcite vein containing hornblende, pyrite and magnetite.
B – A clast/vein boundary illustrating that biotite is clearly and infill mineral that post dated
C – K-feldspar phenocrysts within a clast
D- Infill vein of predominantly calcite and quartz

Observations

Matrix supported breccia with dark magnetic clasts. Lighter pink-red sections exist within the clasts that are less/not magnetitc. Clasts range in size from 2mm-2.3cam. The matrix is comprised predominately of calcite, with magnetite grains, and disseminated sulphides.

Interpretations

Minerals	Primary/Alt/Infill	Grain size and Habit	Modal %	Characteristics
K-Feldspar	Alt	Fine grained alteration of clasts	50%	Fine-grained euhedral crystals that comprise the majority of the matrix component and even [illegible]tz that comprise clasts of red altered rock.
Quartz	Infill	Euhedral, round grains	5%	Matrix component or as infill 'blebs' of quartz
Pyrite	Infill	Large euhedral grains that have been fractured	5%	Pyrite exists in calcite veins as infill. The grains are large but have been highly fractured and infilled in some
Chalcopyrite	Infill	Not observed in hand specimen	>2%	Not observed in hand specimen
Magnetite	Infill	Infill between K-feldspar altered clasts	30%	Irregular shaped infill grains, exhibiting finer infill of fine grained clasts and larger grains in the matrix of the sample
Calcite	Veins	Large aggregates	5%	Highly in-filled by magnetite to the point where only minimal calcite is preserved
Chlorite	Alteration	Not observed in hand specimen	1%	Not observed in hand specimen
Biotite	Secondary	Infill in veins	2%	Most has been retrogressed to Chlorite

SAMPLE 644.1 Sulphide Petrology

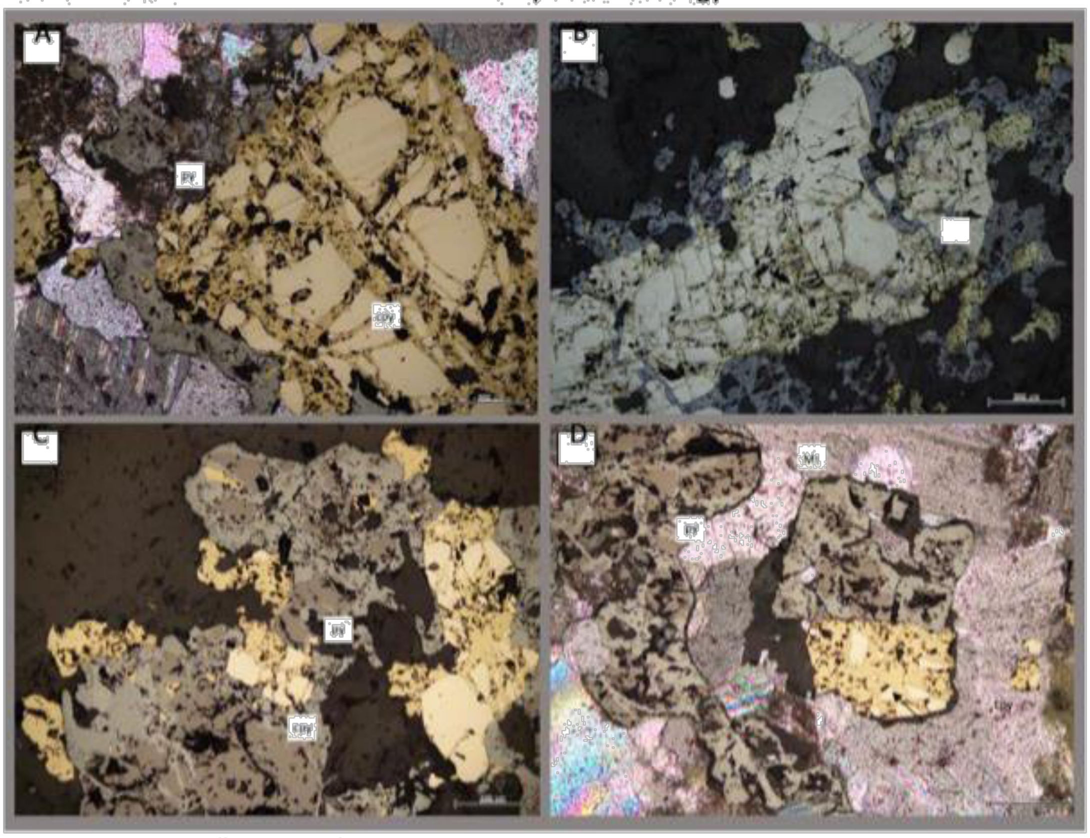

Illustrating the main textural associations of sulphides in sample 504.1.
A – Fractured pyrite and infilling chalcopyrite
B-Fractured pyrite and infilling chalcopyrite and magnetite
C- Fracturing of pyrite within the extent of a calcite vein. Infilling of chalcopyrite and then magnetite.
D-Magnetite, pyrite and chalcopyrite in a calcite vein

Observations

Matrix supported breccia. Clasts are 2mm-2cm across and comprised of altered red clasts in a calcite matrix. Fine magnetic grains border areas of the red clasts as well as occurring within the calcite matrix.

Interpretations

The original host rock has been magnetite then k-feldspar altered, then overprinted pervasively by magnetite – post brecciation. Infill of magnetite + pyrite + chalcopyrite followed.

SAMPLE 779.2 DEPTH:

Minerals	Primary/Alt/Infill	Grain size and Habit	Modal %	Characteristics
K-Feldspar	Primary	Fine grained, euhedral grains	30%	Fine grained matrix hosted
Quartz	Primary	Fine grained, euhedral grains	40%	Equigranular fine veins through the sample
Biotite	Secondary/Alt	Randomly orientated	15%	High amounts of biotite, outside of the ore zone, as indicated by the lack of chalcopyrite
Garnet	Secondary	Fine grained	1%	Fractured and with inclusions of biotite, quartz
Magnetite	Infill	Subhedral grains	7%	Matrix hosted, subhedral grains
Albite	Primary	Elongate grains, twinning present	~3%	Elongate crystals, well preserved in comparison to other samples
Calcite	Infill	Fine-medium grained	5%	Fine- grained through the matrix

SAMPLE 779.2 Mineral Petrology

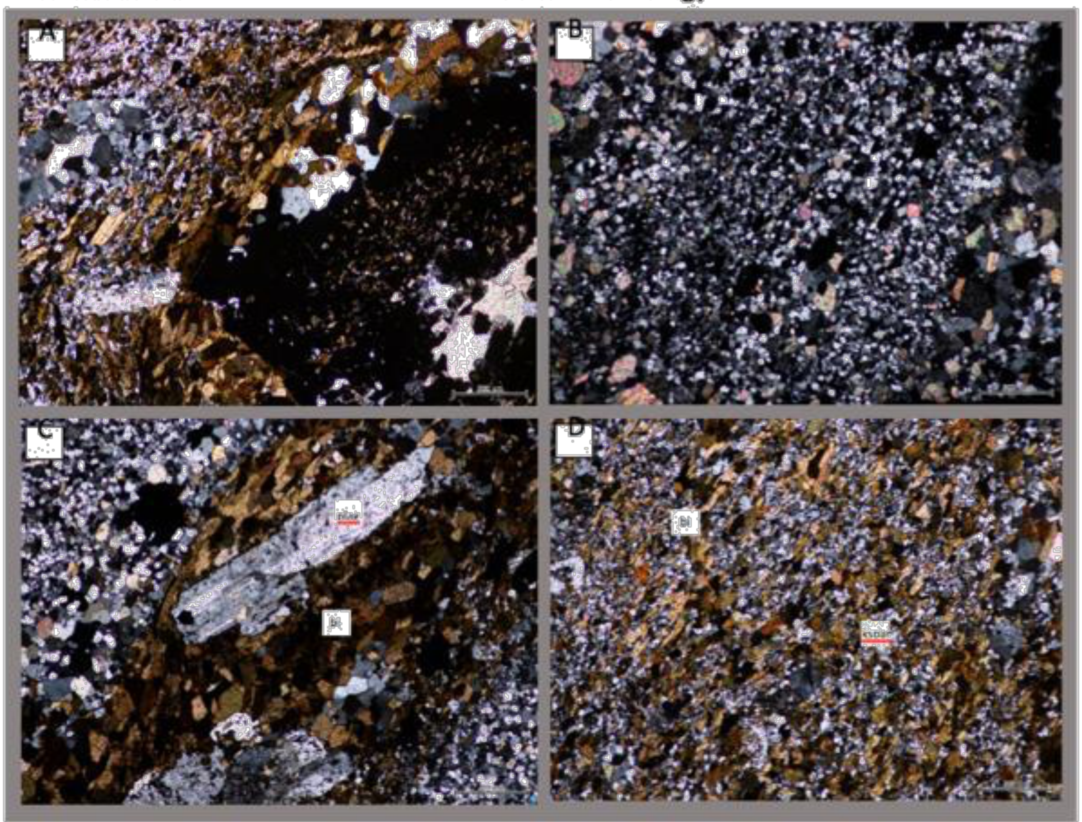

Illustrating the main textural associations of sulphides in sample 779.2.
Matrix of quartz, k-feldspar, magnetite and calcite.
Elongate phenocrysts of a sodic k-feldspar.
Aggregates of intense biotite within parts of this matrix.

Observations

Black rock with randomly oriented pale pink crystals that sometime resemble things 0.5mm veins that are cut off in the clast. These pale ink crystals are hard to scratch. Chalcopyrite is disseminated in quartz veins, and within the magntetite/calcite matrix. Rounded garnets of a orangey-red colour are also present and have 0.5mm grains of a non-magnetic black mineral within them.

Interpretations

SAMPLE 777.3 DEPTH:

Minerals	Primary/Alt/Infill	Grain size and Habit	Modal %	Characteristics
K-Feldspar	Alt	Replaces fine grains of the matrix	40%	Fine grained, matrix hosted, pervasive alteration mineral
Quartz	Infill/Primary	Subhedral veining	10%	Late stage fine veining
Pyrite	Infill	Large fractured grains	10%	Infill, large sulphide phase with magnetite
Chalcopyrite	Infill	Not observed in hand specimen	>1%	
Magnetite	Infill + alt	Anhedral grains	25%	Intense within infill space in veins not occupied by pyrite, likely deposited after pyrite
Calcite	Infill	Edges of large grains preserved	5%	Mostly replaced by infill minerals
Chlorite	Alt	In matrix infill after biotite	5%	Intense alteration at the site of most intense k-feldspar alteration
Accessory	Not identified in hand specimen		5%	

SAMPLE 777.3 Sulphide Petrology

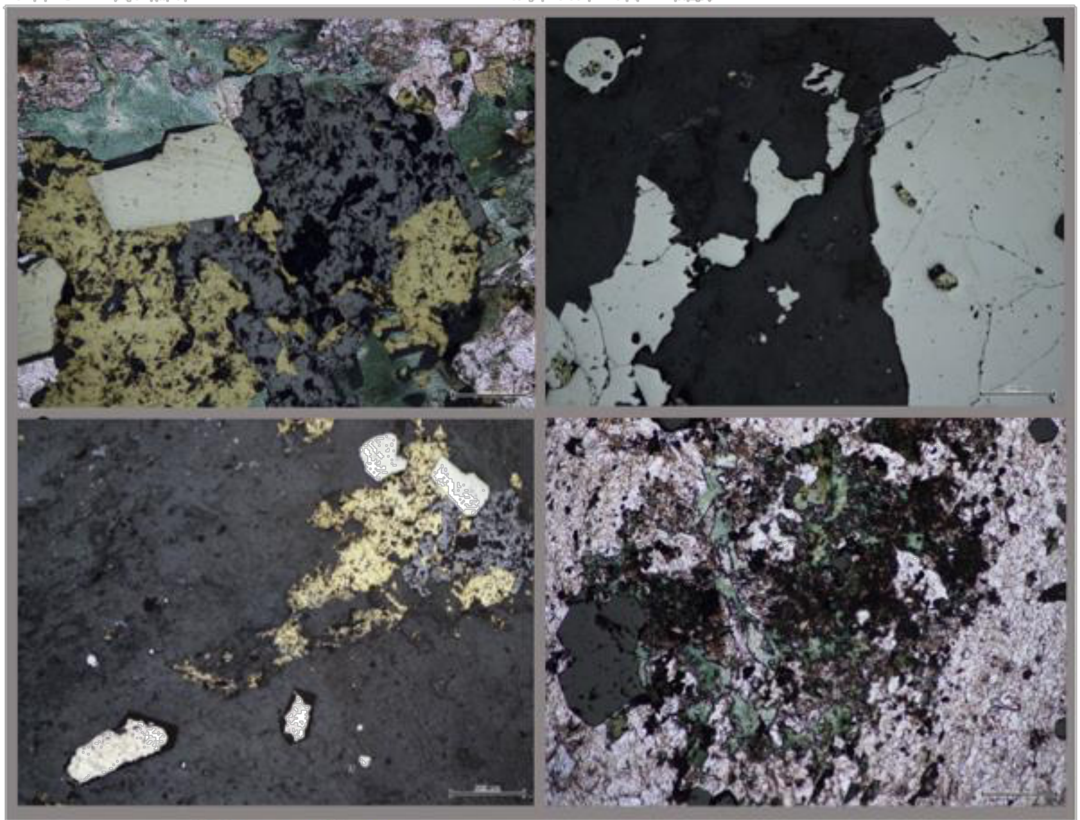

Figure 1. Illustrating the main textural associations of sulphides in sample 777.3.
Vein hosted pyrite, chalcopyrite and magnetite. Pyrite is fractured in some veins. Intense alteration also present (chlorite and k-feldspar)

Observations

Clast supported breccia. Sulphides occur with magnetite. Quartz veins appear to graduate to pink at the edges and are broken up by pyrite, chalcopyrite grains that are sub rounded. The quartz veins are the basis of the matrix.

Interpretations

Light pink alteration of quartz suggests that the lighter pink areas of the hematite altered clasts may have originally been quartz. As there is no calcite in this sample, it may have been overprinted by magnetite or alternatively may not have been in the sample to begin with.

SAMPLE 728.C DEPTH:

Minerals	Primary/Alt/Infill	Grain size and Habit	Modal %	Characteristics
K-Feldspar	Primary	Euhedral – subhedral well preserved rounded grains	75%	[illegible]ix component, creates a mosaic texture with quartz
Quartz	Primary	Euhedral – well preserved rounded grains	5 %	Very fine grained matrix component, creates a mosaic texture with k-feldspar
Pyrite	Infill	Large grains, minimal fracturing.	7.5%	Late stages pyrite grains are fractured and post date 'red rock' alteration. Small inclusions of quartz at grain boundaries between pyrite grains
Chalcopyrite	Infill	Observed under thin section	2%	Subhedral grains, significantly finer grained than pyrite and occurs predominantly as infill in calcite veins
Magnetite	Infill/replacement	Anhedral grains	7.5%	Fractured grains and associated with pyrite and chalcopyrite,
Hematite	Alteration	Surface feature		Intense hematite alteration throughout. Intensity of alteration is most intense on remnant clasts.
Calcite	Infill	Large euhedral grains where not overprinted	5%	Large grains, with well preserved cleavage.
Chlorite	Alteration	Diffuse grain boundaries	1%	Alteration of biotite
Biotite	Infill	Randomly oriented	2%	Infill with the ore assemblage in calcite veins

SAMPLE 728.C Sulphide Petrology

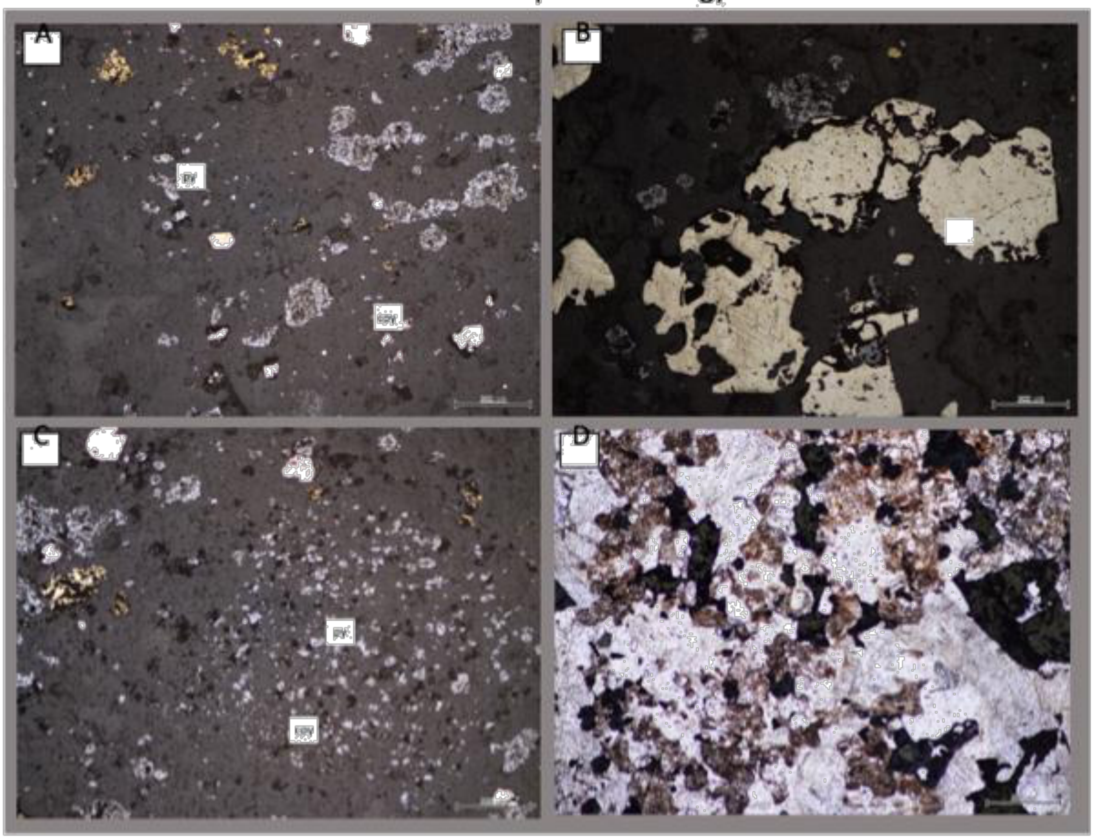

Figure 1. Illustrating the main textural associations of sulphides in sample 728.C
A – Matrix sulphides, disseminated through k-feldspa matrix. Anhedral magnetite and chalcopyrite.
B- Fractured pyrite with infilling magnetite
C- Clast within matrix, infilling smaller magnetite grains
D- Intense hematite + K-feldspar alteration of quartz?

Observations

Clast-supported breccia. Within the clasts of brick coloured rock, there are fine-2mm magnetite grains, in which sulphides are disseminated and dispersed. Large chalcopyrite grains are bordered by calcite

Interpretations

Strong association of vein hosted sulphides with magnetite – need to work out the paragenesis between magnetite and sulphides

SAMPLE 504-5

Minerals	Primary/Alt/Infill	Grain size and Habit	Modal %	Characteristics
K-feldspar	Alt		2%	Alteration at the edge of calcite veins
Quartz	Primary and secondary	Fine grained in primary rock and larger euhedral crystals in veins		Equigranular grains of subhedral interlocking crystals
Pyrite	Infill	Euhedral grains, un-fractured	1%	Vein hosted only within this sample
Chalcopyrite	Infill	And the edges	2%	Irregular grains indicate an infill texture. Close association with magnetite, though magnetite exists without chalcopyrite.
Magnetite	Infill	euhedral- highly irregular	10%	Outside the vein, magnetite forms euhedral crystals that are fractured.. Not infill though?
Garnet	Metamorphic	Large grains, once euhedral but now fractured	35%	Large grains within a vein, that have been pervasively fractured and broken apart in some places.
Calcite	Infill	Euhedral grains	2%	Have magnetite inclusions
Chlorite	Alteration	Partial-complete Alteration of biotite	20%	Highly fractured and broken grains with inclusions of magnetite, quartz and chlorite.
Biotite	Primary		25%	Aggregates of randomly oriented clusters of grains , much of which has retrogressed to chlorite in proximity of garnet grains.

SAMPLE 827.3

Mineral Petrology

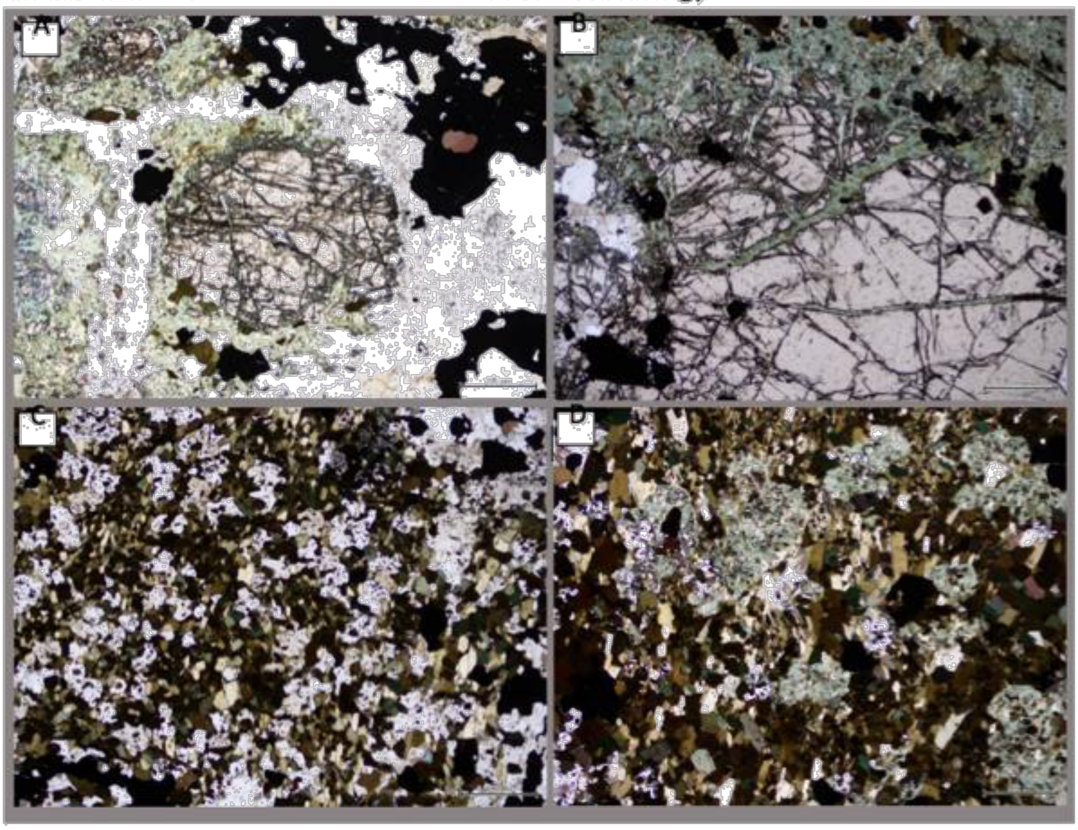

Figure 1. Illustrating the main textural associations of sulphides in sample 827.3.
A – Highly fractured garnet surrounded by chlorite alteration of biotite
B- Intense chlorite alteration in between fractured garnet
C- Quartz and biotite matrix being altered by chlorite
D- Alteration of biotite to chlorite in patches within a biotite rich matrix

Observations

Rich in biotite and chlorite and minimal k-feldspar alteration. Minor sulphides are present. Garnet dominated this samples, with large fractured crystal aggregates.

Interpretations

This sample represents a vein that has formed garnet, fractured and infilled with quartz and biotite/chlorite alteration only observed outside the k-feldspar altered

SAMPLE 728.2

Minerals	Primary/Alt/Infill	Grain size and Habit	Modal %	Characteristics
K-Feldspar	Primary	Fine grained, euhedral grains	5%	Fine grained matrix hosted at the edge of the vein
Quartz	Primary	Fine grained, euhedral grains	40%	Equigranular in the vein with calcite
Biotite	Secondary/Alt	Randomly orientated	40%	High amounts of biotite, outside of the vein zone, as indicated by the lack of chalcopyrite. Biotite lines up between k-feldspar and quartz rich 'bands' indicating a foliation fabric
Magnetite	Infill	Subhedral grains	10%	Matrix hosted, subhedral grains, intense as alteration of the host rock and as infill, larger crystals within the vein
Pyrite	Infill	Vein hosted	~3%	Variable crystal sizes – euhedral to subhedral crystals
Calcite	Infill	Fine-medium grained	5%	Fine- grained through the matrix

SAMPLE 728.2 Mineral Petrology

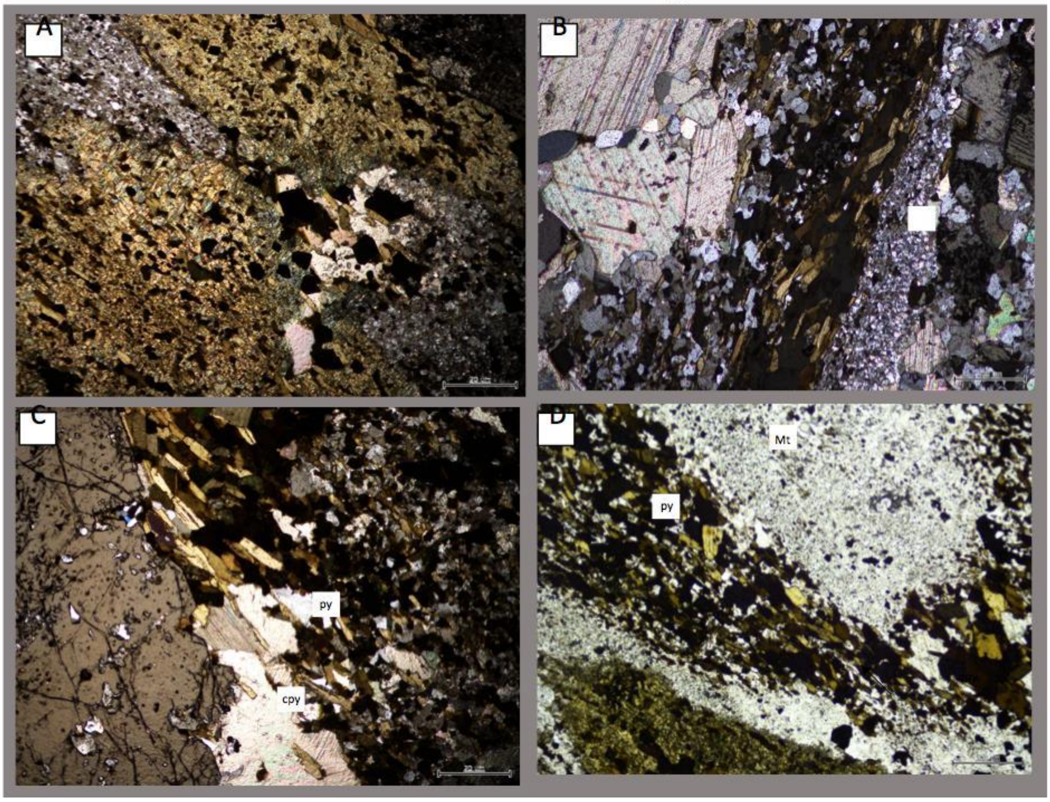

Illustrating the main textural associations of sulphides in sample 728.2.
A – Intensely altered crystals of ? By chlorite? Hornblende?
B- Calcite vein with finer grained quartz crystals included between calcite crystals. Aggregate of biotite Forming a line between a fine-grained mosaic textured quartz and k-feldspar matrix.
C- Garnet in a calcite vein between a matrix of intense magnetite and biotite alteration
D- Clast of volcanics within a matrix of intense magnetite and biotite alteration

Observations

Rich in biotite and magnetite alteration. Minor sulphides are present. Clasts of volcanics in the richly altered matrix. Infill of magnetite and pyrite in the calcite vein.

Interpretations

Foliations of clasts between magnetite and biotite alteation.

SAMPLE 690.6 DEPTH:

Minerals	Primary/Alt/Infill	Grain size and Habit	Modal %	Characteristics
K-Feldspar	Primary	Fine grained, euhedral grains	20%	Fine grained matrix hosted
Quartz	Primary	Fine grained, euhedral grains	5%	Equigranular fine veins through the sample
Biotite	Secondary/Alt	Randomly orientated	15%	High amounts of biotite, outside of the ore zone, as indicated by the lack of chalcopyrite
Pyrite	Infill	Fine-grained in calcite vein	1%	
Magnetite	Infill	Subhedral grains	25%	Matrix hosted, subhedral grains
Albite	Primary	Elongate grains, twinning present	~3%	Elongate crystals, well preserved in comparison to other samples
Calcite	Infill	Fine-medium grained	25%	Fine- grained through the matrix

SAMPLE 644.3 Mineral Petrology

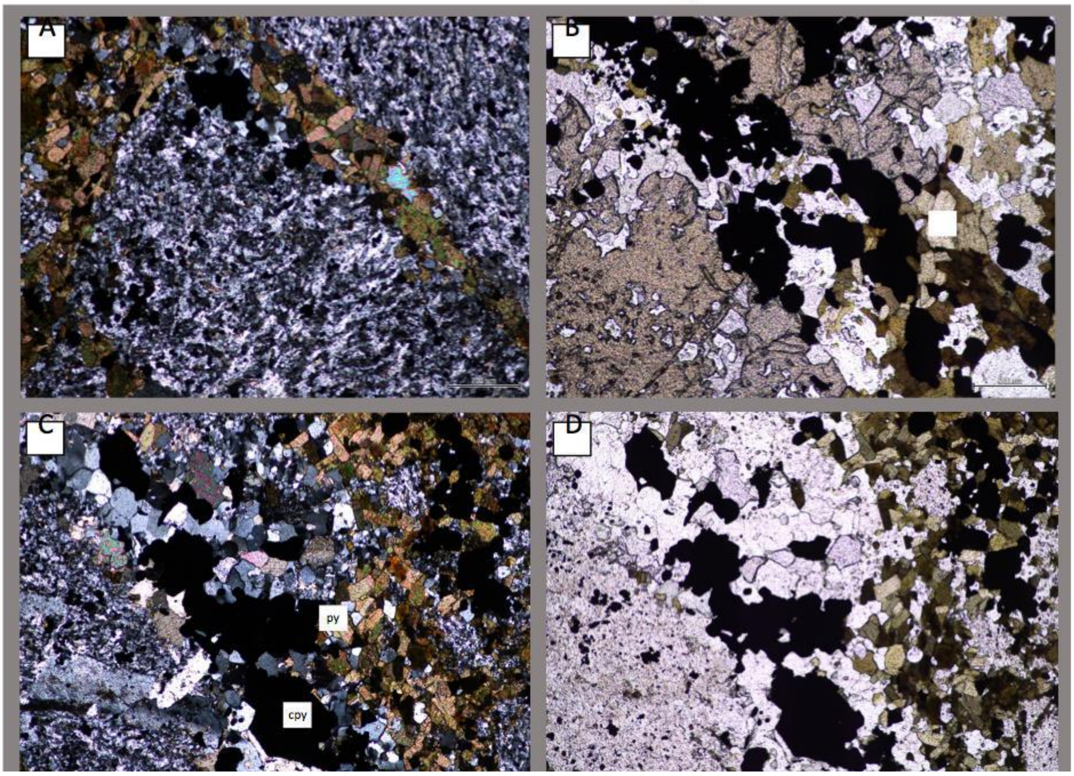

Figure 1. Illustrating the main textural associations of sulphides in sample 690.6
A – Trachyeandesite textured clasts of plagioclase/ albite in-between biotite and calcite.
B- anhedral garnet grains within quartz veins, in between magnetite and randomly orientated biotite.
C- Veins of quartz and magnetite between an albite bearing andesite clast and a biotite rich altered clasts.
D- The same as C but in PPL.

Observations

Rich in biotite and magnetite alteration. Minor sulphides are present. Clasts of volcanics in the richly altered matrix. Infill of magnetite and pyrite in the calcite vein.

Interpretations

Foliations of clasts between magnetite and biotite alteration.

SAMPLE 690.5

Minerals	Primary/Alt/Infill	Grain size and Habit	Modal %	Characteristics
K-Feldspar	Alt	Fine grained alteration of clasts	50%	Fine grained euhedral crystals that comprise the majority of the matrix component and even finer grains with quartz that comprise clasts of red altered rock.
Quartz	Infill	Euhedral, round grains	5%	Matrix component or as infill 'blebs' of quartz
Pyrite	Infill	Large euhedral grains that have been fractured	5%	Pyrite exists in calcite veins as infill. The grains are large but have been highly fractured and infilled in some
Chalcopyrite	Infill	Not observed in hand specimen	>2%	Not observed in hand specimen
Magnetite	Infill	Infill between K-feldspar altered vein aggregates	30%	Irregular shaped infill grains, exhibiting pervasive infill/alteration
Calcite	Veins	fine aggregates	5%	Highly in-filled by magnetite to the point where only minimal calcite is preserved
Chlorite	Alteration	Not observed in hand specimen	1%	Not observed in hand specimen
Biotite	Secondary	Infill in veins	2%	Most has been retrogressed to Chlorite

SAMPLE 690.5

Mineral Petrology

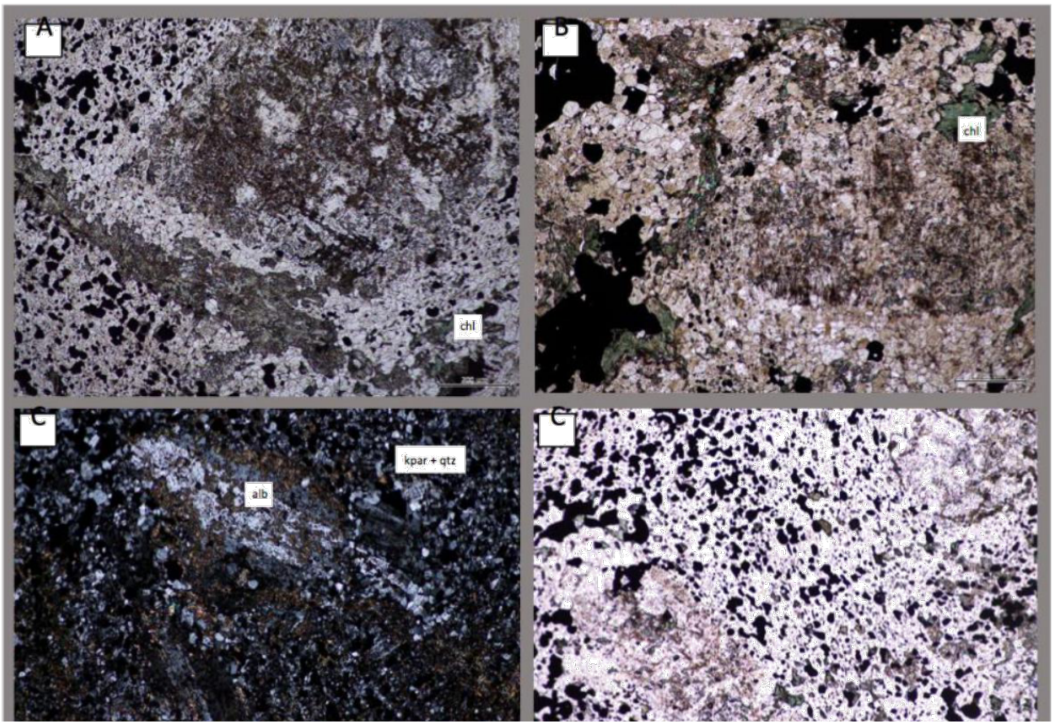

Figure 1. Illustrating the main textural associations in sample 690.5
A – Intense hematite alteration of a past-albite phenocryst
B- K-feldspar and quartz dominated matrix with intense alteration the only preserved feature of overprinted phenocryst. Chlorite alteration along altered veins.
C-Sericitic alteration of albite phenocryst in a magnetite, quartz and albite rich matrix.
D- PPL light image of remnant phenocryst that is not exposed to the magnetite alteration in the matrix

Observations

Intense alteration of phenocrysts by sericite and K-feldspar alteration in a highly magnetite altered matrix.

Interpretations

Albite phenocrysts are targeted by k-feldspar alteration before it overprints the whole groundmass observed closer to the ore body.

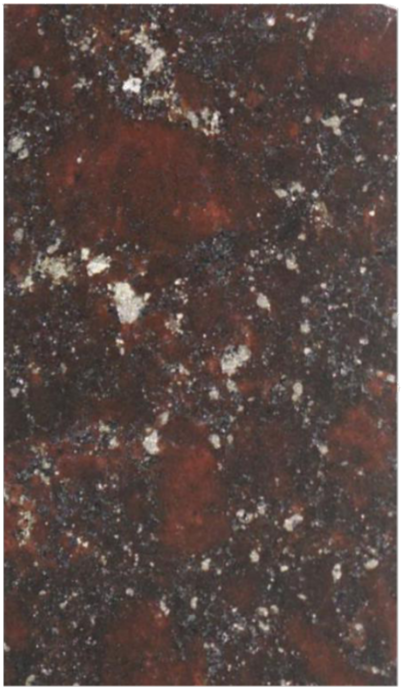

SAMPLE 690.1

Minerals	Primary/Alt/Infill	Grain size and Habit	Modal %	Characteristics
K-Feldspar	Alt	Fine grained alteration of clasts	[illegible]	Fine-grained euhedral crystals that comprise [illegible] and even finer grains with quartz that comprise clasts of red altered rock.
Quartz	Infill	Euhedral, round grains	5%	Matrix component or as infill 'blebs' of quartz
Pyrite	Infill	Large euhedral grains that have been fractured	7%	Pyrite exists in calcite veins as infill. The grains are large but have been highly fractured and infilled in some
Chalcopyrite	Infill	Not observed in hand specimen	>2%	Not observed in hand specimen
Magnetite	Infill	Infill between K-feldspar altered vein aggregates	30%	Irregular shaped infill grains, exhibiting pervasive infill/alteration that infills between red altered clasts.
Calcite	Veins	fine aggregates	5%	Highly in-filled by magnetite to the point where only minimal calcite is preserved
Chlorite	Alteration	Not observed in hand specimen	2%	Not observed in hand specimen
Biotite	Secondary	Infill in veins	>2%	Most has been retrogressed to Chlorite

SAMPLE 690.1

Mineral Petrology

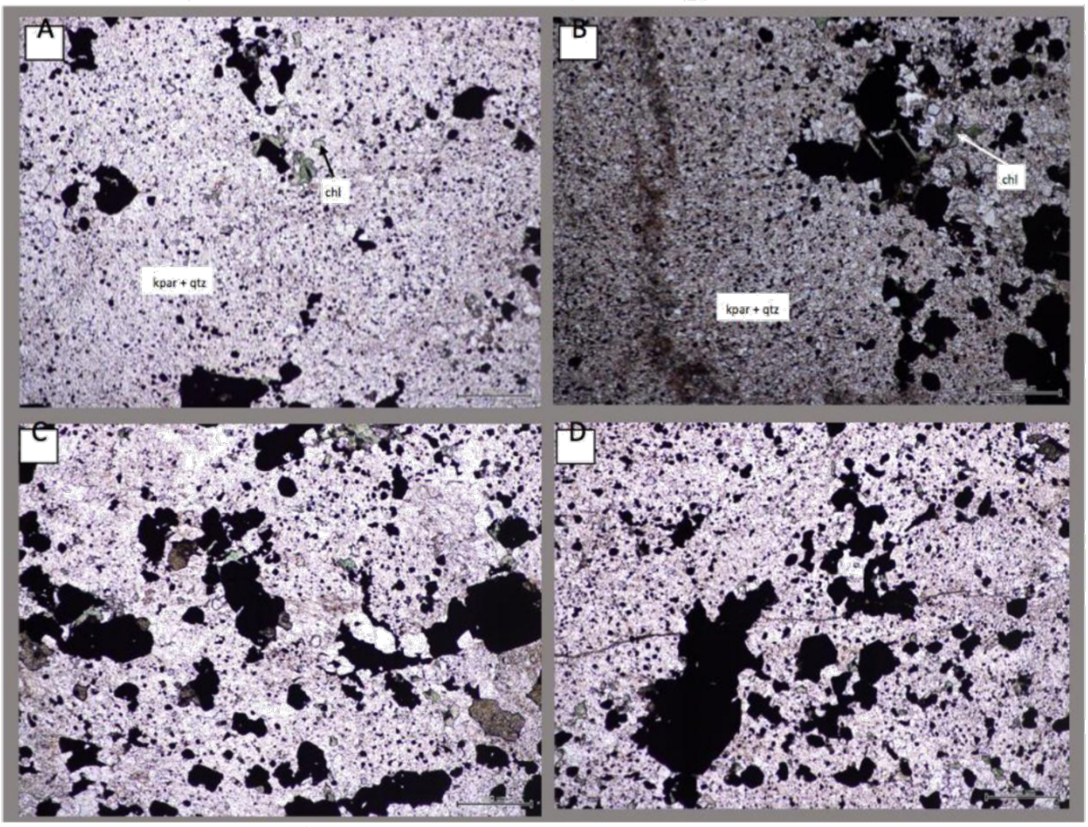

Figure 1. Illustrating the main textural associations in sample 690.1.
A – Fine-grained matrix of K-feldspar and magnetite with minor chlorite.
B- Intense alteration along a fine vein. Aggregate of magnetite with chlorite infill in fractures.
C- Same as A and B – sample is pretty homogeneous.
D- Fine veins – need further identification under SEM

Observations

This sample is a matrix supported breccia. Clasts range in width from 2mm-3.5cm across and display a dark-pinky red colour. Within these clasts, are variable, with a lighter pink colouration. The clasts have a rounded appearance to them. Disseminated sulphides sit within the matrix of the rock. Larger pyrite grains have an irregular shape.

The matrix is comprised predominately of magnetite. The matrix consists of a darker alteration colour, its hard to determine at the hand specimen scale as to whether this is very fine-grained disseminated magnetite.

Interpretations

Hematite alteration has affected the clasts, which may have already had some very fine veining through them, explaining the lighter pink colour within the clasts. Magnetite, once again in the matrix may be the result of overprinting of calcite veining.

The larger pyrite grains may be a cluster of smaller grains that have grown in proximity to each other. Chalcopyrite distribution will need to be undertaken at the thin section level.

SAMPLE 644.3

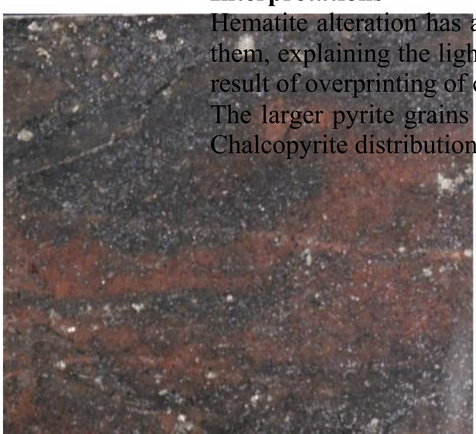

Minerals	Primary/Alt/Infill	Grain size and Habit	Modal %	Characteristics
K-Feldspar	Alt	Fine grained alteration of clasts	50%	Fine-grained euhedral crystals that comprise the majority of the matrix and clast component and even finer grains with quartz that comprise clasts of red altered rock.
Quartz	Infill	Euhedral, round grains	5%	Matrix component or as infill 'blebs' of quartz
Pyrite	Infill	Large euhedral grains that have been fractured	7%	Pyrite exists in calcite veins as infill. The grains are large but have been highly fractured and infilled in some
[illegible]	Infill	Not observed in hand specimen	>2%	Not observed in hand specimen

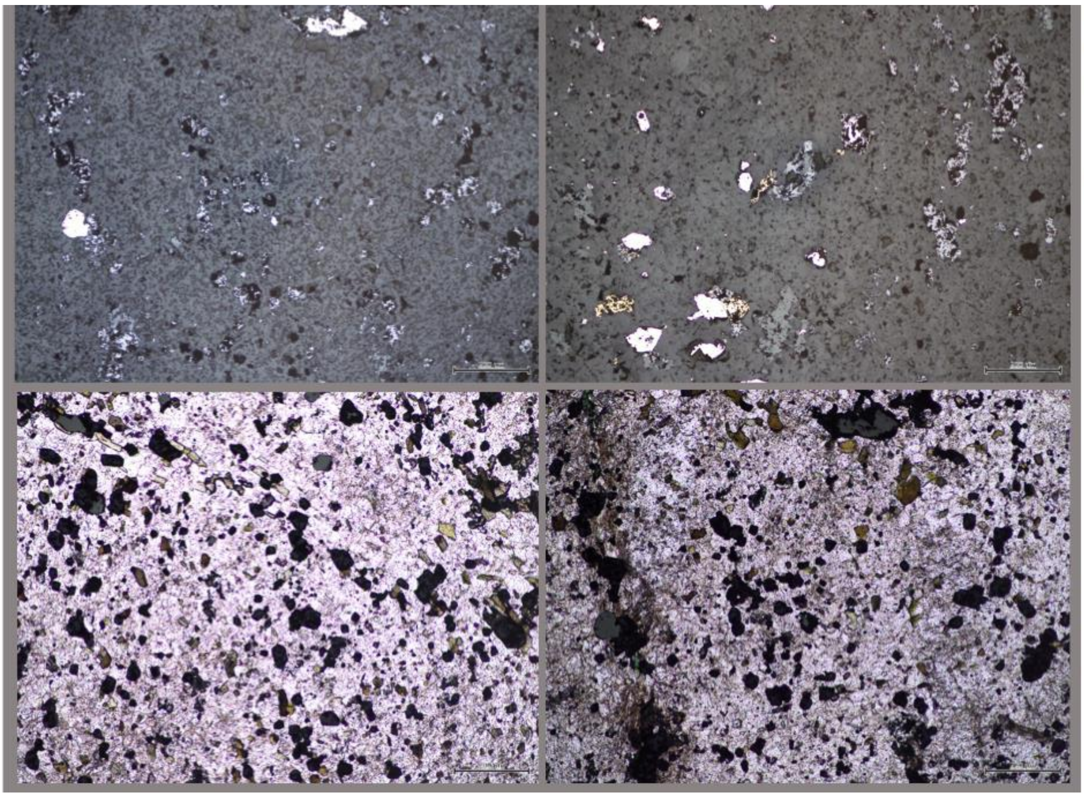

Figure 1. Illustrating the main textural associations of sulphides in sample 504.1.
A – Minor magnetite and pyrite in the matrix
B- chalcopyrite (yellow) disseminated through the matrix, anhedral grains
C- XLP: Magnetite and minor biotite in a k-feldspar rich matrix
D- intense k-feldspar/hematite alteration along a vein hosting magnetite. Minor pyrite in the matrix.

Observations

Fine- grained matrix of k-feldspar with magnetite minor magnetite, pyrite and chalcopyrite.

Interpretations

Variable alteration but not brecciation outside the intensely k-feldspar alteration zone.

SAMPLE 644.5 DEPTH: 1062.5

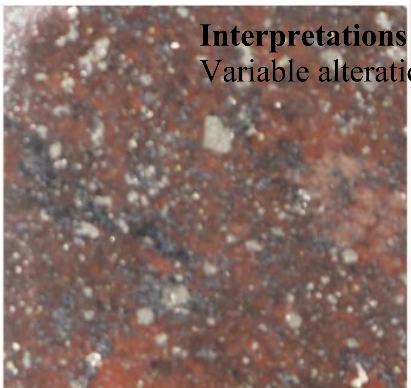

Minerals	Primary/Alt/Infill	Grain size and Habit	Modal %	Characteristics
K-Feldspar	Alt	Fine grained alteration of clasts	50%	Fine-grained euhedral crystals that comprise the majority of the matrix and clast component and even finer grains with quartz that comprise clasts of red altered rock.
Quartz	Infill in veins	Euhedral, round grains	5%	Matrix component or as infill 'blebs' of quartz
Pyrite	Infill	Large euhedral grains	7%	Pyrite exists in infill spaces, through the whole sample
		Not observed in	>2%	Not observed in hand specimen

SAMPLE 644.5 Mineral Petrology

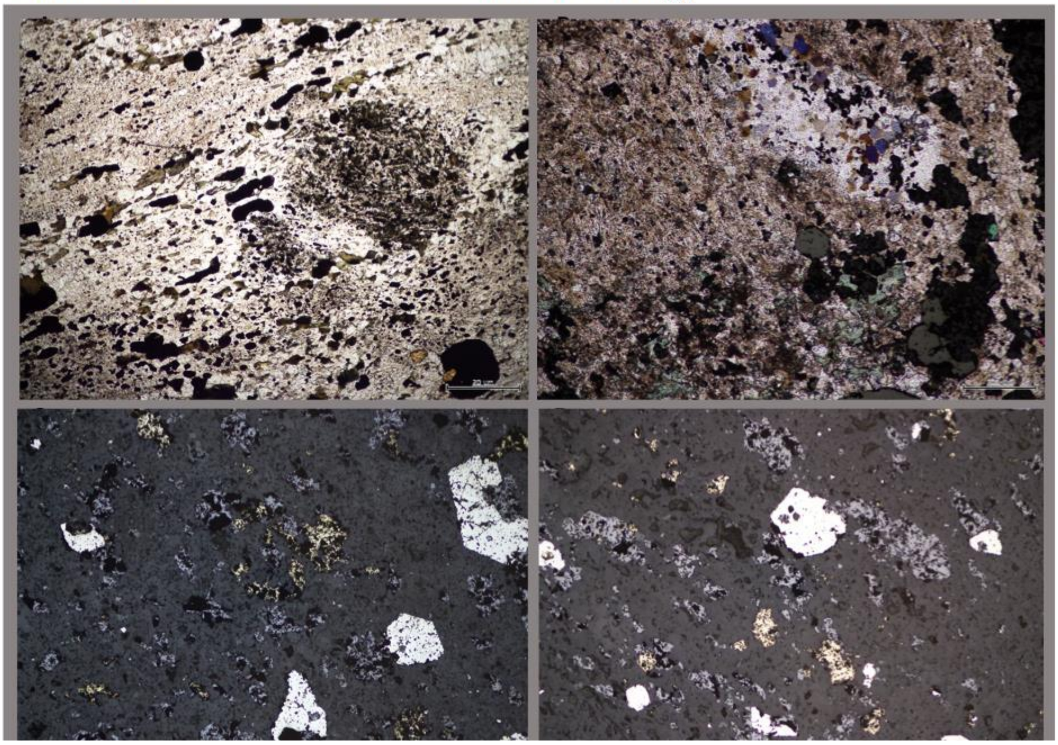

Figure 1. Illustrating the main textural associations of sulphides in sample 504.1.
A – Shear fabric? Rotated, highly altered magnetite clast within a k-feldspar, magnetite and minor biotite matrix.
B- some trachyandesite texture preserved in the matrix. Quartz vein with later magnetite infill. Chlorite alteration of biotite?
C- sulphides through the matrix, disseminated with anhedral magnetite and biotite and minor fractured pyrite.
D- Reflected light image of sulphide phase ore minerals. Minor alignment with a fabric? Pyrite and magnetite in the same phase.

Observations

Fine- grained matrix of k-feldspar with magnetite minor magnetite, pyrite and chalcopyrite.

Interpretations

Infill assemblage is representative of the ore bearing phase.

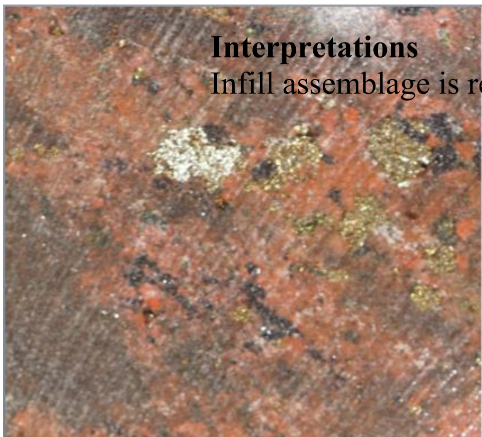

SAMPLE 644.1 DEPTH: 1026.5

Minerals	Primary/Alt/Infill	Grain size and	Modal %	Characteristics
K-Feldspar	Primary	Euhedral alteration of prior assemblage	40%	Very fine grained matrix component, creates a mosaic texture with quartz
Quartz	Primary	well preserved rounded grains	10 %	Very fine grained matrix component, creates a mosaic texture with k-feldspar
Pyrite	Infill	Large grains, minimal fracturing.	15%	Late stages pyrite grains are fractured and post date 'red rock' alteration. Small inclusions of quartz at grain boundaries between pyrite grains

SAMPLE 644.1 Sulphide Petrology

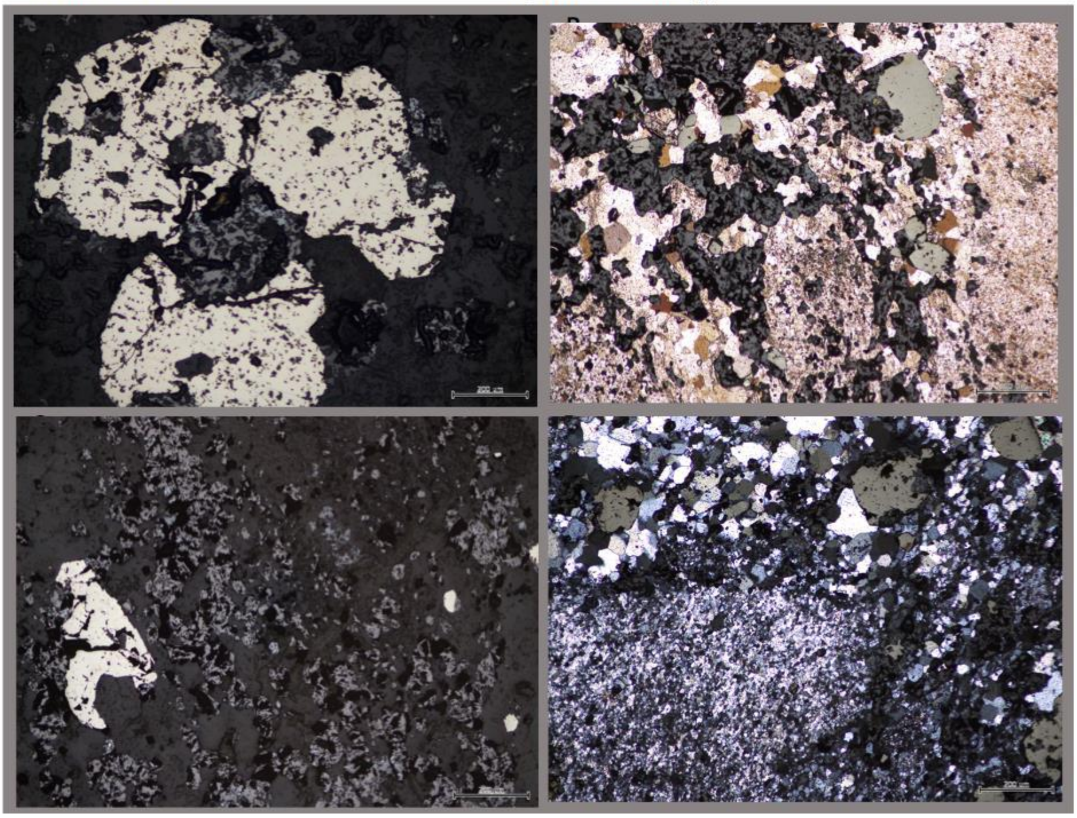

Figure 1. Illustrating the main textural associations of sulphides in sample 504.1.
A – Fractured pyrite with infilling magnetite.
B- K-feldspar and quartz matrix with intense magnetite infill with pyrite.
C- Magnetite rich matrix and a fractured grain of pyrite.
D- Reflected and XPL. Clast of fine grained volcanics in a matrix of quartz, pyrite, magnetite.

Observations

Fine- grained matrix of k-feldspar with magnetite minor magnetite, pyrite and chalcopyrite. Both sulphides and k-feldspar alteration dominated around veins.

Interpretations

Variable alteration but not brecciation outside the intensely k-feldspar alteration zone.

SAMPLE 504.6 DEPTH 539 m

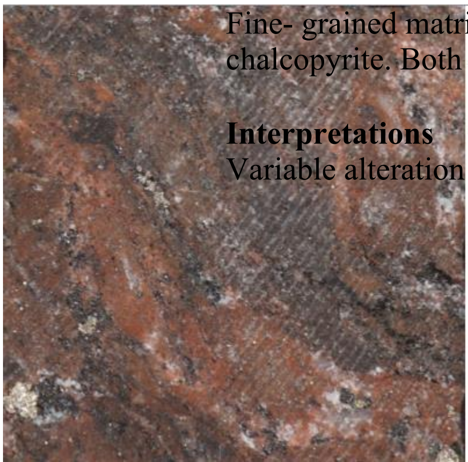

Minerals	Primary/Alt/Infill	Grain size and Habit	Modal %	Characteristics
K-feldspar	Primary	Euhedral alteration of prior assemblage	50%	Very fine grained matrix component, creates a mosaic texture with quartz
Quartz	Primary	well preserved rounded grains	10 %	Very fine grained matrix component, creates a mosaic texture with k-feldspar
Pyrite	Infill	Large grains, minimal fracturing.	5%	Late stages pyrite grains are fractured and post date 'red rock' alteration. Small inclusions of quartz at grain boundaries between pyrite grains

SAMPLE 504.4 Sulphide Petrology

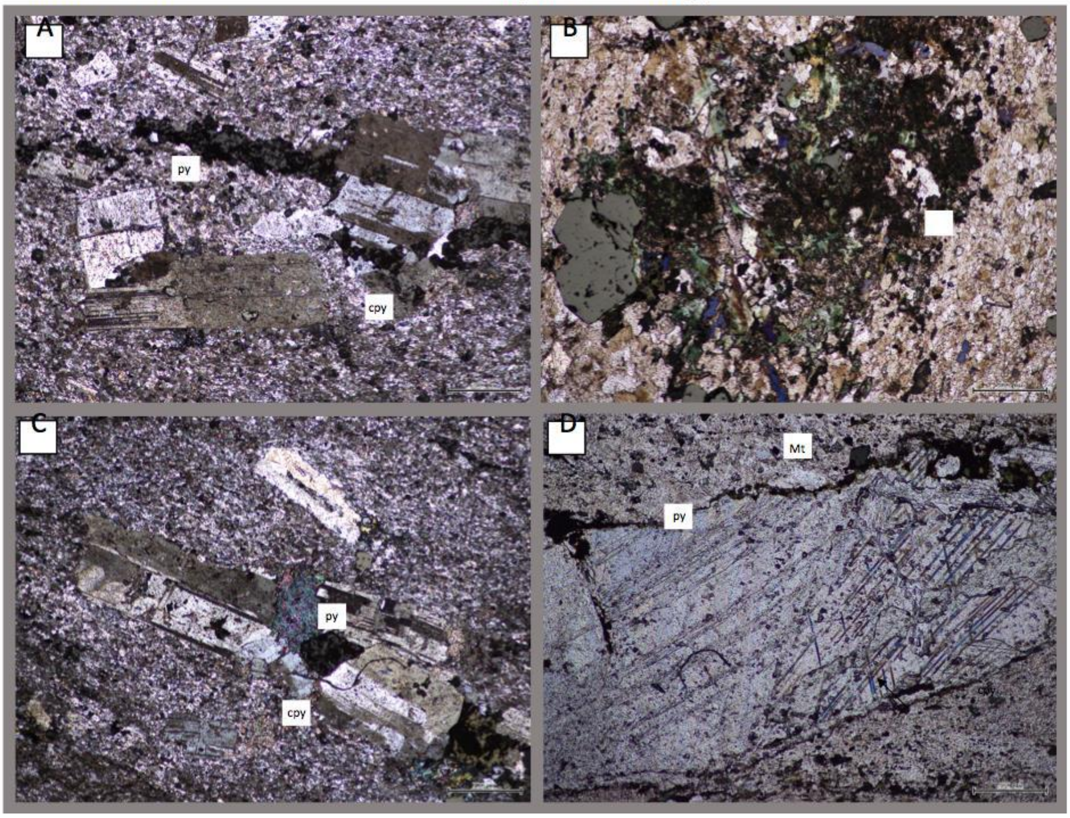

Illustrating the main textural associations of sulphides in sample 504.1.
A – feldspar phenocrysts within a fine grained matrix of k-feldspar alteration. Minor magnetite alteration.
B- Intense hematite and chlorite alteration of an unidentified minerals.
C-feldspar phenocrysts within a fine grained matrix of k-feldspar alteration. Minor magnetite alteration.
D- well preserved late stage calcite vein with minimal infill

Observations Magnetite and sulphides in calcite veins. Dark clasts Some quartz crystals inside the calcite veining and pink minerals. Calcite veining is pervasive and vary from 1- 8mm in width.

Interpretations
Where does the biotite come in?

APPENDIX D: STRUCTURAL MEASUREMENTS

Appendix D: Raw Structural Data and strike conversions.

		Foliations			Veins		
Hole ID	**Depth (m)**	**Dip**	**Dip Direction**	**Converted strike value**	**Hole ID**	**Dip/ Direction**	**Converted Strike Value**
504		42	146	42	504	50/220	310
504		60	150	60	504	30/240	330
504		80	150	80	504	20/290	380
728		86	330	420	504	20/260	350
728		45	115	205	504	40/295	386
728		82	180	270	728	58/338	428
728		75	170	260	728	48/340	430
728		80	140	230	728	64/310	400
728		20	190	280	728	52/90	180
728		82	150	240	728	39/172	262
728		78	160	250	728	59/123	213
728		70	154	244	777	46/077	167
728		46	136	226	777	38/056	146
644		65	207	297	777	52/090	178
644		50	218	308	777	40/046	136
644		40	205	295	777	50/055	145
644		60	275	365	777	62/017	107
779		62	125	215	777	22/305	395
779		38	104	194	777	10/289	379
779		48	88	178	690	50/220	310

779		58	88	178	690	30/240	330
779		69	80	170	690	20/290	380
779		44	92	182	690	20/260	350
779		52	90	180	690	40/296	386
779		64	92	182			
779		56	98	188			
690		42	146	236			
690		60	150	240			
690		80	150	240			